SQUID Magnetometers for Biomagnetism and Nondestructive Testing: Important Questions and Initial Answers

John P. Wikswo, Jr.
Vanderbilt University, Nashville, TN U.S.A.

Abstract—**For two decades, academic and industrial researchers worldwide have used SQUID magnetometers to measure magnetic signals from the heart, brain, lungs, liver, nerves, skeletal muscle, stomach, intestines, eyes, and other organs, and have invested heavily in developing and promoting this technology. While there are as yet few accepted clinical applications of SQUIDs, various trends are encouraging. The recent introduction of SQUIDs to the nondestructive testing (NDT) of aircraft and other structural systems and materials is following a strikingly similar course: most of the effort is directed towards instrumentation development and demonstrations in simple systems, and instruments suitable for specific commercial applications are just now being prototyped. To assess the potential of either technology, it is useful to ask critical questions: why are we doing this, what have we learned so far, how easy is it, what does it cost, how might we best utilize advances in digital SQUIDs and high-temperature superconductivity, and what can competing technologies provide? Answers to such questions can help identify those specific technological niches for which SQUIDs are uniquely suited, and guide the optimization of SQUID systems that are targeted for particular NDT or biomagnetic measurements.**

I. Introduction

My objective in this paper, as in the plenary lecture from which it is derived, is to provide a broad overview of the state of the art in the application of Superconducting QUantum Interference Device (SQUID) magnetometers to biomagnetism and nondestructive testing (NDT). This paper is based closely upon my plenary lecture and provides my personal views about the capabilities and limitations of SQUIDs for these applications based upon my experience with biomagnetism, NDT and SQUIDs over the past 25 years. The references are not exhaustive, but are given in part to provide the curious reader with key historical papers and examples of current research. More detailed treatments of the subject can be found in several books, conference proceedings, and review articles[1]–[8]. A number of highly relevant papers are included elsewhere in these proceedings.

The approach I will take will be to ask and attempt to answer a number of simple questions, such as: What is a SQUID? What is biomagnetism? What is nondestructive testing? There are other important questions that are often asked in response to requests for funding: Why are people developing SQUIDs for biomagnetism and NDT? Will SQUIDs always be confined to magnetic shields in laboratories? Will SQUIDs using high-temperature superconductors be of any practical use? Is there a role for digital SQUIDs? Will anyone ever make money with SQUIDs? As I hope to show in this paper, I believe that the answers to these latter questions, while not universally positive, suggest that SQUIDs are just now coming of age, and their expanded application to a variety of research and commercial applications is a certainty. In order to strike what I hope will be a reasonably balanced perspective between the scientific, engineering, clinical and commercial issues, I will also discuss in some detail not only specific SQUID applications, but also the competition offered by other, nonSQUID technologies.

A. What is a SQUID magnetometer?

A SQUID is a Superconducting Quantum Interference Device, and has as its active element one or more Josephson junctions. A Josephson junction is a weak link between two superconductors that can support a supercurrent below a critical value I_c. An rf SQUID uses a single Josephson junction that is connected to a superconducting loop; an rf current bias is inductively coupled to the SQUID to measure its impedance. A dc SQUID uses a superconducting loop with a pair of Josephson junctions, and a dc current is applied directly to the SQUID to measure the loop impedance, as shown in Fig. 1. In either type of SQUID, the special properties of the Josephson junction cause the impedance of the SQUID loop to be a peri-

Manuscript received January 2, 1995.

J. P. Wikswo, Jr., e-mail wikswojp@ctrvax.vanderbilt.edu, fax 615-322-4977, phone 615-322-2977.

Preparation of this manuscript was supported in part by grants from the Air Force Office of Scientific Research, the Electric Power Research Institute, DuPont, and the National Institutes of Health.

Address reprint requests to John P. Wikswo, Jr., Living State Physics Group, Department of Physics and Astronomy, Vanderbilt University, Box 1807 Station B, Nashville, TN 37235, U.S.A.

1051-8223/95$04.00

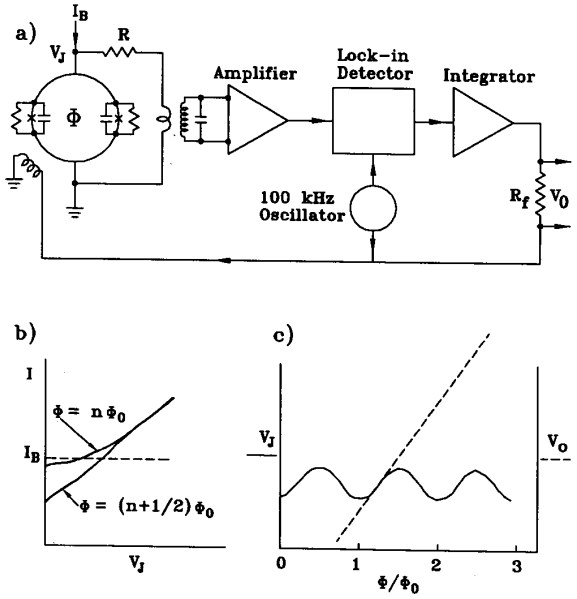

Fig. 1. A dc SQUID. a) A simplified circuit for a dc SQUID magnetometer. b) The current-voltage characteristic of a SQUID without feedback with two different values of the flux ϕ threading the SQUID loop. c) The dependence upon the applied flux for the voltage across the SQUID junctions, V_j, for a SQUID without feedback (solid), and the output voltage, V_o, measured across the feedback resistor, R_f, for a SQUID with feedback (dotted). Adapted from[7].

odic function of the magnetic flux threading the SQUID, so that a modulation signal applied to the bias current is used with a lock-in detector to measure the impedance and to linearize the voltage-to-flux relationship. The net result is that a SQUID functions as a flux-to-voltage converter with unrivaled energy sensitivity.

While early SQUIDs were made with point contacts, subsequent designs used thin-film tunnel junctions and toroidal input and rf coils in a toroidal niobium cavity. Hybrid dc SQUIDs, such as those produced for many years by Biomagnetic Technologies, Inc. (BTi), used a pair of tunnel junctions in a toroidal coupling cavity. Today, a growing number of dc SQUIDs are made in a general geometry developed by Mark Ketchen at IBM, as shown in Fig. 2, in which the SQUID loop is partially formed by a large washer that couples the SQUID to the external flux transformer. The dc bias current is applied to one side of the washer, and the other side of the SQUID loop is grounded. This geometry provides SQUID loops with low inductance and hence high sensitivity, while allowing efficient coupling to an external flux transformer.

In most practical systems in use today, the SQUID is located inside a small cylindrical, superconducting magnetic shield in the middle of a liquid helium dewar, as shown in Fig. 3. Superconducting pickup coils, typically configured as gradiometers that detect the difference in one component of the field between two points, are located at the bottom of the dewar, and the subject's head,

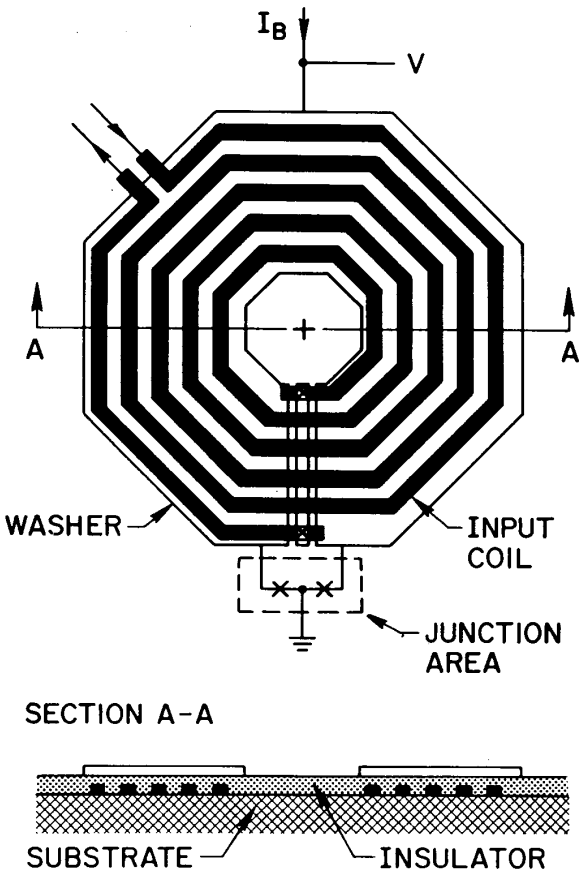

Fig. 2. A schematic drawing of a washer-type dc SQUID. The Josephson junctions are the pair of x's below the large octagonal washer, which forms part of the superconducting loop containing the Josephson junctions, and also serves as a one-turn winding in the transformer that couples magnetic flux from the input coil to the SQUID. The pickup coils, which are not shown, are connected to the input coil by the two leads at the upper left edge of the input coil. The bias current, applied to the upper edge of the washer, is divided between each side of washer and the series-connected Josephson junction. The hole in the center of the washer is on the order of 50 μm to 100 μm in diameter, so that the diameter of the entire washer is typically a fraction of a millimeter. (Courtesy of Mark Ketchen of the IBM Thomas J. Watson Research Center)

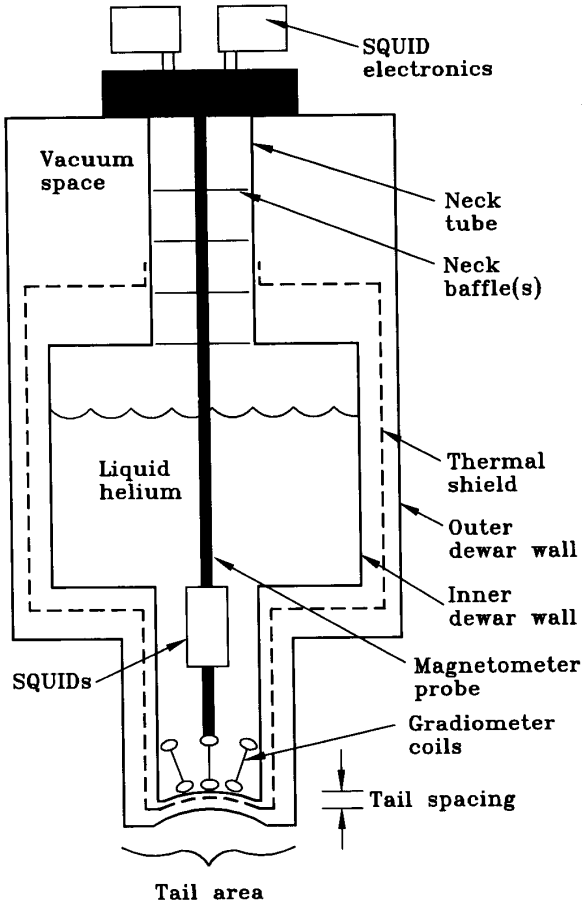

Fig. 3. A cross-sectional schematic of a typical SQUID magnetometer used for measuring the magnetic field of the brain. The majority of the dewar is fabricated from fiberglass-epoxy composite, although in some designs the helium reservoir is aluminum. (Adapted from[8]).

for example, or another object is placed beneath the magnetometer. The rest of the hardware benefits from clever cryogenic engineering and is designed to minimize helium boil off, eliminate rf interference, and to not contribute Johnson noise or distort any external ac fields.

B. What are nondestructive testing and biomagnetism?

Nondestructive Inspection (NDI), Nondestructive Testing (NDT) and Nondestructive Evaluation (NDE) are three interchangeable names for the development and application of technical methods to examine materials or components, in ways that do not impair their future usefulness and serviceability, in order to detect, locate, measure and evaluate discontinuities, defects and other imperfections; to assess integrity, properties and composition; and to measure geometrical characteristics[9]. NDT is used in process control, in post-production quality control, and in the testing of systems that are already in use. While biomagnetism has been described as the measurement of magnetic fields produced by biological systems, so as to distinguish it from magnetobiology that is the study of the effects of magnetic fields on biological systems, it is worthwhile to at least examine a somewhat broader definition of biomagnetism: the development and application of magnetic field measurements on people, in ways that do not impair their future usefulness and serviceability, in order to detect, locate, measure and evaluate discontinuities, defects and other imperfections; to assess integrity, properties and composition; and to measure geometrical characteristics, *i.e.* nondestructive testing of humans.

The earliest biomagnetic measurements were made with million-turn, room-temperature pickup coils and were limited by both external noise and the lack of adequate sensitivity or bandwidth[10]. SQUIDs were first applied to biomagnetism in 1970, when Edgar Edelsack at the Office of Naval Research convinced Jim Zimmerman, one of the inventors of the SQUID, to bring one of his first SQUID magnetometers to David Cohen's magnetically shielded room at the National Magnet Laboratory at MIT, where they recorded the magnetocardiogram (MCG) from the heart of a subject sitting in the shield[11]. Cohen later used SQUIDs to study the magnetoencephalogram (MEG) from electrical activity of the brain[12], which he had measured earlier using room-temperature coils[13]. Cohen and numerous other investigators subsequently recorded signals from a wide variety of sources within the brain, including the spontaneous alpha and delta rhythms, spikes associated with epilepsy, and evoked responses resulting from auditory, visual, tactile, and other stimulation[1],[4].

Biomagnetic signals have also been detected from the eye as the magnetooculogram and the magnetoretinogram, the stomach as the magnetogastrogram (MGG), the small intestine as the magnetoenterogram (MENG), skeletal muscle as the magnetomyogram (MMG), periph-

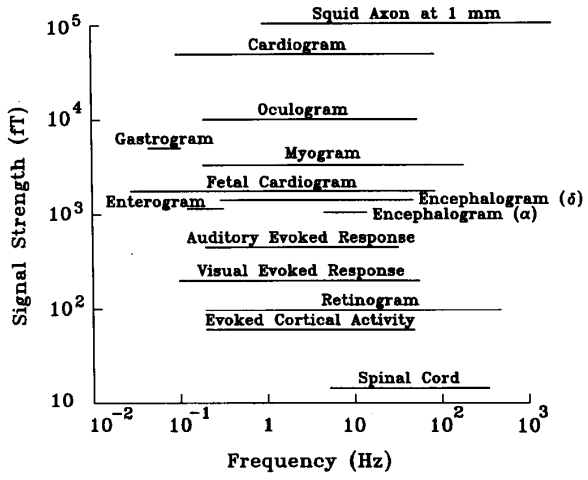

Fig. 4. A logarithmic graph of the strength and frequency bandwidth of various biomagnetic signals. (Adapted from[8]).

eral nerve as the magnetoneurogram (MNG), and the fetal heart and brain as the fetal magnetocardiogram (F-MCG) and magnetoencephalogram (F-MEG). As shown in Fig. 4, the strength of these signals ranges from 10 femtotesla (fT) to more than 10,000 fT, at frequencies from a fraction of a hertz to a kilohertz. The weak field strength, the substantial information content at low frequencies, and the broad measurement bandwidth all suggest that SQUIDs will remain the magnetometer of choice for the immediate future, with exception of measurements on isolated, one-dimensional nerve and muscle tissue preparations using miniature toroidal pickup coils[14] and possibly the measurement of the adult MCG using optical magnetometers[15], [16]. (Optical magnetometers based upon Faraday rotation may eventually provide competition to SQUIDs in some applications, since sensitivities of 100 $fT/Hz^{1/2}$ have already been achieved with a 1 mm long, 3 mm diameter, gallium-substituted yttrium iron garnet crystal, and a noise of 1.4 $pT/Hz^{1/2}$ was achieved at 1 kHz with the addition of a pair of tapered, 13 mm long, 25 mm diameter ferrite flux concentrators[17]. However, it may prove difficult to create highly balanced gradiometers with these systems, the noise at 1 Hz and below has not been reported, the problems of separating signal and noise must be addressed, and the cost and size of the requisite optical systems may not be trivial, since the devices require a diode-pumped YAG laser and the optical systems of the most sensitive systems can occupy a volume as large as 1 m^3 and the simplest single-channel system may cost in excess of $30,000 [18].) As we will see later, the strength of some of the biomagnetic signals shown in Fig. 4 already places them within the range of sensitivity provided by high transition-temperature SQUIDs, and these systems could in the near future cost less than $1,000 per channel.

C. *Why are people developing SQUIDs for biomagnetism and NDT?*

The first major question that we need to address is the one that reviewers occasionally ask pejoratively: "Why in the world are you bothering to develop SQUIDs for biomagnetism or NDT?" There are a number of reasons. The magnetic fields exist and we can build good SQUIDs. This is the Matterhorn response: You climb it because it's there! More importantly, some existing clinical and NDT techniques are clearly inadequate, and it appears that in some cases SQUIDs are the best and possibly the only way to make the desired measurements. Clearly, some people need SQUIDs today, and from present trends, it is reasonable to expect that more people will need SQUIDs tomorrow. A variety of people are willing to pay to develop the technology, including government and nonprofit funding agencies, industrial organizations with specific problems that need to be solved, or venture capitalists interested in developing new industries.

II. Instrumentation

The single channel SQUID systems, such as those originally marketed by BTi and CTF Systems, Inc., have found widespread use for various applications in biomagnetism and NDT. The very first biomagnetic studies were directed towards measurements of the MCG, but early clinical studies revealed little additional diagnostic information beyond that recorded with the simpler and less expensive electrocardiogram (ECG). Recently, several multichannel systems have been built for more sophisticated and promising cardiac studies, which will be discussed later.

A. *SQUIDs for measuring the magnetic field of the brain*

The widest scientific and commercial interest has concentrated on the MEG and hence this is the area with the most active instrumentation development. As shown in Fig. 5, the cortex of the human brain is filled with nerve cells that have distributed dendritic networks. In the course of the electrical activity of the brain, currents in these dendrites act like small electric dipoles. If the dipole is located tangential to the approximately spherical surface of the brain, it will produce an external magnetic field; collections of 10^4 dendrites active in a 1 mm^2 area of cortex can produce magnetic fields that are measurable outside the surface of the scalp with a SQUID magnetometer[19].

Although a single magnetometer can be used to map the spatial variation of the magnetic field from a repetitive, evoked process in the brain, such studies are tedious and prone to errors in determining the location of the SQUID pickup coils relative to the subject's brain. Furthermore, single channel SQUIDs are of little use in study-

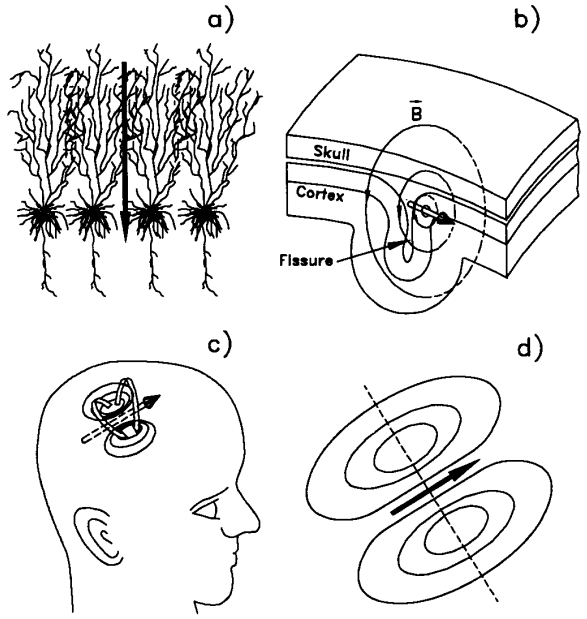

Fig. 5. The magnetic field from the brain. a) A collection of simultaneously active cortical dendrites whose summed electrical activity produces electric and magnetic fields similar to that of a current dipole. b) Equivalent dipole sources adjacent to a sulcus (fissure) in the brain oriented so that the dipole is tangential to the surface of the skull produce externally detectable magnetic fields in (c), which produce the characteristic dipolar pattern of isofield contours in (d). (Adapted from[20])

ing the spatial distribution of asynchronous electrical activity such as the alpha rhythm, or the interictal spikes that occur between seizures of epilepsy patients. This limitation was first addressed with a 5 channel SQUID system produced for Sam Williamson by BTi in 1983; subsequently, BTi introduced a pair of 7-channel magnetometers that could study signals occurring on opposite sides of the head. Unfortunately, the 7 channel systems covered only a small fraction of the cortex, and provided insufficient data for accurate localization and characterization of many sources. BTi and others then introduced 37 channel systems; BTi subsequently developed a dewar that could be operated with the SQUIDs located above the helium reservoir so that it could be placed beneath the subject's head; thus a pair of 37 channel systems could be operated simultaneously above and below a reclining subject's head. Elsewhere, the University of Twente developed a 19 channel system[21], a research group at the Institute of Radio Engineering and Electronics of the Russian Academy of Sciences in Moscow formed a company, Cryoton, that has built a 19-channel system[22],[23], and Philips[24] in Hamburg has built a double SQUID system with 31 channels in each dewar. Flat bottomed dewars for the MCG are used in 37 and 63 channel systems built at the PTB in Berlin[25], and in a 256 channel system developed at the Superconducting Sensor Laboratory (SSL) in Japan[26].

The real advance with SQUIDs for measuring the MEG came with the introduction of helmet-shaped dewars that have a hundred or so SQUIDs and cover much of the head. The advantages of these systems are that they provide partial or full head coverage so that you can do measurements that acquire data from multiple regions at the same time. They also reduce the length of time required for measurements. The advantage that has not yet been fully realized is that multiple channels should allow imaginative digital signal processing to eliminate noise. The 64 channel, whole head system from CTF, shown in Fig. 6, has first order gradiometers connected to SQUIDs with digital feedback and uses digital signal processing and 27 reference gradiometers to synthesize third-order gradiometers[27],[28]; a 140-channel system with 28 reference SQUIDs is under construction. The Neuromag system developed at the Helsinki University of Technology and being sold by Instrumentarium/Picker has 122 channels in the form of pairs of orthogonal, planar thin-film gradiometers. A 256 channel helmet system is being developed at SSL[29], and BTi is now constructing several helmet systems with 148 SQUID magnetometers and 12 reference SQUIDS. Researchers at the Consiglio Nazionale delle Ricerche in Rome are developing a 153 channel system.

The real limitation of helmet systems arises from their fixed geometry: the CTF helmets come in two sizes, one for a standard Japanese head and other for a standard

Fig. 6. The CTF whole-cortex SQUID system. Top: A subject having her magnetoencephalogram recorded with the 64-channel unit[27]. Bottom: A mock-up of the form that holds the first order gradiometer coils in the 140 channel system. (Courtesy of Jiri Vrba of CTF)

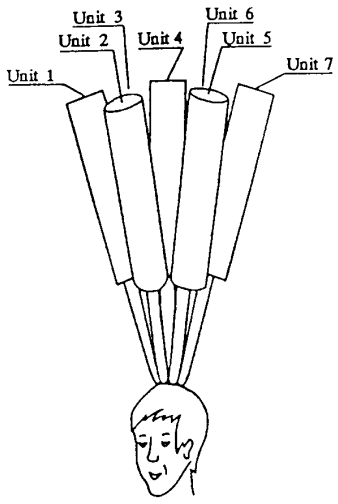

Fig. 7. A seven-channel neuromagnetic system using separate single channel modules[30], [31] (Courtesy of Andrey Matlashov of the Institute of Radio Engineering and Electronics of the Russian Academy of Sciences)

Canadian head. The design of the Neuromag system is based on military studies of the distribution of head sizes of adult males in the Finnish army. As a result of variation in the size and shape of the subjects' heads, and the cryogenic difficulties encountered with building large, concave dewars, the source-to-pickup coil separation is typically larger by a centimeter or more over what was achieved with simple, 7-channel systems. As a result, the signal amplitude is reduced, and more importantly, the high spatial frequencies present in the magnetic field close to the scalp are selectively attenuated by the increased distance. I believe that before long, the users of the helmet systems, particularly those who do extensive mathematical processing of the data, will recognize that the increased and variable coil-to-source spacing is unwise, and it will be necessary to develop alternative approaches, such as segmented or otherwise adjustable helmets, as shown in Fig. 7, but this does present problems with dewar cost, increased tangential separation between the channels at the edges of adjacent segments, and multiple cryogen transfers. The approach that BTi is taking with its new helmet systems is to use magnetometers rather than gradiometers, so that each sensor has increased sensitivity to deep or distant sources as compared to a gradiometer configuration. The helium consumption of the present helmet systems is also significant, between 10 and 20 liters per day, due to the large surface areas where the coil-to-room temperature spacing must be kept small, the thermal leak that arises from the six to ten wires required to operate each dc SQUID, and from the size of the neck tube in some dewar designs.

It is important to recognize that these systems are be-

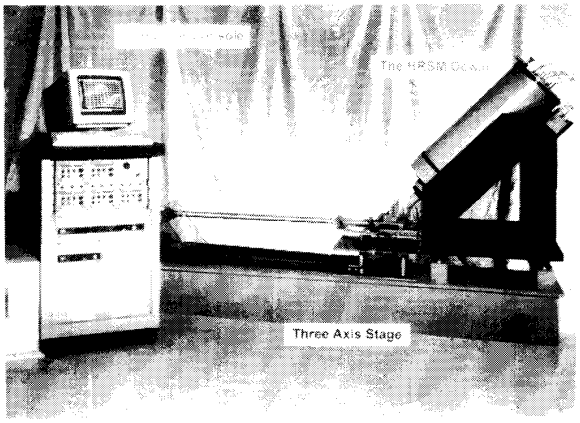

Fig. 8. The Quantum Magnetics High Resolution Scanning Magnetometer set up to scan a corrosion cell in an unshielded environment[32],[33]. (Courtesy of Andy Hibbs of QM)

coming quite complicated and expensive: The CTF system has 168 channels of SQUID electronics with digital feedback, and various other electroencephalogram and other signal channels that create a great deal of costly and bulky hardware. These systems also generate a tremendous amount of data quite quickly, which in turn makes demands upon data processing, display, and storage. While the CTF system is presently unique among the helmet systems in that it can be used in an unshielded environment, other systems require a magnetically shielded room; the performance of the CTF system is improved within a shield. Helmet systems cost between one and two million dollars, and the cost of the shield can increase this by another half million dollars. Thus the helmet systems are just that: major systems with all the inherent problems of systems integration and escalating costs; the SQUIDs and their electronics probably contribute only 10% of the total cost!

B. SQUIDs for NDT

Several companies build SQUID systems specifically for NDT. The first high resolution SQUID used for NDT and biomagnetism, MicroSQUID, was built for me by BTi and Quantum Design. Quantum Magnetics (QM) has developed a five-channel High Resolution Scanning Magnetometer (HRSM) that is designed to scan a corrosion cell in an unshielded environment[32],[33]. The system, shown in Fig. 8, is equipped with a custom-made fiberglass (G-10) translation stage. The stepper motor controller and the data acquisition process are controlled by a desktop computer. Figure 9 shows a 6-channel SQUID magnetometer with built-in magnets for 1 mT ac and 0.1 T dc fields developed by Conductus for use with a robot for nondestructive evaluation of components in a reactor. SQM Technology has developed an electromagnetic

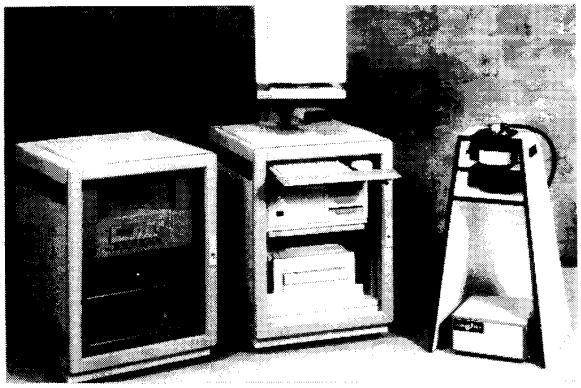

Fig. 9. The Conductus 6-channel NDT system with ac and dc magnets. The small dewar at the top of the test stand at the right would be held by a robot moving within a nuclear reactor. (Courtesy of Richard Kirby of Conductus).

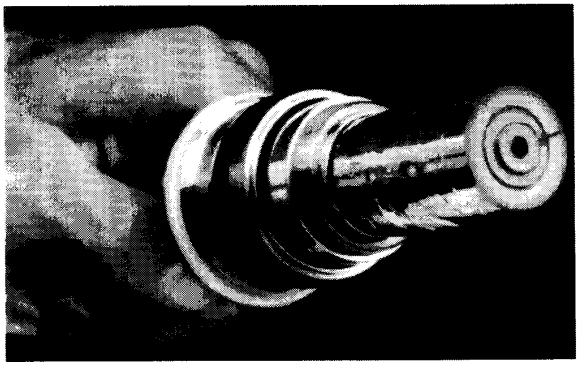

Fig. 10. The SQM Technology Electromagnetic microscope. The 2 mm diameter, differential pickup consists of two counterwound, semicircular loops[34],[35]. Current oscillation in a 10 turn, 10 mm diameter superconducting source coil concentric with the pickup induces eddy currents in conductive objects under test. The 16 mm coil is for compensation. Axisymmetric currents induced in unflawed test pieces generate a null response in the gradiometer pickup; flaws break symmetry and cause a signal. (Courtesy of SQM Technology)

microscope (Fig. 10) which has an ac source coil and a pickup coil on the end of a flexible thermal link connected to a closed cycle refrigerator[34],[35].

III. Applications - Biomagnetism

While there is inadequate space in this review to cover all applications of SQUIDs to biomagnetism, it is worthwhile to provide selected examples in cognitive science, clinical neurology, cardiology, and gastroenterology. However, before we can do that, we need to look at how to interpret the data.

A. Modeling of biomagnetic fields

Much of the MEG work to date has been done by looking at biological signals from sources that are highly localized in space, and hence are suitable for analysis as a

single electric dipole. As an example, cognitive science studies benefit from determining the location of the cortical neurons that respond first to a particular auditory or visual stimulus. The potential for MEG to locate such sources was clearly demonstrated in the early studies by Sam Williamson and Lloyd Kaufman at New York University[36], [37]. If one uses the rather drastic simplification that the head can be modeled as a sphere, information about the depth of the source can be obtained directly from a map of the component of the magnetic field that is perpendicular to the scalp: in this approximation, the effective source dipole lies midway between the maximum positive and negative values in the MEG map, at a depth that is $\sqrt{2}/2$ times the spacing between the two extrema shown in the isofield pattern in Fig. 5d. While this approximation was used extensively in early MEG studies and it still provides useful results for some regions of the head, such as over the visual cortex at the back of the head, more advanced models that account for the non-spherical shape of the inner surface of the skull are more uniformly applicable. Because of the high conductivity of the scalp and the low conductivity of the skull, such simplistic models have not proven useful for the electroencephalogram. As shown by Fig. 11, the ability to localize sources from the MEG is improved by using more realistic models of the head that include the shape of the head surface, and the inner and outer surfaces of the skull; typical accuracies for a single sphere model are on the order of 0.5 cm at the cortical surface, and 2.5 cm near the center of the head, whereas an accuracy of 0.23 and 0.5 cm can typically be achieved using a realistic three-layer model[38], [39]. It is worthwhile to note that while there have been a number of studies to ascertain the localization accuracy of the MEG, the accuracy of the competing, conventional imaging techniques is not widely studied – one study demonstrated that MRI images of the head had an average 1 to 1.5 mm distortion due to field gradients[40], dependent in part upon the pulse sequence and field gradients used. Later, we will discuss the problems with localization using the EEG.

The fundamental limitation of dipole models is that some sources either are not dipolar, or are distributed over such a large area that the dipole moment conveys only a fraction of the information about the nature of the source. A detectable interictal spike from an epilepsy patient may be the result of the simultaneous activation as much as 6 cm^2 of cortical surface[41], [42]. The temptation is then to attempt to solve the generalized inverse problem of determining the distribution of cortical currents that produced the magnetic field. Unfortunately, this problem has no unique inverse solution, and can be solved only with the addition of physiological constraints or mathematical regularization. A variety of approaches have been taken; examples are shown in Figs. 12 and 13. Figure 14 compares the three types of minimum norm

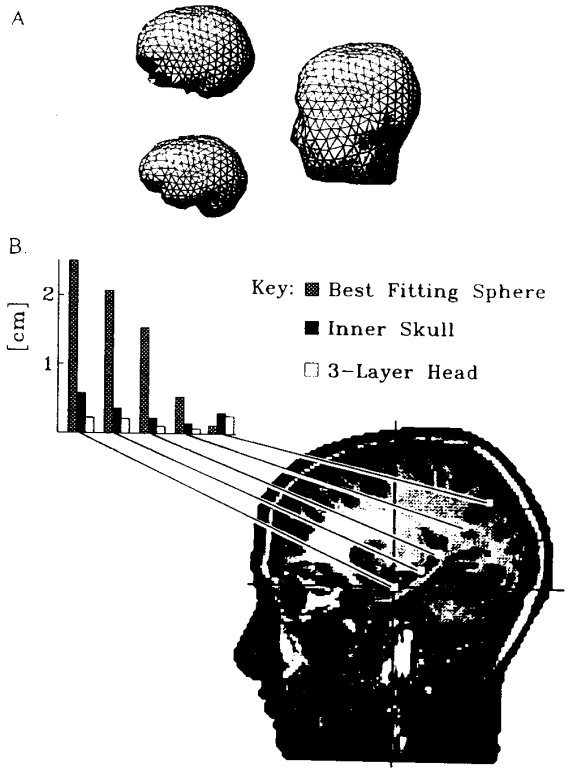

Fig. 11. Error in dipole localization for head volume-conductor models of increasing anatomical realism[39]. a) A series of computational meshes defining major conductivity barriers in the head: the head surface, the outer and inner surfaces of the skull. These meshes are used for boundary integral computations of the head surface potential and magnetic field distributions due to current dipoles at arbitrary locations and orientations within the head. b) A series of assumed dipole sources relative to an MRI anatomical rendering. The input data from the forward model simulated a 127-channel SQUID system with a 10:1 signal-to-noise ratio. The bar graphs illustrate the error for each source location for three models: the sphere that best-fits the inside of the head, a single-surface model representing the inner surface of the skull, and the full three-layer model. (Courtesy of John George of Los Alamos National Lab)

Fig. 12. The Philips model of the head and the MEG, in which an MRI image is automatically segmented and an arbitrary cut was made in order to look inside the head[43]. The locations of the coils are shown by the circles, above the isocontour lines of the magnetic field. An algorithm computes the minimum norm estimate of the distributed sources of the magnetic signal that occurs 20 ms after median nerve stimulation. (Courtesy of Olaf Dössel of Philips)

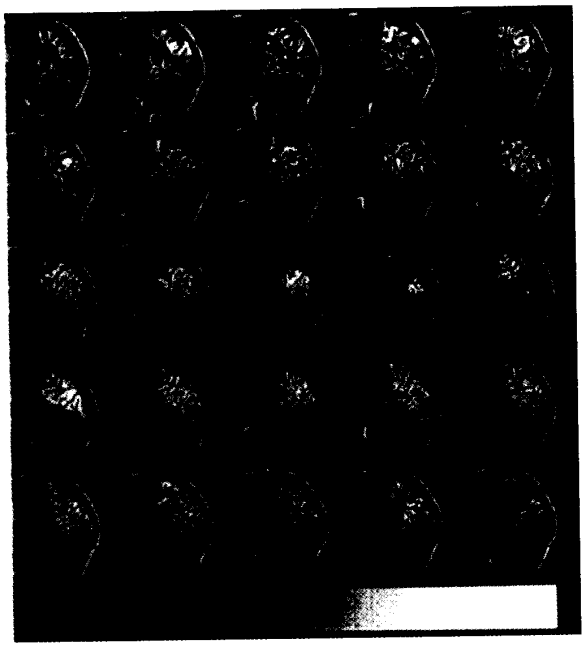

Fig. 13. The Los Alamos MUltiple SIgnal Classification (MUSIC) algorithm[44]. Slices of the MRI anatomy with superimposed, as brighter regions, the values of the cortically constrained MUSIC metric - a functional measure derived from MEG in a series of slice images. MUSIC allows assessment of the distribution of probability of a dipole source by systematically scanning a predefined grid. By adding constraints based on the location and orientation of the local cortical surface, the MUSIC metric becomes more diagnostic, with sharper peaks corresponding to (relatively) localized regions of neural activity. This figure illustrates a region of the occipital lobe of the brain and suggests several discrete areas of activation. (Courtesy of John George of Los Alamos National Laboratory).

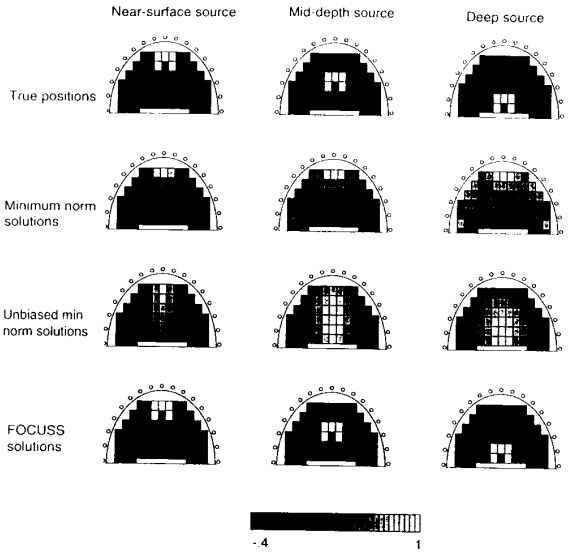

Fig. 14. Reconstructions achieved with different techniques for an extended source at different depths[45]. Each column illustrates a different depth source, and each row illustrates a different reconstruction method (minimum norm, unbiased minimum norm, and FOCUSS (FOCal Underdetermined System Solution) solutions; the top row is the simulated current distribution. Each subimage is normalized by dividing each element by the maximum value in the image. (Courtesy of Irina Gorodnitsky of the University of California, San Diego)

solutions; the success of the FOCUSS (FOCal Underdetermined System Solution) algorithm demonstrates that a series of carefully designed constraints, including that the number of active generators not exceed the number of measurements, can produce reasonable reconstructions for certain types of source distributions[45]. Work on improved inverse calculations should prove to be a fruitful area of research for years to come.

B. Cognitive science

Given the fact that many sources are highly dipolar, SQUIDs can be used for some interesting cognitive science, such as providing a noninvasive, tonotopic map of the response of the auditory cortex to auditory stimulation at different frequencies, studies of tonal memory[46], [47], brain activity during eyeblinks[48] and picture naming[49], mapping of the visual field on the retina onto the cortex, and mapping of the hand and face to the cortex. As shown in Fig. 15, Chris Gallen and Tony Yang at the Scripps Institute in La Jolla have applied a nonmagnetic mechanical stimulator to various points on the hand and mapped the locations on the brain that corresponded to the hand locations[50]. Similar studies on subjects who had one arm amputated showed that the signals from the face and shoulder for the amputated side had moved closer together, and overlapped into the space that would have otherwise corresponded to the hand, providing the first direct demonstration of cortical plasticity in humans, and proving that some phantom sensations from the amputated limb arise from the cortex[51].

C. Clinical applications

A wide variety of clinical applications of biomagnetism have been examined in neurology, including studies of epilepsy, stroke, trauma, and the recording of signals from the spinal cord, nerves, and skeletal muscle. One of the problems with the acceptance of magnetometry as a clinical tool is the length of time that it has taken to demonstrate clinical utility. This is hard in any one field, and biomagnetism is being applied to many different ones. More importantly, because the technique represents a significant departure from existing clinical techniques and few clinical centers will purchase an expensive and unproven instrument, corporate involvement has been required in developing clinical applications: BTi and its collaborators worldwide have recorded from over 3,400 patients and normal subjects. Other groups have also been demonstrating clinical applications, but generally in a more limited way.

The first application that has been clinically proven and recognized for third party reimbursement is the presurgical functional mapping for brain tumors, arteriovenous malformations, and epilepsy, in which the MEG is used to identify key regions of functioning cortex before they

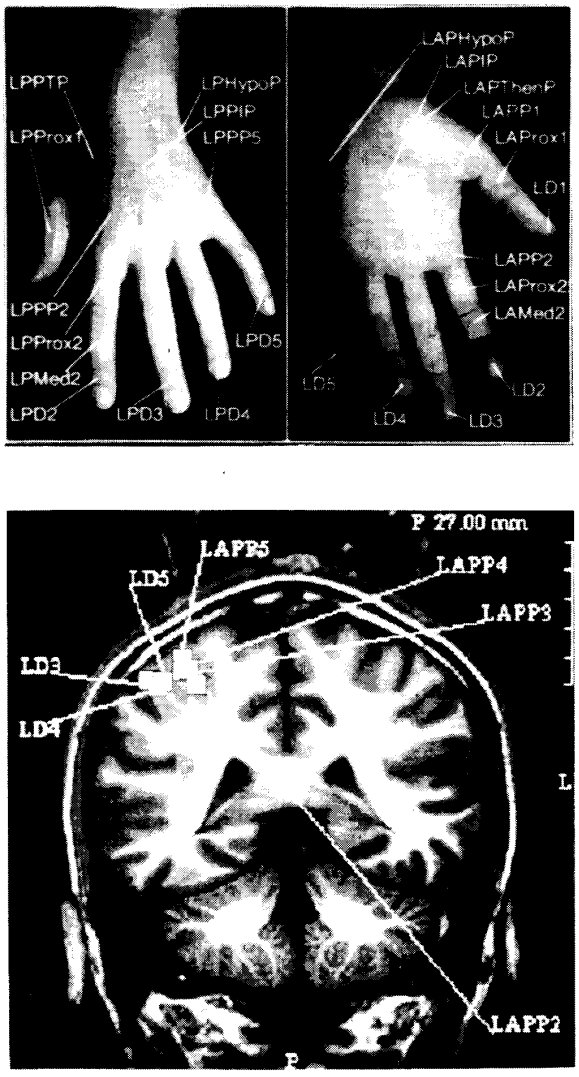

Fig. 15. Demonstrations of noninvasive mapping of hand stimulation sites onto the cortex[50]. Top: Sites of mechanical stimulation; Bottom: the sites of cortical response. (Courtesy of Christopher Gallen of the Scripps Institute and Gene Hirschkoff of BTi).

are inadvertently removed or otherwise damaged during surgery. This procedure is now accepted by a number of insurance companies - in part because there is a 20% morbidity rate for the 100,000 intracranial surgeries performed each year, and the MEG is proving useful for reducing the risk.

Clinical applications that are still in the process of being proven include the use of the MEG to provide a more definitive diagnosis of stroke, head trauma, and transient ischemic attack (TIA) in the brain, and the use of the MCG to localize and classify cardiac arrhythmias. Promising applications that are just now being examined include the use of SQUIDs for fetal heart monitoring[52], [53], studies of the signals from the spinal cord and peripheral nerves[54], the diagnosis of bowel function disorders, and the study of schizophrenia and metabolic brain disorders such as uremic or hepatic encephalopathy. I will now discuss some of the applications in more detail.

1) Studies of the brain: Because patients with epilepsy often exhibit electrical spiking in the interictal period between seizures, substantial effort has been directed towards using the MEG to localize the site of origin of the spikes, which is believed to coincide with the site of origin of the seizure. Early studies by groups in Rome and at UCLA demonstrated the validity of this approach[55], [56]; Fig. 16 shows how a helmet MEG system can quickly localize the source of the spikes, and also shows how the mirrored activity on the left side of the brain of the subject being studied lags after the activity on the right side[57].

One of the more recent and interesting applications under development is the use of the MEG to diagnose head trauma and damage from transient ischemia, being pursued by Jeffrey Lewine and William Orrison of the University of New Mexico and the Veterans Hospital in Albuquerque[58]–[60]. The activity of the normal brain is dominated by alpha waves in the 8-13 Hz range. Patients with neurological disorders often show slowing of the EEG, and also show extensive, large amplitude, abnormal low frequency magnetic activity (ALFMA) in the theta and delta range. The MEG ALFMA examination is quite sensitive to demonstrating pathophysiology in these patients. Many patients who suffer mild traumas have normal MR and CT examinations, but significant postconcussive psychological changes. As an example, the circles in Fig. 17a correspond to the locations of ALFMA activity at 2.5 Hz in a 65 year old woman who had three episodes of facial numbness and slurred speech within the four hours prior to her admission to the hospital. Her clinical symptoms resolved by the time she went to the hospital 10 hours after the last episode. Computerized tomography and magnetic resonance imaging could find no abnormalities. Magnetic source imaging with the MEG found multiple sites of ALFMA slow wave activity that confirmed the suspicion of multiple middle cerebral artery transient ischemic attacks (TIAs) that were undetectable

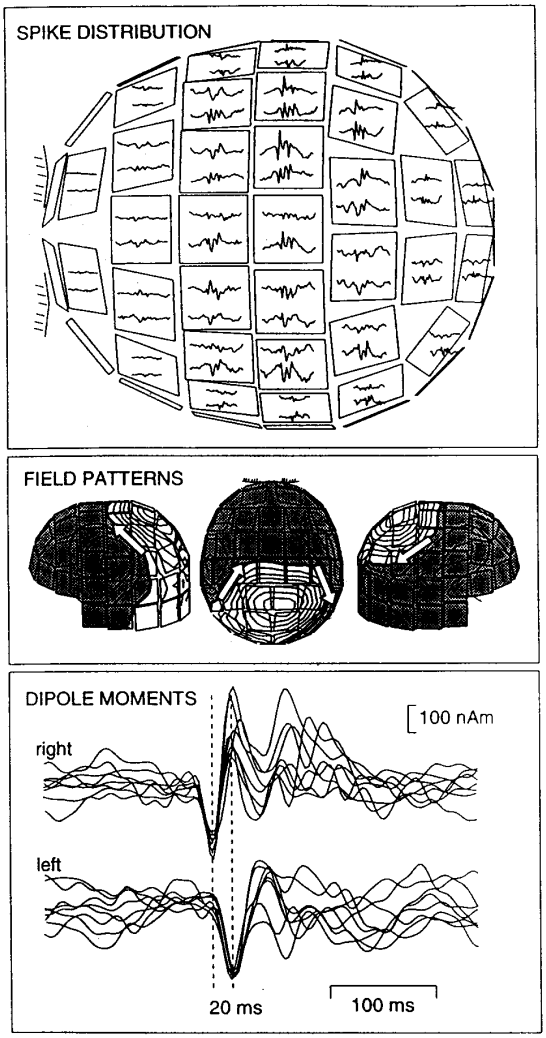

Fig. 16. Top: Spatial distribution of one interictal spike displayed on the sensor array; only about half of the measured signals are shown in this projection. The two traces on each sensor unit illustrate the two orthogonal derivatives of the magnetic field measured at that location. Middle: Field patterns during a single time moment of one spike. The sensor array is viewed from the left, from above, and from the right. The shadowed areas indicate magnetic flux emerging from the head; the isocontours are separated by 400 fT/cm. The arrows indicate the sites and orientations of the two equivalent current dipoles required to account for the field pattern. Bottom: Dipole moments as a function of time in both hemispheres. Each trace corresponds to one unaveraged spike, whose distribution was explained by the two-dipole model. (From[57], with permission).

with other imaging methods or the EEG. The patient was treated to reduce the risk of stroke.

In the example shown in Fig. 17b, an 18 year old boy suffered severe beating at school 3 months prior to the examination and showed a serious decline in school performance. There was no evidence of traumatic injury on EEG, CT or MRI, yet psychological tests supported the explanation of brain trauma instead of an aversion to school for fear of repeated attack. The MSI study demonstrated dense bilateral focal slow wave activity that confirmed serious brain injury.

Surgeons are very reluctant to perform operations that may cause a hemiparalysis because this significantly compromises the quality of a person's life. The data in Fig. 17c are from a 58 year old combat veteran who had a tumor, and the issue was whether the tumor could be resected. The groove in the brain known as the central sulcus contains the motor cortex, but it was not possible to discern from anatomical images whether A or B was the central sulcus. Without this identification, no surgeon would operate. The only technique that could identify that noninvasively was the MEG, which showed that the motor signals from the hand were at A, hence this was the central sulcus. Given this data, a surgeon agreed to perform the surgery.

As a final neurological example, Fig. 17d shows an MRI image of the cortex of a 5-year-old male with intractable partial-complex seizures. Two prior surgical interventions in the inferior frontal cortex failed to alleviate the epilepsy. Functional mapping by MEG and Transcutaneous Magnetic Stimulation (TMS) showed that the resection zone could not be extended more posteriorly without compromise of motor cortex. However, the MEG showed that the epileptic activity was arising from a region far removed from the prior resection zones. Re-examination of the patient's MRI data showed a small vascular malformation in this region that had been previously overlooked. Surgical intervention in this area has controlled the patient's seizures.

2) Cardiac Studies: In contrast to the brain, in which magnetic signals are produced by innumerable asynchronous sources, the electrical activity of the normal heart is a highly synchronized yet distributed current source that propagates through the heart as a wave. From the surface of the chest, as shown in Fig. 18, the heart looks like an electric battery whose amplitude and orientation varies in time. The peak magnetic field from the heart exits the chest on the left side and enters the abdomen lower on the right; the strength and orientation of the source and hence its magnetic field vary throughout the cardiac cycle. The magnetocardiogram in Fig. 19 was recorded by the PTB group in Berlin in their magnetically shielded room[25]. The noise in this signal, with a bandwidth of 250 Hz, is a fraction of a picotesla (pT) (inset) and does not come from the SQUID or the mag-

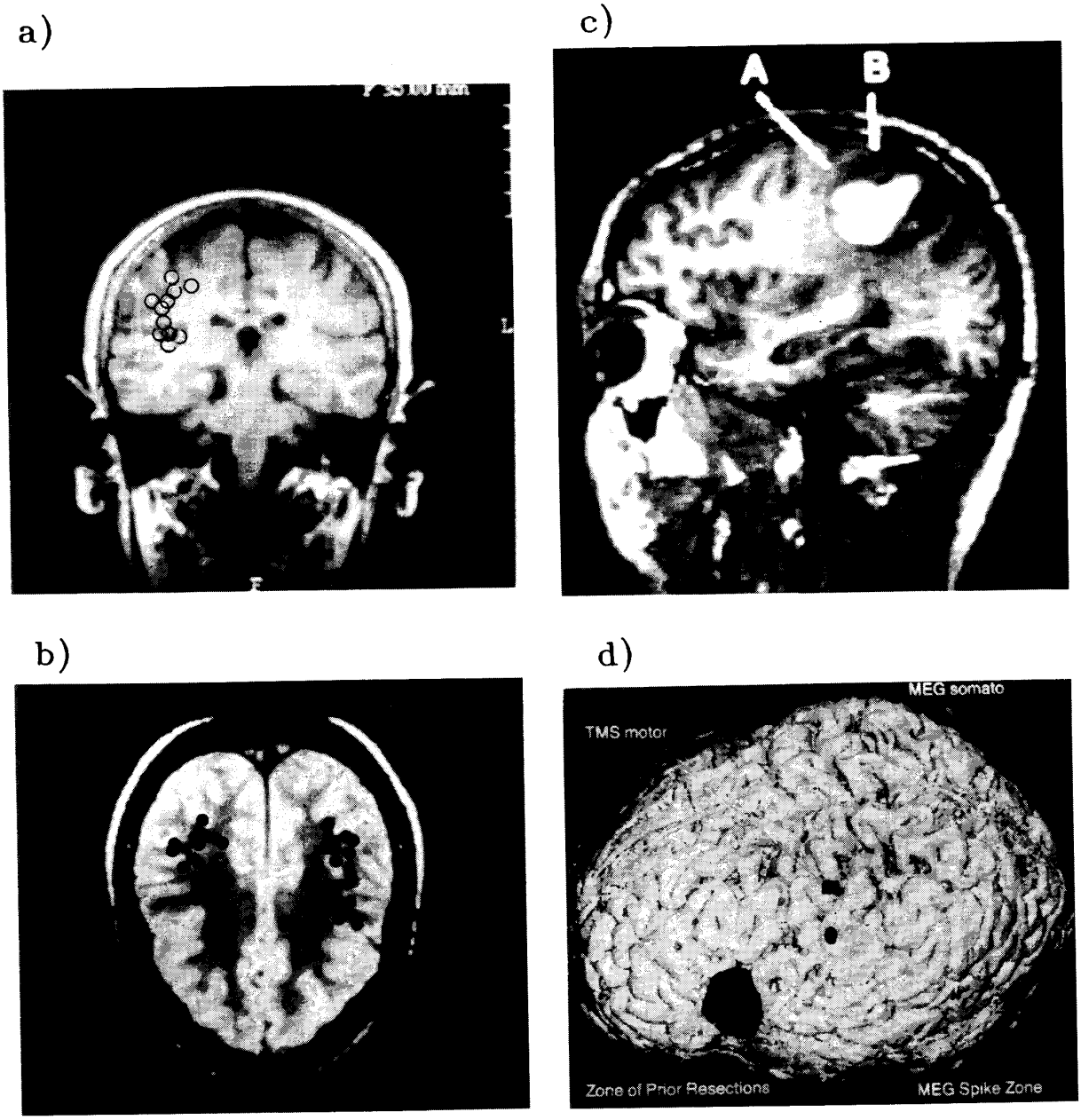

Fig. 17. Examples of the use of the MEG recorded with the BTi 37-channel Magnes^{tm} system for clinical diagnosis and treatment[60]. a) Sites of abnormal low frequency magnetic activity in a 65 year old woman with transient facial numbness and slurred speech. b) Magnetic source imaging of focal slow wave activity, indicated by the dots in one of several different slices of the MRI scan, in an 18 year old boy 3 months after a severe beating. c) Magnetic determination that the location of the central sulcus that contains the somatosensory cortex was at A and not B, thereby allowing surgical resection of the tumor. d) Magnetic determination that the source of recurring, intractable epileptic seizures was a previously-unnoticed vascular malformation far from the site of two previous resections. (Courtesy of Jeff Lewine and BTi)

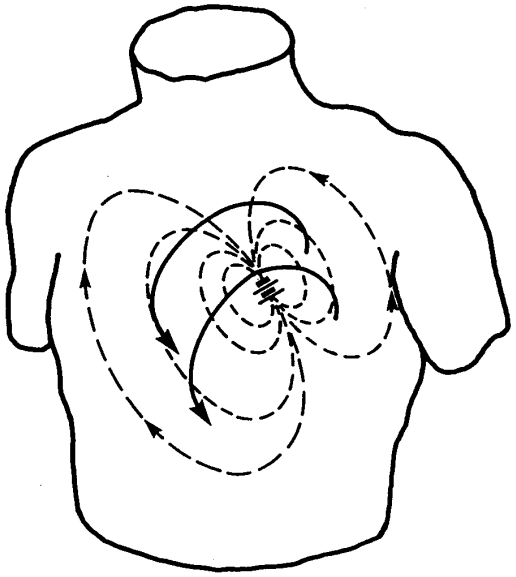

Fig. 18. The magnetic field from the heart at the time of peak signal.

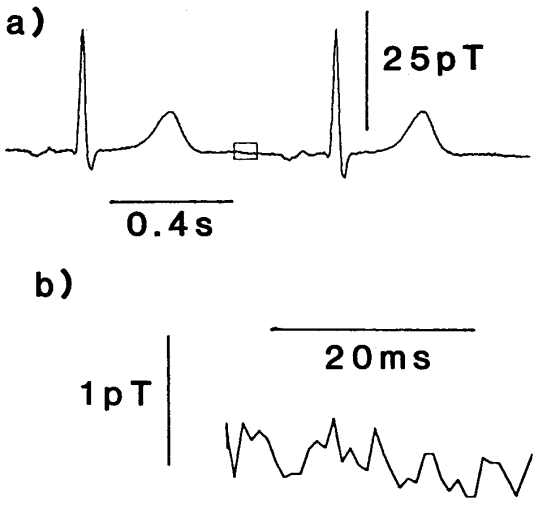

Fig. 19. Unaveraged MCGs taken with the 63-channel SQUID system in the low-noise PTB clinical lab on low-noise patients[25]. a) Two cardiac cycles showing the sharp QRS complex followed by the broader T-wave. b) An expanded view of the small box in (a) showing the noise, which is from the patient. The sampling rate was 1000 Hz with a bandwidth of 0.016 to 250 Hz. (Courtesy of Lutz Trahms of PTB)

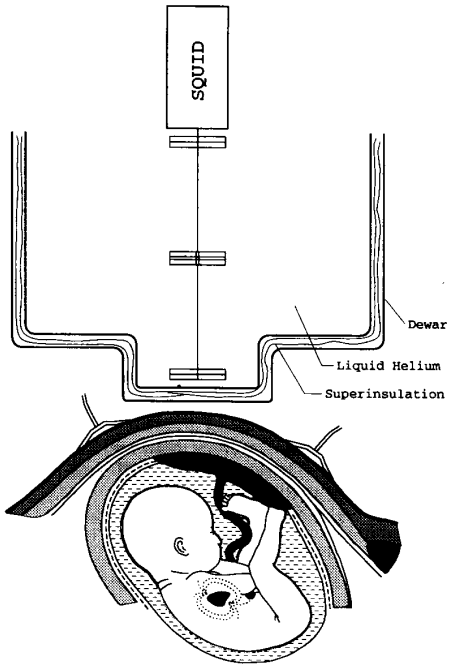

Fig. 20. A schematic view of a SQUID gradiometer positioned above the fetal heart.

netic shield but is magnetic noise from the patient. As we will show later, a filtered, high-frequency MCG has been shown to be superior to the comparable ECG measurement. Another promising application of the MCG, being pursued by Michael Lesh at the University of California in San Francisco, is to use the MCG to localize noninvasively the site of origin of cardiac arrhythmias, such as those responsible for atrial or ventricular tachycardias, in advance of a catheter ablation procedure to remove the source of the abnormal activity. Currently, the invasive catheterization procedures used to localize an arrhythmogenic focus require several hours of concentrated effort by a large staff, are costly in both personnel and supplies, are not without risk to the patient, and can result in a significant X-ray exposure to the patient and particularly the physicians. Possibly the MCG could mitigate some of these problems. One of the difficulties is that the ablation of the site of the tachycardia beat still requires invasive catheterization. Furthermore, some cardiac arrhythmias are normally silent, and can be provoked experimentally only during catheter stimulation and with the administration of drugs. Thus the as yet unanswered question is to what extent the noninvasive MCG study simplifies or shortens the catheterization procedure required for the ablation.

The SQUID magnetometers can also be used to record the fetal magnetocardiogram (F-MCG). Figure 20 shows a SQUID placed over the fetal heart. Note the substantial distance between the SQUID and the heart. Figure 21

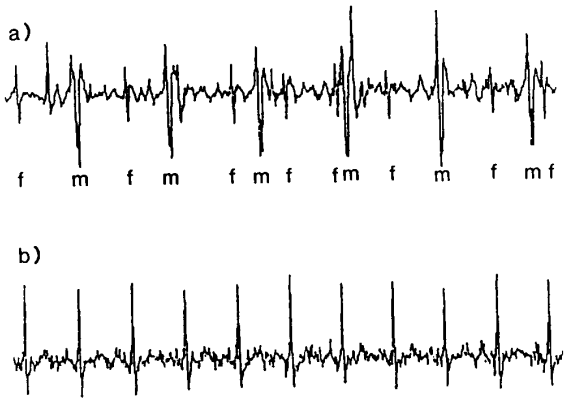

Fig. 21. The fetal electrocardiogram and magnetocardiogram. Upper: the electrical recording showing maternal (m) and fetal (f) cardiac signals. Lower: The magnetic recording showing minimal maternal contribution. (Adapted from[52])

shows F-MCG data from Ron Wakai at the University of Wisconsin in Madison, where the upper trace is the electrical recording that shows very strong maternal electrocardiogram (ECG) signals interspersed by small fetal ECG signals[52]. There are times during the gestation of the fetus where the fetal electrocardiogram signal disappears because of an insulating layer that covers the fetus. In contrast, the fetal magnetocardiogram in the lower trace shows negligible maternal contamination, and clear fetal signals can be recorded throughout the electrically silent period. The net result is that it should be possible to build compact SQUID instruments for recording the fetal magnetocardiogram in the hospital, possibly with digital SQUIDs. Because of the small size of the fetal heart and its depth below the SQUID, it is unlikely that mapping of the F-MCG over the abdomen will produce much more than a dipolar map, so that it may be sufficient to use a vector SQUID magnetometer to record three orthogonal F-MCG components[61], which could then be used to correct at least in part for the effects of the variable and often unknown fetal orientation. The challenge will be to develop sufficiently sensitive SQUIDs and suitable noise rejection algorithms so that signal-to-noise ratios are high enough that the entire P-QRS-T complex can be clearly resolved without signal averaging, which could then make the fetal MCG an invaluable tool for the diagnosis of fetal cardiac arrhythmias and overall fetal cardiovascular stress.

Another application of SQUIDs to cardiac studies, being studied by Daniel Staton and me at Vanderbilt, is the use of a high resolution SQUID to map the spread of current through thin slices of cardiac tissue, which will provide information about the electrical properties of the three-dimensional, anisotropic cable-like behavior of the heart[62]. Examples of these data will be shown later.

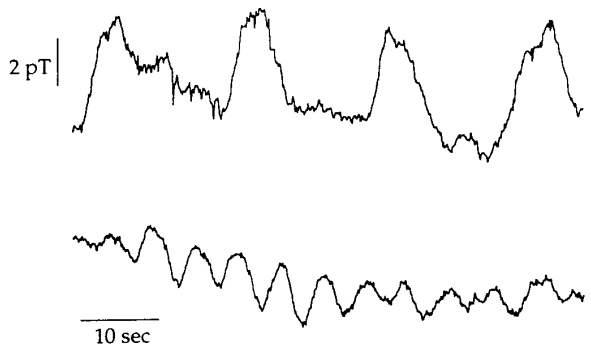

Fig. 22. The magnetogastrogram (upper) from the stomach, and the magnetoenterogram (lower) from the small intestine, recorded with a BTi SQUID system at the Scripps Institute in La Jolla. (Adapted from[63])

3) Gastroenterology: A new application of SQUIDs, being pursued by William Richards and other members of our group at Vanderbilt, is the magnetoenterogram. The electrogastrogram, the electrical signal from electrical activity in the stomach, was first recorded in the 1930's. David Cohen first recorded the magnetogastrogram, the magnetic equivalent, twenty years ago. While it is relatively easy use electrodes on the surface of the abdomen to record electrical signals from the stomach, the multiple layers of fat and muscle between the small intestine and the abdominal surface make it virtually impossible to record noninvasively the electrical activity of the small intestine. As with the brain, these intervening layers serve as a harsh, spatial low-pass filter that smears and attenuates the electric signals, but this tissue has little effect on the magnetic fields. Hence we have been able to use SQUIDs to record the magnetoenterogram, which does not have an equivalent electrical recording. Figure 22 shows typical magnetogastrogram and magnetoenterogram data[63]. Our signals, recorded for the first time in humans a year ago[64], may be of potentially great clinical significance in diagnosing electrical disorders of the intestine, such as arrhythmias, angina, ischemia, and infarct: Death often occurs within two days of an intestinal infarct. The SQUID may provide an early, noninvasive diagnosis.

IV. SQUIDS FOR NONDESTRUCTIVE TESTING

We can now switch and look at applications for SQUID NDT. As shown in Fig. 23, SQUIDs can be used in a number of different NDT modes[65]. You can look at intrinsic currents, for example in a printed or integrated circuit[66]–[69]. You can image remanent magnetization, perturbations in applied currents, or Johnson noise in metals. You can apply an ac field and image the eddy currents, or use either cyclic stress or simultaneously applied ac and dc magnetic fields and look at the hysteretic mag-

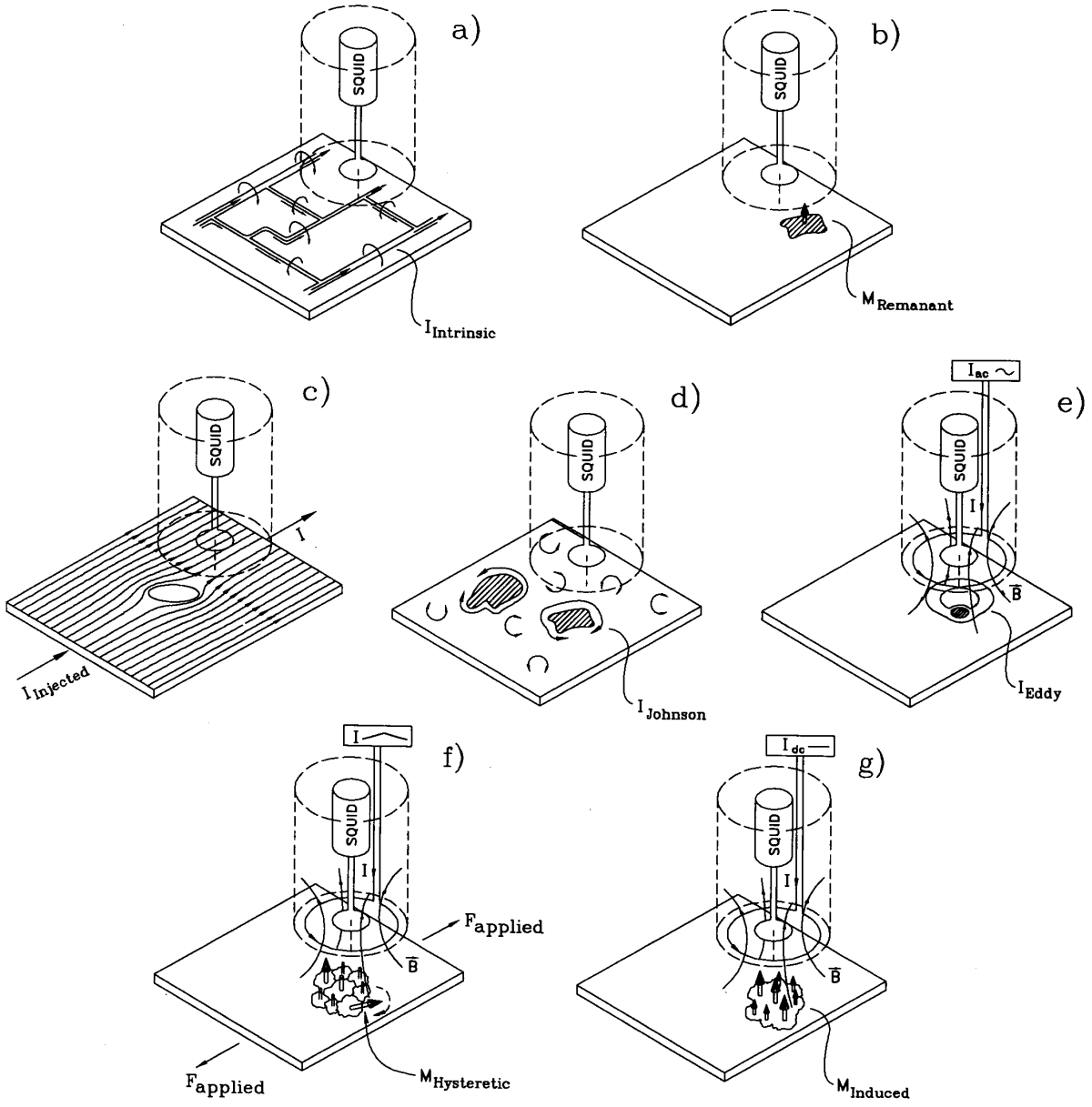

Fig. 23. Modes of SQUID NDT. By scanning the sample beneath the SQUID, it is possible to image a) intrinsic currents, b) remanent magnetization, c) flaw-induced perturbations in applied currents, d) Johnson noise in conductors, e) eddy currents and their perturbations by flaws, f) hysteretic magnetization in ferromagnetic materials in the presence of an applied stress, and g) diamagnetic and paramagnetic materials in an applied field. (From[65], with permission)

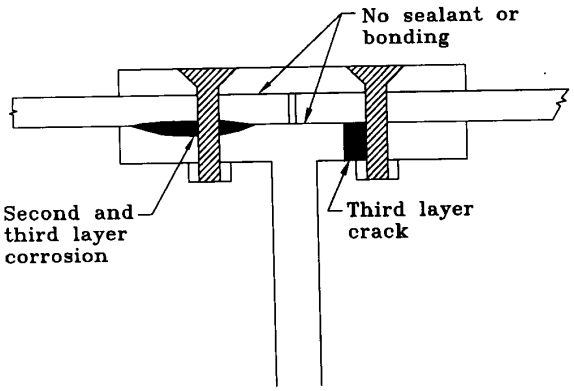

Fig. 24. A schematic representation of an aircraft lap joint that would be well suited for SQUID NDT and not suitable for ultrasonic or eddy current tests.

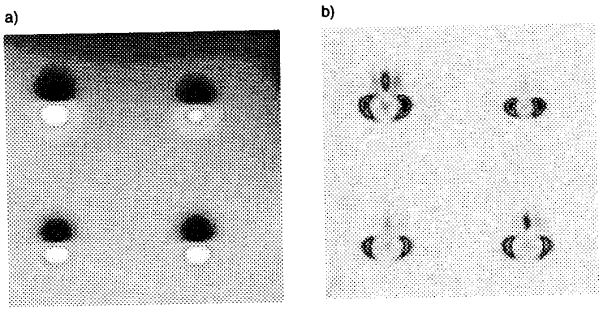

Fig. 26. An example of blind convolution for enhancing SQUID data[77]. a) The magnetic field map from the data in Fig. 25 obtained from a two-layer sample simulating an aircraft lap joint. b) The results of the blind deconvolution algorithm operating on the data in a). The signal in the upper right has no cracks, while that at the upper left has a 6 mm crack in both layers. The signal at the lower left has a crack in the upper layer alone, while that at the right has a crack in the lower layer only. (Courtesy of James Cadzow of Vanderbilt University)

netization in steel, or you can apply a dc magnetic field and image the magnetization of diamagnetic and paramagnetic materials.

A. Aircraft NDT

If you ask when one might use SQUID NDT, you quickly come upon the aging aircraft problem. Airplanes are aluminum, they corrode and crack, and they must not fail. In the typical aircraft lap joint shown in Fig. 24, there are three layers of metal. If there is no sealant or bonding between the layers, you cannot use ultrasound to find second and third layer corrosion. The metal can be sufficiently thick that, because of the skin depth of eddy currents, conventional eddy current techniques cannot find the deep flaws and the deep cracks. To give some idea of the nature of the problem, 7075-T6 is a typical aircraft aluminum. If you're trying to find a flaw that's a centimeter down through a wing structure in an airplane, you find that you need to operate at frequencies as low as 100 Hz. It's very difficult to obtain adequate sensitivity with conventional eddy current testing at 100 Hz. SQUIDs work well at 100 Hz, or 10 Hz, or even dc[70], [71].

The preliminary data obtained so far suggests that SQUID NDT may live up to its promise of great sensitivity with high spatial resolution[72]–[76], [34]. As can be seen in Fig. 25, Yu Pei Ma at Vanderbilt took a section of simulated aircraft wing that has cracks in both layers, neither layer, lower layer, upper layer, and found very clear signatures that were related to the depth and size of the crack[76]. In Fig. 25, the test sample is made of two layers of 7075-T6 aluminum panels bolted together by four 6 mm diameter aluminum flat-head pins and nuts. Each panel is 25 × 25 mm^2 and 3 mm thick. The crack defects beneath the surface are simulated by 6 mm long EDM slots beneath the fasteners. Adjacent to pin a are 6 mm slots in both the top and bottom layers. Pin b has a slot in the bottom layer and pin d has a slot in the top layer (see cross section AA′ and BB′ in (c)). Pin c is without slots and for reference only. The dashed line indicates the 150 × 150 mm^2 mapping area. A sheet inducer, which was a set of strips carrying a current of 15 mA and 1017 Hz in the x direction, was placed below the sample. The induced eddy current is disturbed by both the pin and slot. Fig. 25b shows the surface plot of the magnetic field obtained at a phase angle of 50°. The field has been squared for better visualization. The signal is largest for pin a (with slots in both layers), and smallest for pin c (without slots). In (d), the cross sections are taken from the peak of the signal. The dashed line was taken from section AA′, which shows the signal from bolt b (left) and bolt a (right). The solid line was taken from section BB′ which shows the signal from d (left) and c (right). Each signal has four peaks: the sharper peaks reflect the contribution of the current densities near the surface, while the broader peaks reflect the contribution of the current densities below the surface, as predicted by theory. The signal for bolt c, which is without the crack, shows small and symmetrical peaks. The peak signal from the bolt d, which has a top layer crack, is slightly larger than the peak signal from the bolt b, which has a second layer crack. All three signals from the bolts with cracks show the asymmetric peaks, with the larger peak on the side for which there is a crack. Figure 26 provides an example of how advanced deconvolution algorithms such as blind deconvolution[77] can enhance the image in Fig. 25.

B. NDT on Steel

Harold Weinstock has done a number of studies over the years that use SQUIDs to measure the response of ferromagnetic materials to stress[2], [78]. He has shown

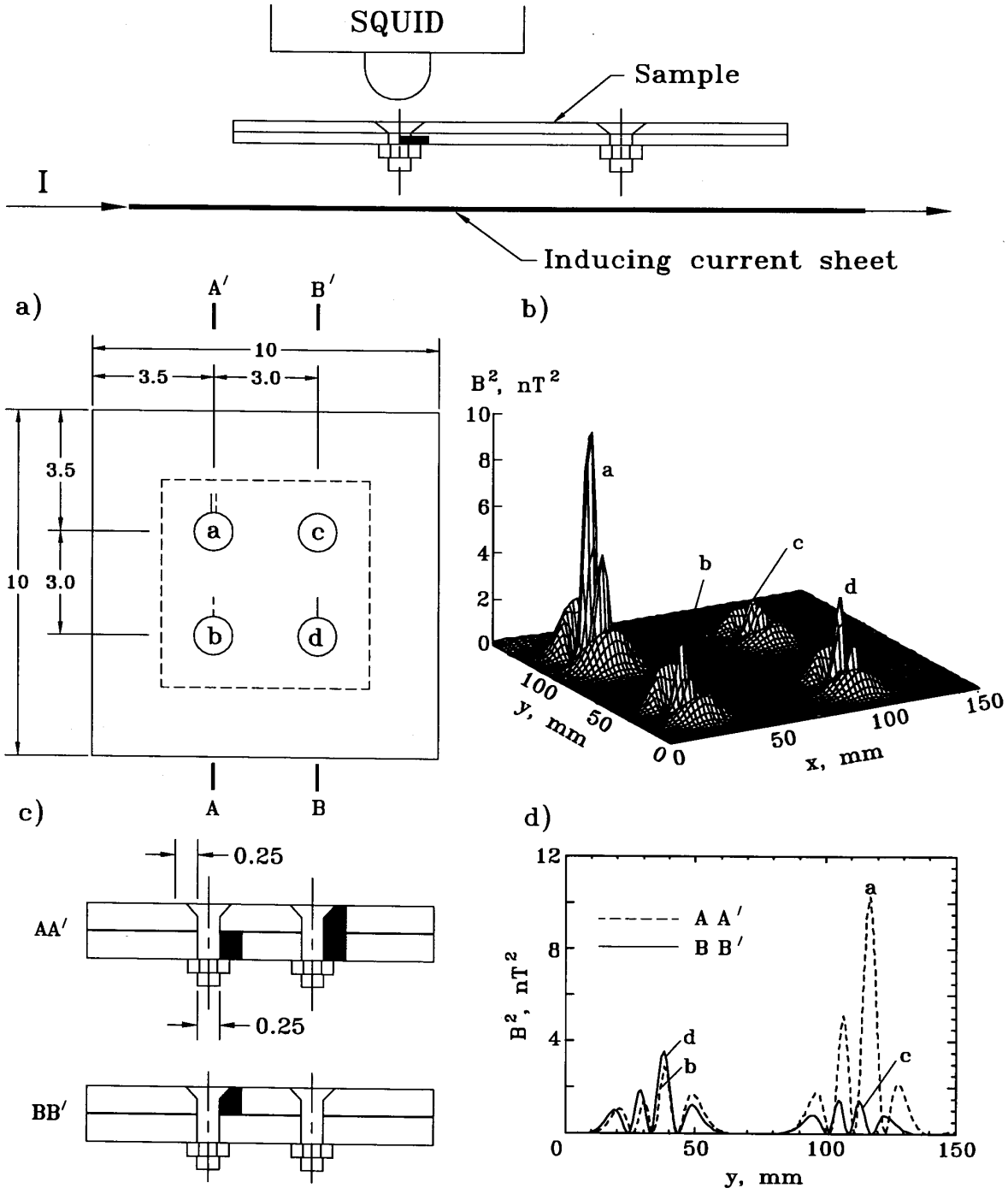

Fig. 25. SQUID Images of the cracks beneath rivets obtained at Vanderbilt with the BTi/Quantum Design MicroSQUID magnetometer and a sheet inducer. Top: the experimental setup (not to scale). a) The test sample. b) A surface plot of the data. c) A cross-section of the sample. d) Cross-sections of the data through the peaks. See text for additional details. (Adapted from[76])

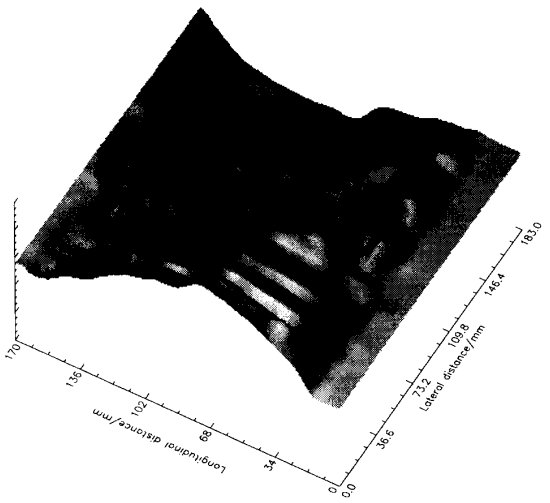

Fig. 28. Field map of a mild steel plate with heat treated regions and a manufacturing flaw. A surface plot of the static field above a sample of mild steel as rolled from the mill, without surface finishing[81]. Two spots were heated dull red with an oxyacetylene torch then allowed them to cool slowly in air. Experimental scanning stand-off was about 5 mm and the polarizing field was about 10 mT. One spot feature is larger in amplitude than the other because that spot was heated slightly more. Also visible is a linear feature along the plate which was caused by an inconsistency in manufacturing, visible on the plate surface as a series of faint bubble-like marks along the direction the plate was rolled. (Courtesy of Sandy Cochran and Luke Morgan of the University of Strathclyde)

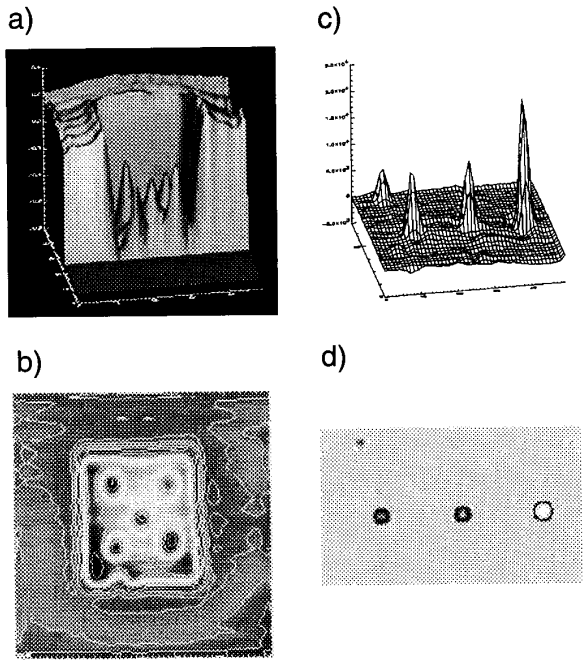

Fig. 30. Susceptibility images. (a-b) A 25.4 mm square sample of plexiglas containing five 1.8 mm diameter holes was magnetized in a 110 μT applied field and scanned at a distance of 2.0 mm. The images show the distribution of diamagnetic material (Adapted from[84]). (c-d) A nickel NDE sample containing EDM slots with dimensions of about 100 μm was surface decorated with paramagnetic microspheres. The magnetic field was mapped 2.0 mm from sample with a 174 μT applied field. The images display the location and size of surface defects, including one (upper left) that was the result of a previously undetected scratch. (Adapted from[85])

that a SQUID can remotely detect changes in the flux expelled from the sample as it is stretched multiple times, as indicated in Fig. 27. This may have applications to the nondestructive testing of steel structures.

Gordon Donaldson, Sandy Cochran and their colleagues at Strathclyde have done a great deal of work on steel plates[79], [80], [82] and have shown that they can detect flaws induced in a steel plate both thermally and in the manufacturing process, as shown in Fig. 28. They can find hidden, simulated fatigue cracks in a ship hull plate, shown in Fig. 29. In this measurement, a fatigue crack was artificially induced in a standard issue UK Admiralty steel hull plate. The crack grew from the underside in the view shown in (a), with the tip finally visible over a 137 mm length near its center. Note that crack was uneven; it developed most near the ends of the loading bar where the stresses were highest, and towards higher lateral distances because of the alignment of the three point loading machine. The eddy current map of the cracked plate in (b) was made with a induction-coil current of 5.25 mA peak to peak at 175 Hz (skin depth about 0.5 mm), giving a field of about 6 μT at the surface of the plate. The stand-off distance was 3.6 mm. A lock-in amplifier was used for demodulation of the SQUID signal. In (c), the static field map of the cracked plate was obtained with a polarizing field of 20 mT and a stand-off of 4.1 mm. For current injection into the plate, the inversion in (d) of the magnetic map of current flow around the artificially induced crack was for a 190 Hz, 1.73 A peak-to-peak current was injected diagonally across the plate between the points shown in (a); a lock-in was used for demodulation. From these preliminary data, we see that it may be possible to use SQUIDs to look deep into steel plates and find cracks that would not be readily detectable otherwise. A group at Hitachi has also used SQUIDs to study ferromagnetic materials[83].

C. NDT on Diamagnetic and Paramagnetic Materials

In a DuPont-funded project, Yu Pei Ma, Ian Thomas and I found that we can use our MicroSQUID magnetometer to image plexiglas[84], which is a diamagnetic material, as shown in Fig. 30. We found that it is also possible to image water, titanium and non-metallic composites magnetically[65]. As demonstrated in Fig. 30, we can detect minute amounts of paramagnetic tracer trapped in flaws on a surface of test blocks[85], allowing us to detect flaws with volumes as small as 2×10^{-12} m^3.

D. Corrosion Studies

In terms of basic studies on corrosion, SQUIDs are ideal because you can map dc or ac currents without having to contact the sample. Relative to the sensitivity of a SQUID, it takes a lot of electric current to dissolve an airplane - approximately 300 coulombs of charge are re-

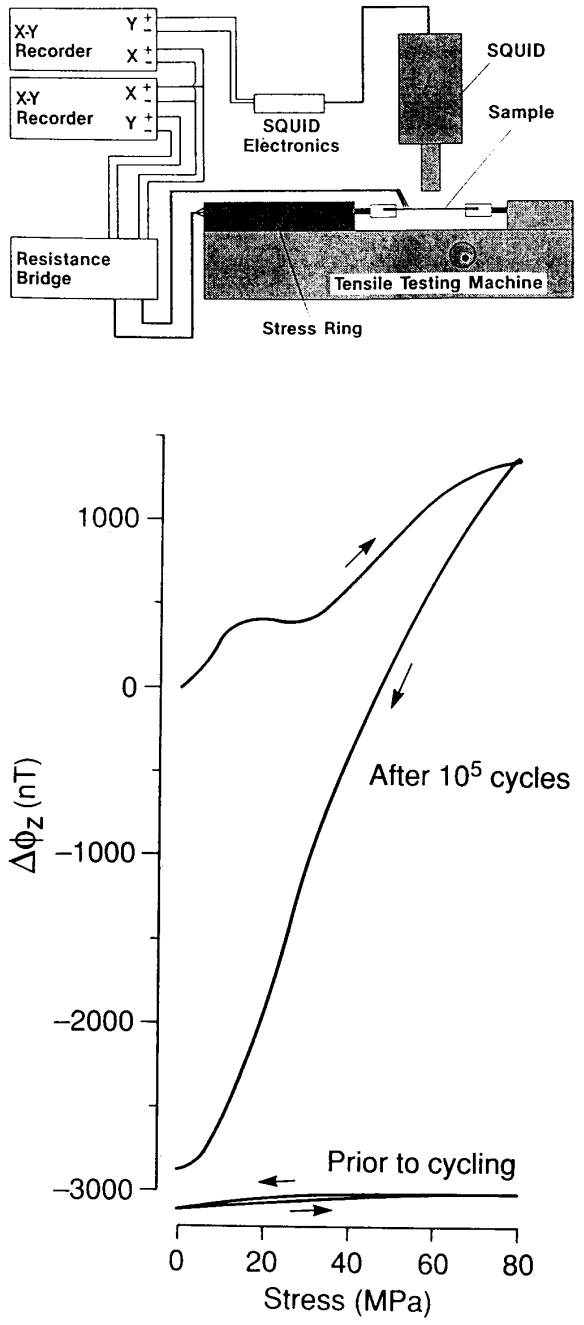

Fig. 27. The test setup (upper) and typical data (lower) from SQUID measurements on the effects of cyclic stress on the magnetic field outside of a steel sample. (From[78], with permission).

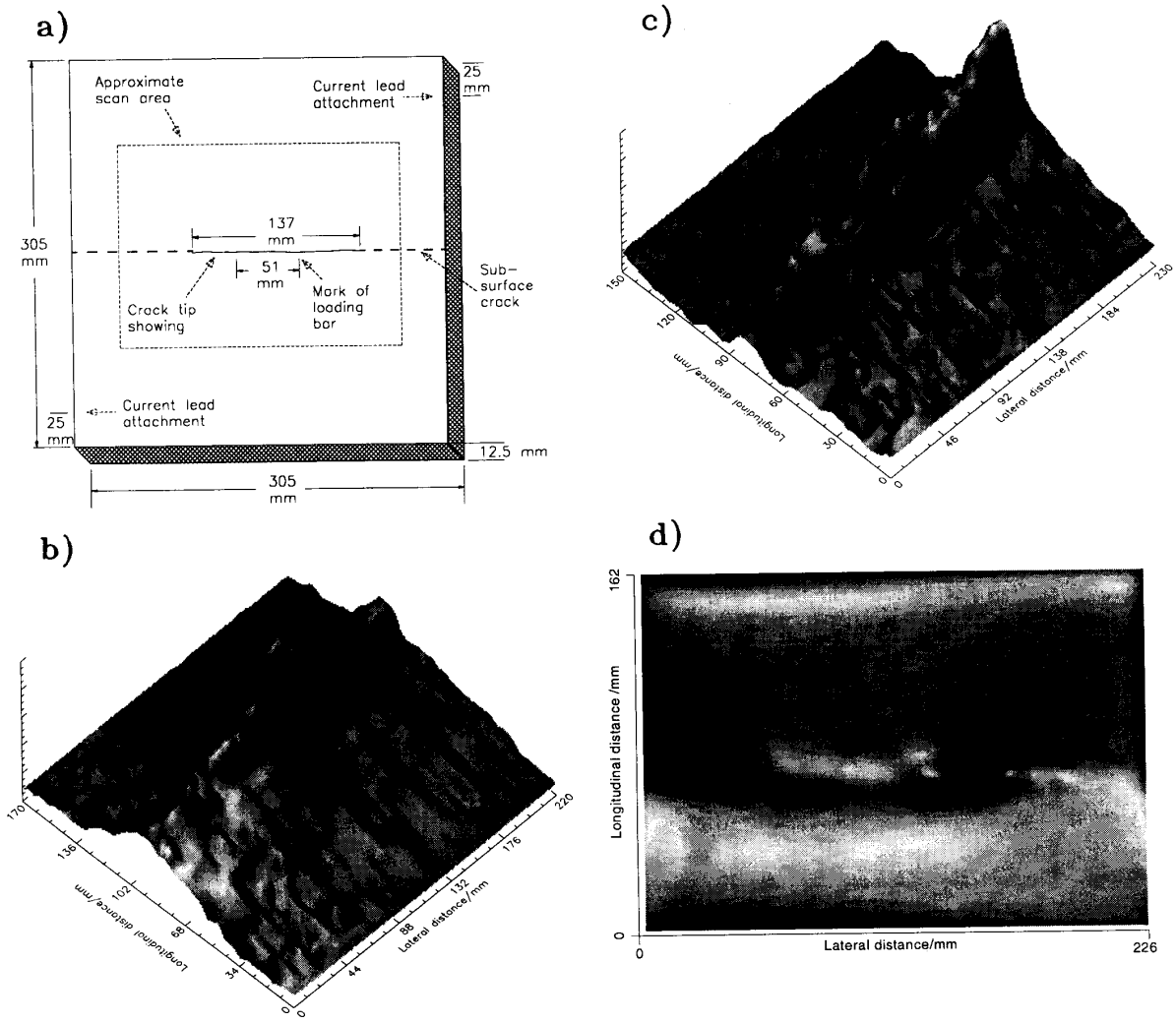

Fig. 29. SQUID measurements on an artificially cracked steel hull plate[82]. a) A fatigue crack was artificially-induced in a standard issue UK Admiralty steel hull plate. b) Eddy current map of the cracked plate. c) Static field map of the cracked plate in a 20 mT polarizing field. d) Inversion of the magnetic map of current flow around the crack. A 190 Hz, 1.73 A peak-to-peak current was injected diagonally across the plate between the points shown in (a). (Courtesy of Sandy Cochran and Luke Morgan of the University of Strathclyde)

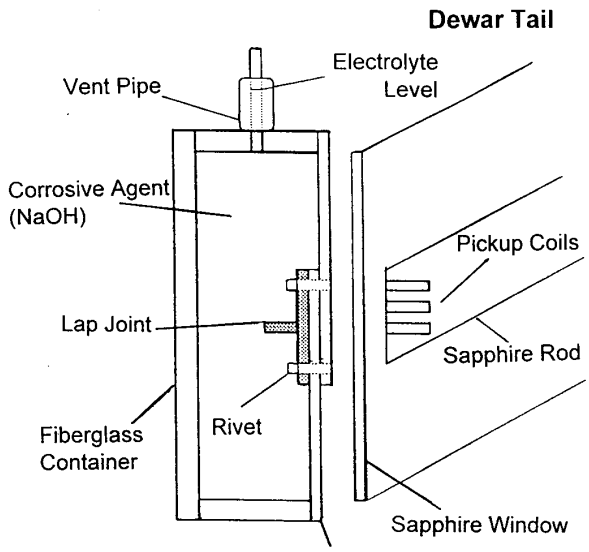

Fig. 31. Cross-section of an experimental arrangement for scanning an aircraft lap joint[33], in which a pristine lap joint was mounted on a custom-made fiberglass cell with epoxy. The cell was then filled with the corrosive agent NaOH and a spatial scan was performed using the Quantum Magnetics (QM) High Resolution Scanning Magnetometer (HRSM) shown in Fig. 8. The HRSM has five sensing coils which are clustered in a "plus" sign: three channels across and three vertical with the center common. These coils are 1.75 mm in diameter and spaced 2.5 mm apart. (Courtesy of Andy Hibbs of QM)

quired to corrode away a 0.1 mm thick layer of aluminum from a 1 cm^2 sample, which would correspond to a current of 160 nA flowing for 80 years. SQUIDs can easily detect nanoamps! Andy Hibbs at Quantum Magnetics has used their 5 channel high resolution scanning system to look at corrosion in simulated lap joints and can in fact image the distribution of currents in the lap joint as it is corroding[33], as shown in Figs. 31 and 32.

Delin Li and Yu Pei Ma at Vanderbilt have taken a plate of 7075 aluminum, placed it in salt water, scanned the magnetometer, and found substantial changes in the distribution of currents in the sample with time[86], as shown in Fig. 33. They have shown that the magnetic fields from corrosion of 7075 aluminum get stronger with time, whereas those for 2024 get weaker with time. So it is possible to monitor corrosion not only without touching but without being able to see the active corrosion in aluminum.

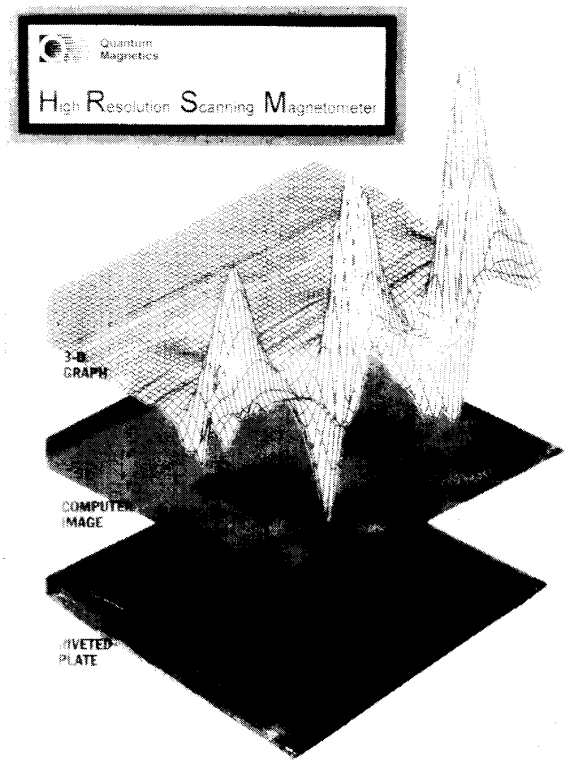

Fig. 32. The magnetic signature of a pristine lap joint during active corrosion with NaOH using the setup in Fig. 31 and one of the channels of the HRSM[33]. A strong magnetic signal was found around the rivets located in the upper portion of the lap joint, and a relatively weaker magnetic signal around the rivets located in the lower portion of the lap joint. Since the upper row of rivets were scanned before the lower row, the difference in signal strength indicates the time-varying nature of the corrosion process. It should be noted that these corrosion activities could not be visually detected from the side of the lap joint facing the HRSM pickup coils. (Courtesy of Andy Hibbs of QM)

E. Other Potential Applications for SQUID NDT

If you review the NDT literature[87], [88], you will find a number of other problem areas that may benefit from SQUIDs, but have yet to be explored in detail. There is a need to detect noninvasively the condition of reinforcing rods in airport runways, bridges and buildings. For example, currently the only accepted way to determine the

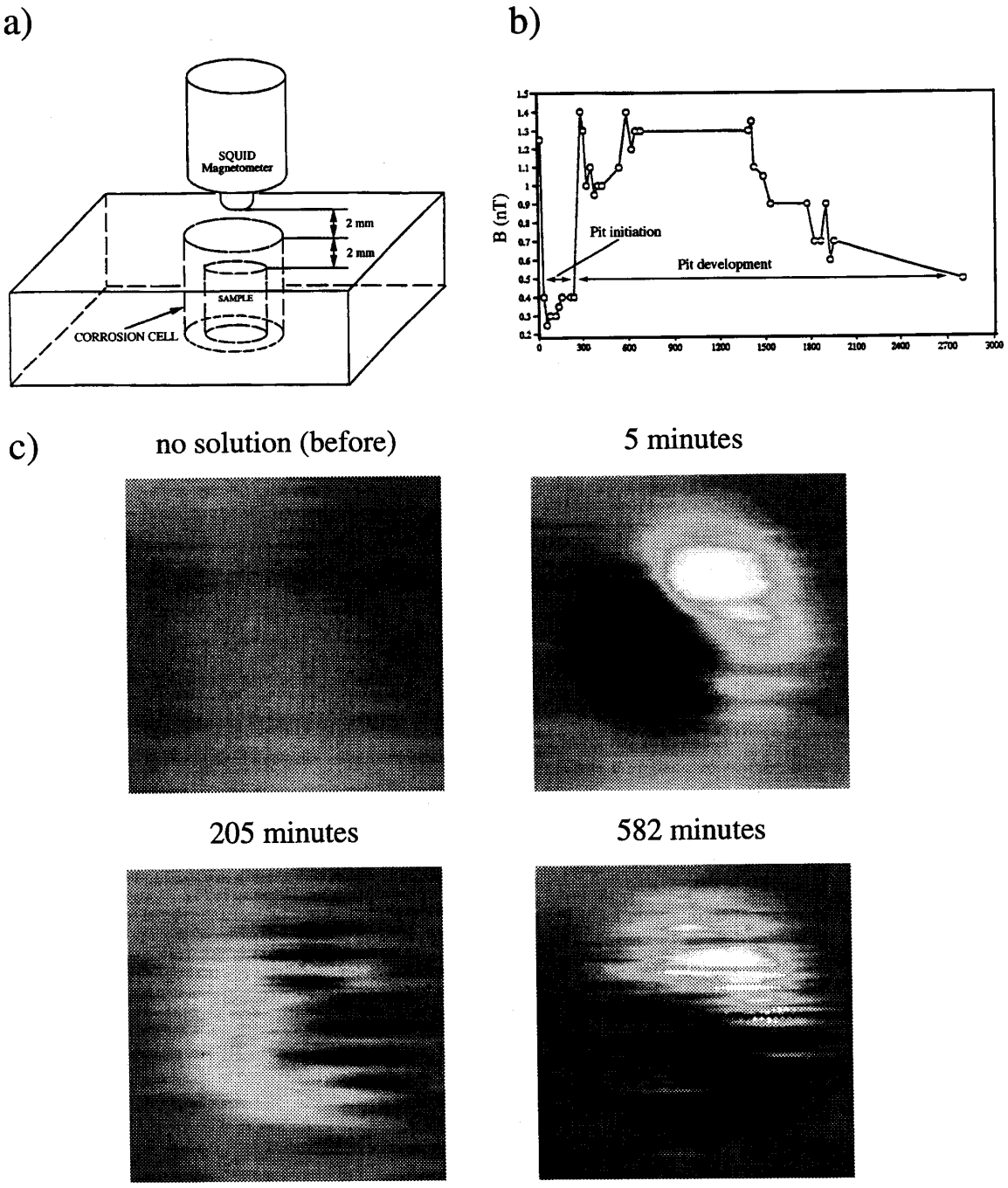

Fig. 33. Active pitting corrosion mapped with MicroSQUID[86]. (a) A schematic of the active in-situ corrosion system, with 7075 aluminum alloy in a solution of 3.5% NaCl + 5ppm Cu^{++}. (b) The maximum magnetic field as a function of time during pitting corrosion. The first 300 minutes represents pit initiation followed by an increase in magnetic field magnitude signifying the onset of the pit development phase. (c) Images of the magnetic field as a function of time. (Courtesy of Yu Pei Ma of Vanderbilt)

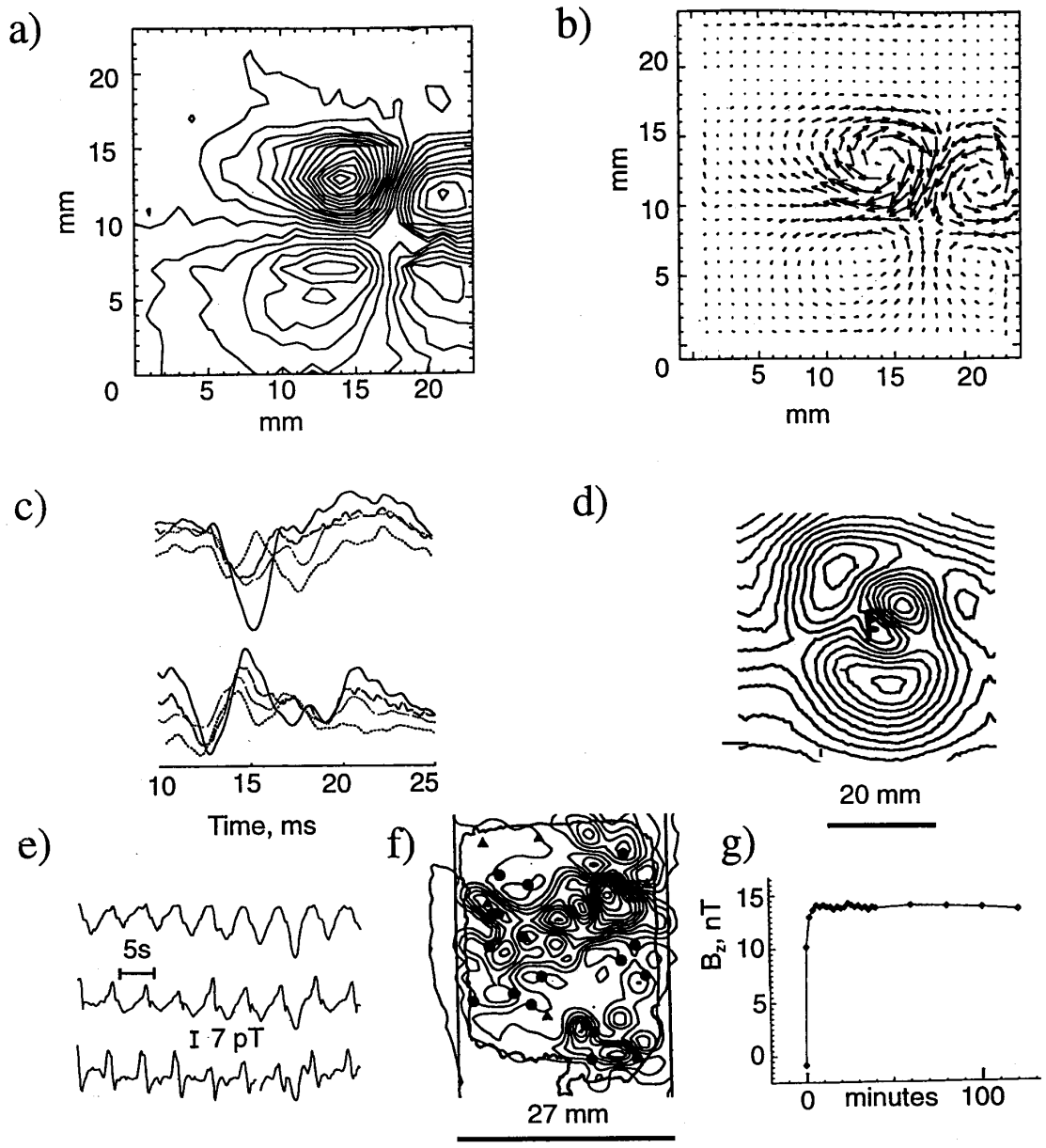

Fig. 34. Representative data from the high resolution MicroSQUID magnetometer at Vanderbilt. a) Magnetic field (25 pT contours) and b) current densities recorded 6 ms after the stimulus in a slice of canine cardiac tissue[62]. c) Simultaneous four-channel recordings of two different single motor units in the human thumb[92]. d) Magnetic field from a 94 hr chick embryo[93]. The embryo is the hook-shaped line. e) Simultaneous, three-channel recording of the magnetic field from the basic electrical rhythm of isolated prairie dog small intestine[94]. f) The induced magnetization distribution from a 50 μm thick slice of pyroclastic rock in a 285 μT applied field with the locations of the magnetic (circles) and biotite (triangles) inclusions[95] (2 mA/m contour spacing). g) The time-course of the uptake of a 900 $\mu\ell$ sample of superparamagnetic microspheres by a rat liver[96] in a 171 μT applied field. The applied field in (f) and (g) was provided by Helmholtz coils outside the cryostat.

integrity of the reinforcing rod in an aircraft runway is to core it. The steel industry has a goal of 100% inspection of all steel production. Detecting corrosion underneath the lagging in pipes is quite a challenge, particularly when the lagging is asbestos. There is concern about finding long term degradation of material in nuclear and conventional power plants. An interesting problem in nondestructive testing is to figure out how to measure the thickness of a beverage can when it's flying past at 5 meters per second, which is a rate of 2000 cans a minute. I personally think that SQUIDs will be a neat way to do it. If you're trying to do quality control on a piece of steel or a forging that is at a thousand degrees centigrade and moving past at 15 meters per second, you may need a dewar anyway to protect whatever instrument you use. You could just as well use a SQUID.

V. High Resolution SQUIDs

The need for high resolution SQUIDs became apparent to me after Dan Barth showed how SQUIDs can detect a variety of signals during epileptic seizures in rats, even though the SQUID pickup coil was larger than the brain of the rat[89]. Several years ago I started pushing for SQUIDS with 1 mm diameter pickup coils 1 mm from room temperature[90]; I've already shown you some data from our BTi/Quantum Design MicroSQUID and from the similar Quantum Magnetics system; additional biological and geophysical MicroSQUID data from Vanderbilt are shown in Fig. 34[62], [91]–[96]. The Strathclyde group has also built a high-resolution system for NDT[79].

Some of the more recent SQUID imaging work has used cold samples, where the SQUID and the sample are in the same cryogenic environment, and the dewar wall doesn't get in the way. The first pretty picture from this approach came last year from Fred Wellstood's group in Maryland, where they used a liquid-nitrogen temperature superconducting magnetometer to image the magnetic field of a portion of the face of George Washington on the dollar bill[97], as shown in Fig. 35. The dollar bill provides an ideal test sample because the ink is ferromagnetic, to the extent that it is often necessary to demagnetize the bill before imaging it. Joe Anderberg at Conductus has built a higher resolution, liquid-helium temperature instrument that can give a close-up of the pupil of the eye and the eyelid of George Washington, as shown in Fig. 36, and can image sub-micron structures with high sensitivity. Dale Van Harlingen at Illinois has used a scanning SQUID system to study vortex structure and dynamics in superconductors[98]. John Kirtley at IBM has mounted a very small SQUID on the end of a cantilever in a scanning tunneling microscope-type setup[99], shown in Fig. 37, and has demonstrated that he can image individual flux quanta trapped in the washer of a high temperature superconducting SQUID at different strengths of trapping

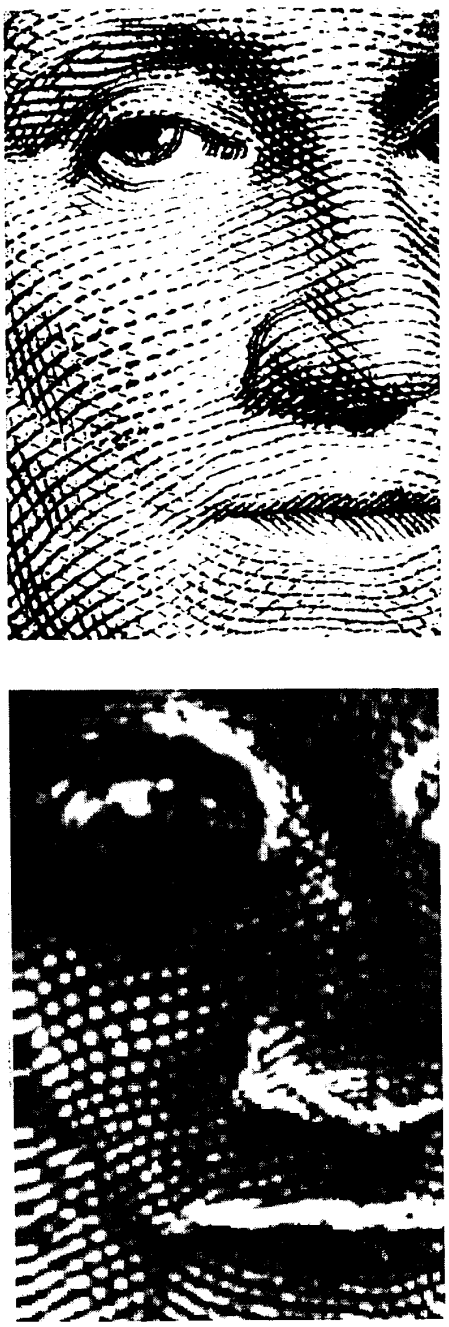

Fig. 35. A magnetic image of George Washington on the U.S. dollar bill, made with the Maryland YBCO SQUID microscope[97]. Top: The actual dollar bill. Bottom: The SQUID image. The sample and the SQUID were both immersed in liquid nitrogen. (Courtesy of Randy Black and Fred Wellstood of the University of Maryland)

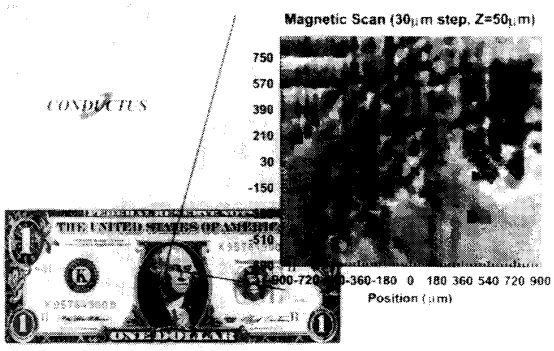

Fig. 36. A magnetic image of the ink in the region of George Washington's right eye in the U.S. dollar bill obtained with the Conductus Scanning Magnetic Microscope. The position scale in the image is in microns. The sample was in exchange gas at liquid helium temperature. (Courtesy of Joe Anderberg and Richard Kirby of Conductus)

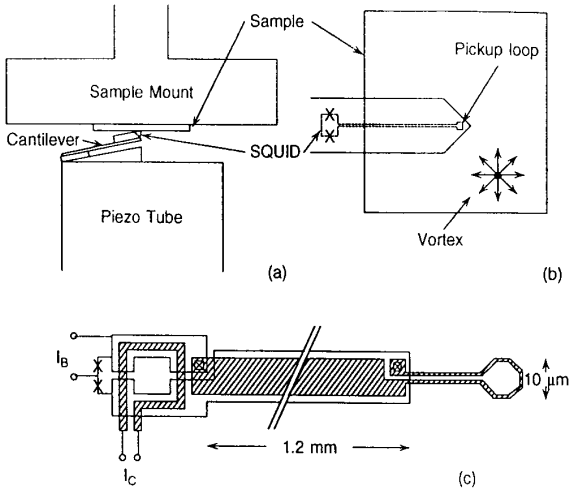

Fig. 37. A schematic of the IBM liquid-helium temperature, integrated, scanning SQUID microscope[99]. (Courtesy of John Kirtley of the IBM Thomas J. Watson Research Center)

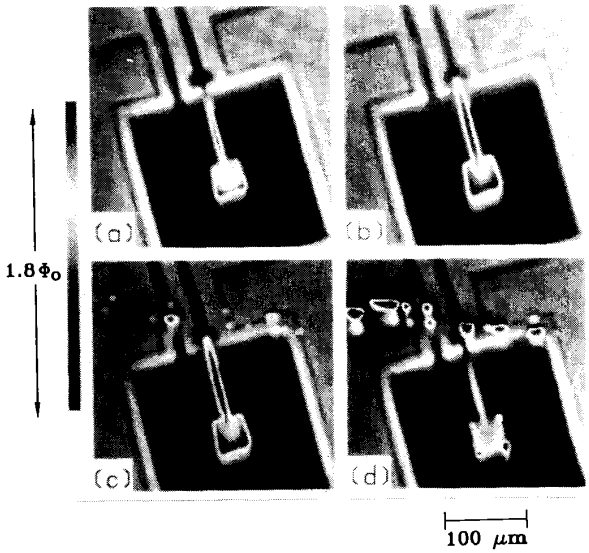

Fig. 38. Images of magnetic flux trapped in a high-T_c SQUID obtained with the IBM scanning SQUID microscope[99]. Both the scanning SQUID and the sample being examined are at 4.2 K. a) The image of the high-T_c SQUID in a 0.2 μT applied field so that the diamagnetism of the superconducting films provides sufficient contrast to visualize the SQUID structure. The black dots within the square washer are single flux quanta. b) An image after a 60 μT field was applied to the high-T_c SQUID and then removed. A flux quantum of the opposite sign to those in (a) is trapped in the upper right corner of the washer. c) After application of a 180 μT field, additional flux lines are concentrated along a scratch in the high-T_c film. d) After warming the sample to 77K and applying 240 μT field. Note the flux lines trapped in the inside corners of the hole in the washer. (Courtesy of John Kirtley of the IBM Thomas J. Watson Research Center)

fields, shown in Fig. 38. He has also used this system to demonstrate that in particular crystalline geometries, high temperature superconductors can trap half-integer flux quanta, thereby providing strong evidence for d-wave superconductivity[100].

VI. What are the key challenges for SQUID NDT?

We can now ask about the key challenges for SQUID NDT. There are a number of technical ones such as rejection of background noise that may be important. When I talk about background noise I don't mean only the temporal noise of the environment, but also the spatial noise from the airplane itself. While airplanes are usually clean and smooth on the outside, they can be highly irregular and quite dirty on the inside, as shown in Figs. 39 and 40.

If you're trying to find corrosion on the fuselage on the opposite side of a wing or fuselage panel, you have to keep track of the fact that the back of the panel may in fact be a complex extrusion (Fig. 39), or there can be all sorts

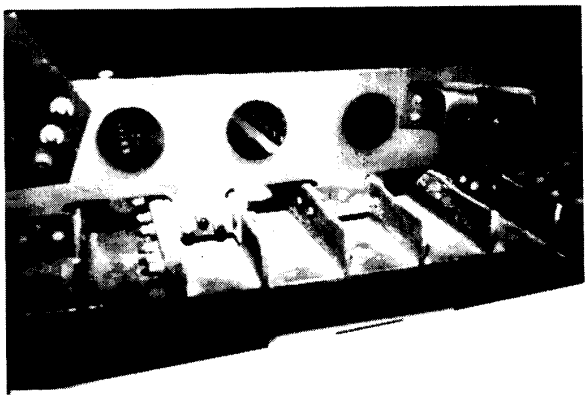

Fig. 39. A section from an airplane wing. (Courtesy of Steve Baughman of Lockheed Aeronautical Systems)

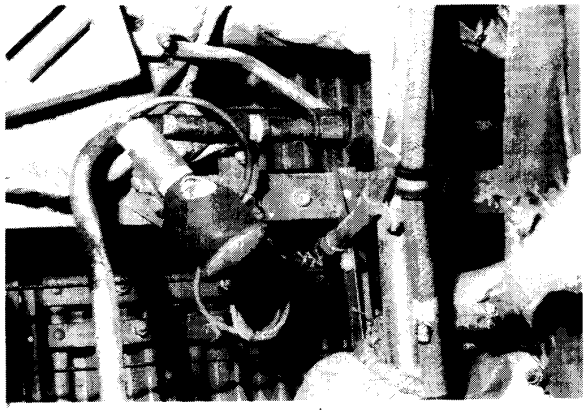

Fig. 40. The interior of an aging aircraft. (Courtesy of Richard Kinzie of Warner Robbins Air Force Base)

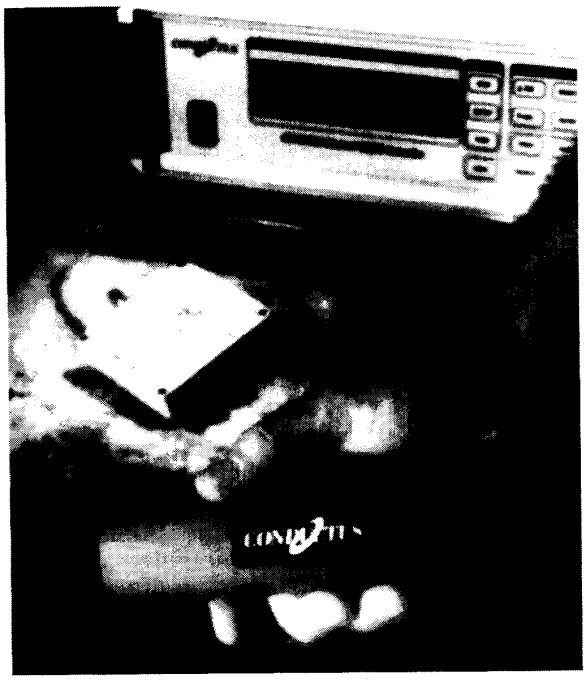

Fig. 42. A hand-sized liquid nitrogen dewar developed by Conductus that has a single high-T_c SQUID in it. It has an 8 hour hold time when vertical and a 4 hour hold time in any other orientation. (Courtesy of Conductus.)

of hardware, tubing, and wiring hidden from view but detectable by the SQUID (Fig. 40). Figure 41 provides an example of how SQUIDs can be affected by this and how properly configured gradiometers can solve it[101]; cancellation plates can be used for removing edge effects when current is injected into some conducting shapes[102].

Other technical issues include portability, refrigeration, and robustness. The Conductus hand-held high-T_c system in Fig. 42 is a step towards a compact, portable SQUID system that could be field-deployed.

There is a need for SQUID systems with more channels that have smaller and closer pickup coils and better eddy-current inducers. If high-T_c SQUIDs are to be used in NDT, it may be necessary to use high-T_c persistent current magnets, which then raises issues about flux creap and field stability. To be competitive, it will be necessary to reduce cost, since some sophisticated SQUID eddy current systems today cost over a quarter of a million dollars. The quantitative interpretation of the data will require improved mathematical models, and it will be necessary to develop specialized measurement techniques. SQUIDs for NDT must be usable on the flight line or a busy bridge! I expect that the various technical problems, including the issue of background noise, are all going to be solved. The key challenge in my mind is to identify suitable problems for which SQUIDs are the best solution. The trick is to use this technique to find flaws that

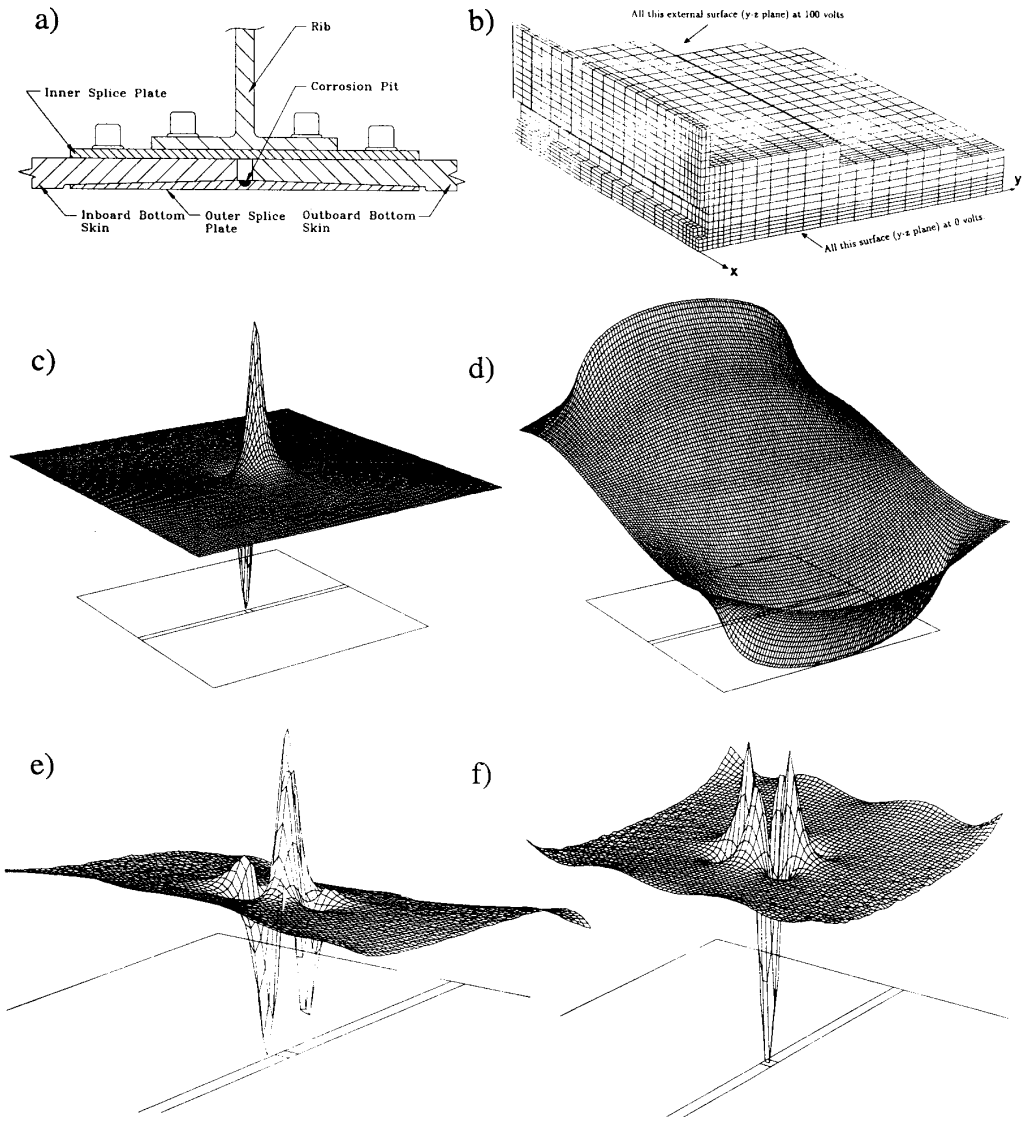

Fig. 41. Simulations of the magnetic signature of a small region of hidden corrosion in an F-15 lower wing splice. a) Schematic cross-section of the splice. b) The finite element mesh describing one-quarter of a section of wing splice. A uniform current is applied parallel to the x-axis. c) The magnetic signature of the flaw alone. d) The magnetic field from the wing structure and the flaw. The peak-to-peak signal arising from the edges of the various plates in the splice is 400 times larger that of the flaw. e) and f) The simulated output of a SQUID gradiometer configured to reject large-scale spatial variations such as from the wing structure and selectively detect fields from localized flaws. (Adapted from[101])

no one else can find and, most importantly, do so in ways that the NDT user community likes.

VII. What is the competition?

In order to assess how difficult the problems are, we need to look at the competition. There are two kinds of competition: within the SQUID industry and between various technologies. Table I lists a number of different companies who are competing within the SQUID industry. We've talked about a lot of them so far. It is important to realize that not all of them will stay in the game. Siemens has decided to drop out of the biomagnetic SQUID business. Experience shows that while small SQUID companies have come and gone over the past 25 years, conservation laws seem to apply to the most highly skilled personnel. However, whether or not the SQUID industry will become large may be determined by the competition with other technologies.

Table I. The competitors within the SQUID industry

Biomagnetic Technologies (Bio*)
Conductus (Lab, NDT, Bio)
Cryoton (Bio, NDT)
CTF Systems/Osaka Gas (Bio, Geo)
General Electric/Mediterranean Quantum Systems (Bio)
Hypres (Digital SQUIDs)
Neuromag/Instrumentarium/Picker (Bio)
Philips (Bio)
Quantum Magnetics (Lab, NDT, SQUIDs)
Siemens (Bio)
SQM Technology (NDT)
Superconducting Sensor Laboratory/MITI (Bio)
2-G Associates (Geo, Lab)
Research laboratories: CNR, IBM, KFA, PTB...
Universities: Berkeley, Helsinki, Illinois, Jena, Maryland, New Mexico, New York, Open, Pontificia Universidade Catolica do Rio de Janeiro, Strathclyde, Twente, Vanderbilt, Wisconsin...

*Bio=Biomagnetism Lab=Laboratory systems
Geo=Geophysics NDT=Non-destructive testing

A. What technologies compete with biomagnetism?

There are a number of technologies that compete with biomagnetism: Electrical measurements such as the electrocardiogram, the electromyogram, the electroencephalogram, the electrogastrogram, and the electroneurogram all compete. Bill Richards and I at Vanderbilt are fascinated by the fact that there is no reliable electroenterogram in normal subjects - just the magnetoenterogram, which is possibly the only electrophysiological signal in biomagnetism without an electrical counterpart. It is also

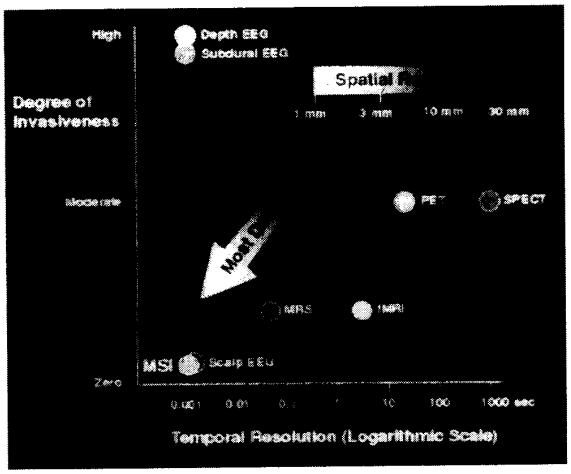

Fig. 43. A comparison of the spatial and temporal resolution and invasiveness of various "windows on the mind." The MEG is shown as MSI (Magnetic Source Imaging). (Courtesy of BTi)

important to realize that for many people, particularly surgeons, invasive surgery is a technology that competes effectively with noninvasive diagnosis. The most serious competition, because of the expense of the systems and their already-widespread acceptance, comes from the clinical imaging techniques such as computerized tomography (CT), magnetic resonance imaging (MRI), positron emission tomography (PET), single photon emission computed tomography (SPECT), magnetic resonance spectroscopy (MRS), and functional magnetic resonance imaging (F-MRI).

These classical imaging techniques and the EEG and MEG all provide "windows on the mind." They have different characteristics, and hence are difficult to compare. Figure 43 shows that the relevant phase space has at least three dimensions. There is the degree of invasiveness: depth electrodes implanted into the brain or subdural electrodes placed on the exposed cortex are highly invasive. Various techniques have different time resolution: single photon emission computed tomography has terrible time resolution. If you look at the combination of spatial resolution, temporal resolution and noninvasiveness, magnetic source imaging and the scalp EEG are the best possible techniques, but they only detect electrical activity and do not provide anatomical images. As discussed in a recent review[103], the EEG and the MEG will always be able to provide electrophysiological information not available from the other imaging techniques.

Now we need to turn to a long-standing controversy about the relationship between bioelectric and biomagnetic recordings and their relative information content[104], [105]. Human studies involving the statistical comparison of the ability of the ECG and MCG to detect cardiac abnormalities suggest that the MCG contains

diagnostic information that is complementary to that in the ECG[106]–[109]. Because electrodes are not required, the MCG is vastly superior to the ECG for measurements of the steady currents of injury that are associated with myocardial ischemia[110]. Animal studies and theoretical calculations in our lab suggest that magnetic recordings can provide new information about the electrical anisotropy of cardiac tissue[62], [111], [112]. The arrhythmia localization studies discussed previously are possible because the magnetic fields outside the body are less affected by internal electrical inhomogeneities than are the surface electric fields. If one wanted to screen any reasonable fraction of the population of an entire country for cardiac disorders, it would probably be easier to do this magnetically than electrically, since it would not be necessary to apply electrodes, and there would be no risk of getting the wrong wire attached to an electrode. Whether these differences are sufficient to justify the widespread acceptance of the MCG is as yet unknown. Until low-cost, hand-held, mechanically refrigerated SQUIDs are created that can record high quality MCGs in an unshielded hospital environment, MCG studies will probably be used only in tertiary care settings such as university hospitals. This could of course change quickly, if, for example, the fetal MCG proves to be an important clinical tool.

From the point of scientific and commercial competition, the EEG and the MEG represent significant mutual competition. Historically, the EEG has been used by clinicians who examined 10 or 20 channels of recordings on a strip chart recorder with little if any signal processing, enhanced visualization, or inverse solutions. Cognitive psychologists learned a great deal about brain processes by careful examination of the time course of signals from selected electrodes. The magnetoencephalogram was developed largely by physicists, who were skilled in the modeling of electromagnetic fields and were not subject to the historical biases intrinsic to the EEG. The MEG proved conducive to quantitative analysis, advanced signal processing, and computer visualization. The physicists building the instruments established collaborations with psychologists, physiologists, and physicians, so that the MEG was used to make previously impossible non-invasive measurements, for example the tonotopic mapping of the auditory and visual cortex[36], [37] and noninvasive measurements of the steady currents associated with epilepsy[89] and migraine headaches[113].

The issue then reduces to which of the two techniques, MEG or EEG, should be used, or both. Electroencephalography is clearly a cheaper, simpler technology. It has tiny electrodes and simple differential amplifiers, rather than SQUIDs with feedback circuits, lock-in amplifiers, liquid helium and magnetic shields. But the EEG has not done all that well as a cutting-edge clinical tool. A very small community of electroencephalographers, most notably Alan Gevins of the EEG Systems Laboratory in

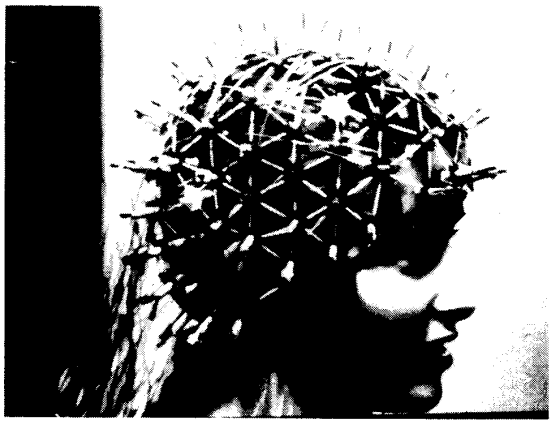

Fig. 44. A 128-channel geodesic net for EEG[114]. (Courtesy of Don Tucker of the University of Oregon)

San Francisco, began independently of the MEG to develop much improved hardware and software for the EEG. Some of the difficulties normally associated with the application of numerous electrodes to the scalp are being addressed with the development of high impedance electrode caps, such as the 128-channel geodesic net in Fig. 44 built by Don Tucker at the University of Oregon[114]. Gevins has developed a 128 channel cap and amplifier system that uses a lap top computer for signal processing[115]. Figure 45 shows his comparison of a conventional, 18-channel EEG with a 128-channel high-resolution EEG[116]. The high electrode densities make it possible to perform sophisticated signal processing such as the surface Laplacian and inward continuation of the electric potentials to the cortex.

With the exception of dc-coupled measurements, the MEG detects the same sources as the EEG, and there is no real issue about fundamental differences in information content (slowly varying electrode and skin potentials generally preclude dc-coupled electrical recordings). However, the EEG and MEG have differing spatial sensitivities, as shown in Fig. 46, which can work to the advantage of one technique or the other, depending upon the location, depth and orientation of the particular source being studied. As the most fundamental difference, the EEG can detect radial dipoles in a perfectly spherical brain whereas the MEG can only detect tangential dipoles, but heads are rarely perfectly spherical. Some people think this radial/tangential difference is an advantage for the MEG, while others view it as a disadvantage; the two techniques together may be much better than either used alone.

From the perspective of the inverse problem of computing cortical sources from measurements of scalp potentials or fields, the EEG has a severe problem with its sensitivity to the differences in the conductivities of the scalp, skull and brain, which work in concert to produce a low-pass filter that causes the scalp potentials to be a highly

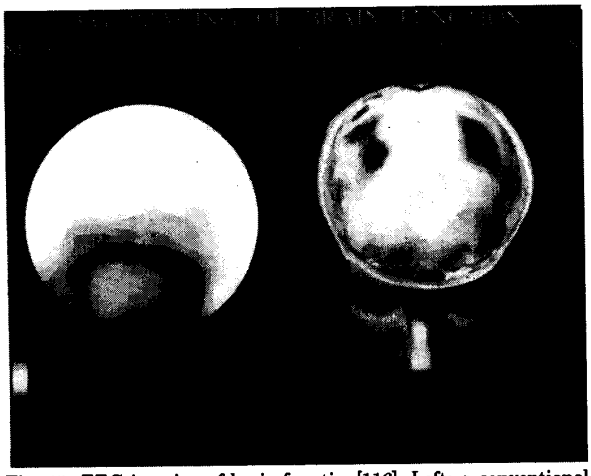

Fig. 45. EEG imaging of brain function[116]. Left: a conventional, two-dimensional, 18-channel topographic map evoked by repetitive electrical stimulation of the left middle and right index finger. As brain electrical activity is conducted through the skull, important spatial details become distorted, to the extent that there is no useful localizing information. Right: A three-dimensional, 122-channel high-resolution topographic map of neural potentials evoked by the same stimuli. The scalp EEG data has been mathematically deblurred and projected down to the surface of the subject's brain and combined with 3-D structural images of the brain from magnetic resonance images. The image shows that the left and right somatosensory cerebral cortical areas, corresponding to the right and left hand fingers, have been activated. (Courtesy of Alan Gevins of the EEG Systems Laboratory)

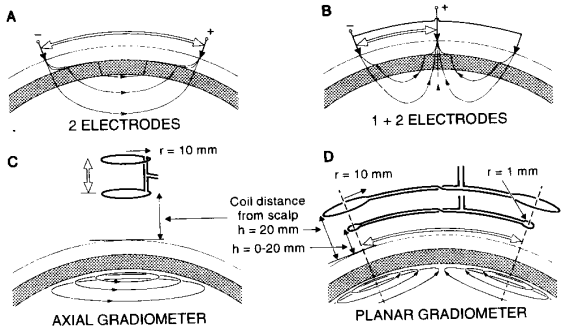

Fig. 46. The lead-field lines for EEG electrodes and MEG gradiometers[118]. The direction of the lines shows the direction of dipole sources to which the detector is sensitive, and the spacing of the lines is proportional to the sensitivity. (Courtesy of Jaakko Malmivuo of the Ragnar Granit Institute of the Tampere University of Technology)

blurred and distorted representation of the cortical potentials. While it has been shown that the EEG can be used to localize dipolar sources, the EEG studies of localization accuracy have in general not been as rigorous as those for the MEG. (It is important to distinguish between imaging and localizing resolution[117]; while localizing resolution for the EEG and MEG may be a few millimeters for least-squares fits to multiple measurements, imaging resolution may be several centimeters and is determined primarily by source-to-detector spacing and noise.) Simultaneous EEG and MEG localization studies with state-of-the-art electrode arrays and SQUID helmets are needed and should be forthcoming. My personal view is that MEG localization will inherently be more accurate than EEG localization, primarily because I believe that uncertainties in the scalp and skull conductivities, variations in the locations of the sensors, and the ill-conditioned nature of the inverse problem will limit the EEG more than the MEG.

At present, the MEG seems easier to use and mathematically more robust than the EEG with a comparable number of channels. As multichannel SQUID helmets become less expensive and more readily available, the price differential between the EEG and MEG may become less important. At some point, the cost of the computer and the programmers who develop the software, and the elapsed time expended by the medical technicians who perform the studies and the physicians who interpret the data will set the effective price of an EEG or MEG procedure, rather than the amortized cost of the actual sensors. For now, there seems to be greater clinical and research interest in MEG systems, and the concomitant financial commitment, than in advanced EEG systems. The recent introduction of numerous helmet MEG systems worldwide may provide sufficient clinical evidence of the utility of the MEG that the EEG might not be able to catch up, even if the recent solutions to its technical limitations are widely adopted. In any event, it may be wisest to use the EEG and MEG simultaneously while remembering that these two techniques are the only windows on the mind with adequate bandwidth to record the detailed electrical activity of the brain[103], [119].

B. Is biomagnetism worth pursuing?

Based on studies such as those presented in this brief overview, I believe that we can answer the question "Is biomagnetism worth pursing?" with a definitive "Yes". Clinical measurements with SQUIDs are often easier than the corresponding electric measurements, in part because there is no need to attach electrodes. As SQUID systems are built with more and more channels, the data is getting more and more useful. The cost of competing technologies can be considerable: positron emission tomography requires a cyclotron and a radiopharmacy!

Obviously, the majority of the clinical applications of SQUIDs discussed so far require a capital investment of

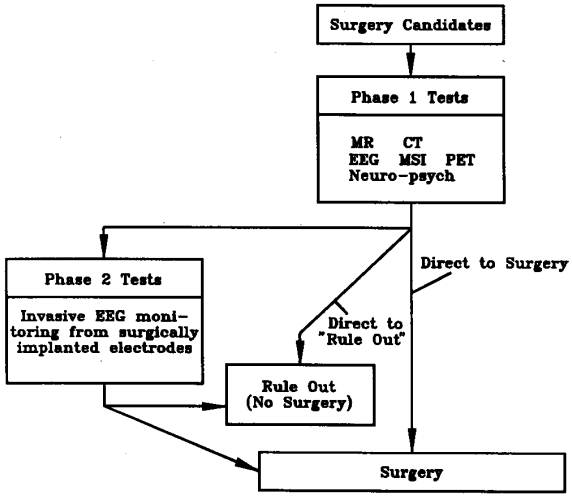

Fig. 47. A decision tree that would be followed during diagnostic tests prior to making a decision for surgery to treat epilepsy. Noninvasive Magnetic Source Imaging (MSI) studies with the MEG may be able to eliminate costly, invasive Phase 2 tests. (Adapted from a drawing by BTi)

one million dollars or more. With this in mind, the goal that has been pursued most aggressively is to use clinical magnetometry to replace costly, invasive procedures with cheaper noninvasive ones. For example, an intraoperative study to map epileptic activity prior to surgery might cost as much as $50,000; an MEG study that could provide much of the same information might cost one tenth of that. Figure 47 shows how Magnetic Source Imaging (MSI) with the MEG might fit into a decision tree that is followed prior to epilepsy surgery. If in fact an MSI study can support a decision to go directly to surgery or rule out the possibility of surgery without the invasive and expensive cortical or depth-electrode monitoring, there can in fact be a substantial cost saving. In balance, one of the difficulties with the commercialization of the MEG is that there is not a gigantic volume of epilepsy surgery cases, approximately 1,500 during 1991 in the United States[120], and now estimated at several thousand annually worldwide and growing rapidly[121].

C. What technologies compete with SQUID NDT?

In terms of SQUID NDT, there are almost innumerable techniques that can compete, including eddy current, magnetic particle inspection, acoustic emission, magneto-optical inspection, x-ray, ultrasound, thermal imaging, Barkhausen noise, optical/laser interferometry, and neutron radiography, just to name a few. If you're trying to find a crack in a bolt hole in an aircraft engine being serviced in a maintenance hangar, you may decide to use a rotating eddy current probe rather than a SQUID. Neither an aircraft maintenance hanger nor a completely assembled jet engine are magnetically friendly, and eddy current probes are small, portable, hand held, and relatively cheap.

Fig. 48. The PRI magneto-optical inspection (MOI) system being used to find fatigue cracks in an airplane fuselage. (Courtesy of Gerald Fitzpatrick of PRI)

Probably the strongest competition for SQUIDs in aircraft NDT is a technique termed magneto-optical inspection (MOI) developed by Physical Research, Inc. (PRI)[122]. It is a video imaging technique that uses a magneto-optic crystal and polarized light to obtain magnetic images of cracks and flaws. A sheet inducer produces planar eddy currents in the test object and thereby eliminates much of the extreme sensitivity to separation between the eddy current probe and the sample, termed liftoff, that plagues conventional eddy current measurements. The MOI is being accepted by an increasing number of aircraft manufacturers, airlines, and aircraft maintenance organizations. The unit in Fig. 48 costs approximately $30,000, which is not that different from what a few channel SQUID might cost in a year or two. The MOI has three major problems: It has limited sensitivity; because it uses a hysteretic magneto-optical crystal as an integrating, imaging memory, it provides no phase information; and as a result it has some difficulty in detecting cracks or corrosion in the second and third layers of an airplane. While SQUIDs may eliminate some of these problems, it is important for us to keep in mind that this is what the successful competition looks like and how it needs to be used and work. I believe that SQUID NDT can give MOI a run for its money, but only if SQUIDs are used cleverly.

VIII. The Market

A. The Biomedical Market

Eighty-nine million Americans suffer neurological impairments. Each year, in excess of 289 billion dollars is spent in the United States on the diagnosis and treat-

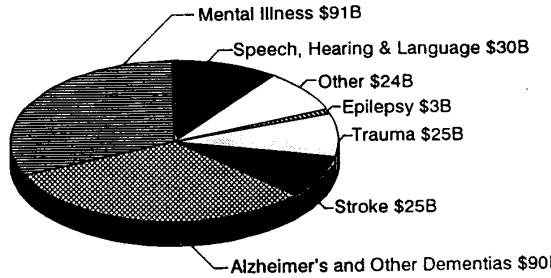

Fig. 49. The annual costs of functional disorders of the brain for the United States. (Adapted from a graph from BTi, which was based upon data from the NIH, the Office of Science and Technology Policy, and the American Psychiatric Association)

ment of these patients, divided as shown in Fig. 49. There is a tremendous need for the development of new, cost-effective diagnostic procedures and treatments, and hence the market opportunity for biomagnetism may be excellent if it can be shown to aid substantively in the diagnosis or treatment of one or more of these disorders. It is important to realize that much of the academic work worldwide in biomagnetism has concentrated on epilepsy and on cognitive science, and to a lesser extent on stroke and trauma. The other areas in the chart are only now being explored; cardiac, fetal, or intestinal applications may provide an additional market.

The rate of growth of the biomagnetism market will in part be determined by its successes. The difficulty is that while the cost per SQUID channel is dropping, users are demanding more and more channels. The system costs must come down, particularly in light of concerns regarding the high cost of medicine. But as we have stated already, SQUIDs offer the potential of replacing even more expensive alternatives. The total worldwide sales for CT and MRI systems was almost 20 billion dollars in 1991, and somewhat less more recently; while SQUIDs are unlikely to approach this scale of market, there is clearly plenty of room for growth.

B. The NDT Market

The NDT market is a bit more complicated, and I want to go into it in a little greater depth to give you some idea of the size of the numbers and the problems. It is clearly recognized that existing NDT techniques for aircraft are inadequate. Certain critical flaws cannot be found before they have grown unacceptably large, and existing techniques are labor intensive and prone to operator fatigue and error. In the most extreme cases, the first demonstration of a flaw is when the technician sticks a finger through the wing or fuselage of the airplane. That is not satisfactory. The United States Air Force spends between 700 million and one billion dollars annually on corrosion[123]; the amount for inspection and maintenance of structural fatigue damage is also significant. The entire U.S. Department of Defense spends an estimated 4.3 billion dollars a year on corrosion[124]. Some of that is for detection of corrosion damage, but much is for repair and prevention. The civilian aircraft market is equally interesting: as of 1990, there were 806 DC-8 and DC-9 aircraft[125] and 1200 Boeing aircraft[126] that were beyond their 20-year design lifetime. The age of these aircraft and the discovery of classes of structural flaws that were not included in the original design has led the FAA to issue multiple airworthiness directives that specify the nondestructive evaluation of literally millions of individual fasteners each year[127], and the FAA has not yet fully addressed the issue of nondestructive testing and airworthiness of commuter aircraft. The capabilities of SQUIDs, coupled with the limitations of other techniques and the need to extend the service life of many aircraft, provides much of the impetus for the development of SQUIDs for aircraft NDT.

Earlier, we mentioned the need for improved NDT techniques for reinforcing rods and concrete in airport runways, bridges, and buildings. This represents a 400 million dollar a year problem, but it is sobering to realize that of that, only 25 million dollars is equipment[87]; the rest is service. The annual NDT market, as a whole estimated at 450 million in the US, and 1.2 billion dollars worldwide, is considered a small market from the perspective of world trade[128]. There is a limited industrial customer base for NDT today: principal users are the aerospace, chemical/petrochemical, utilities, and casting/forging sectors. It is generally accepted that the NDT market is probably going to grow slowly. but there are notable exceptions: the eddy current market share grew from 5% in 1950 to 11% in 1990[129]; thermography was a $106,000,000 market in 1992 and is predicted to be $190,000,000 in 1997[128].

The fundamental problem with the NDT market is that given all of the various applications and competing technologies, the industry is highly fragmented: The total worldwide volume is 36,000 units annually[130], but there are only 5 or 6 NDT instruments or units that sell at volumes greater than a thousand a year. However, I doubt that the existing SQUID community would mind being limited to selling a thousand SQUID magnetometer systems a year. The real challenge is going to be to insert SQUID NDT into the marketplace without becoming a service industry. Can you find people who will buy SQUIDs to find flaws in airport runways without having to do it yourself? Because of the conservatism and the legal ramifications, penetration into the NDT market will in fact be very difficult. Small start-up companies may have a harder time at this than large, vertically organized ones that have access to a captive, internal market.

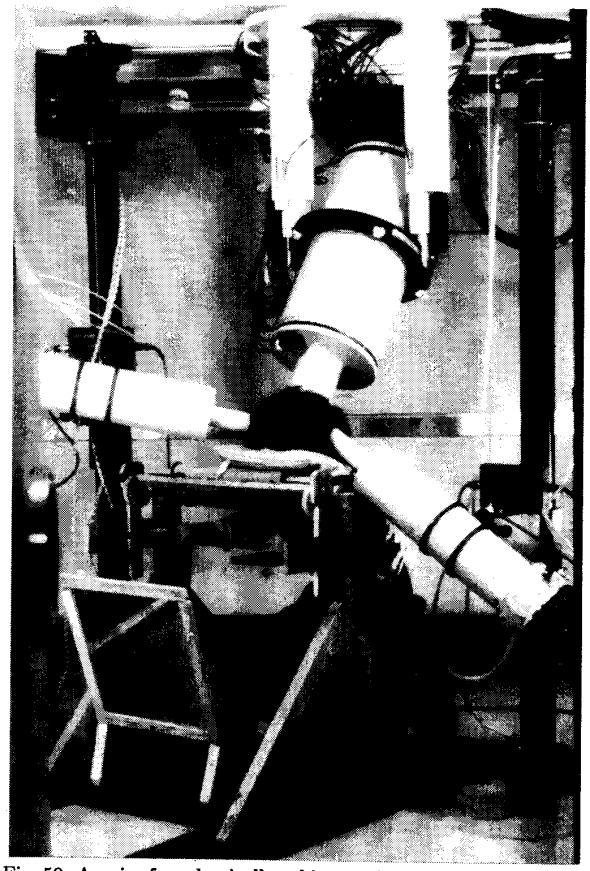

Fig. 50. A pair of mechanically refrigerated CryoSQUIDs operating with the 5-channel SQUID system are arranged to monitor the responses in 3 cortical regions when a subject participates in a forced-choice sensory-motor task[131],[132]. The CryoSQUIDs, built in a BTi/New York University collaboration, required no liquid helium and could operate upside-down. (Courtesy of Sam Williamson of NYU)

IX. What about refrigerators?

People often ask about refrigerators. In 1988, in cooperation with Sam Williamson and with Air Force Office of Scientific Research funding, BTi built a pair of mechanically refrigerated SQUIDs that were used in any orientation for studies of the magnetoencephalogram [131], [132]. As shown in Fig. 50, it can be done. There are all sorts of problems: power consumption, expense, size, weight, vibration and magnetic noise. The benefit is the absence of liquid cryogen. It may be that systems such as Bill Little's microminiature refrigerators[133],[134] will get around some of these problems. One way or the other, these technical problems are going to be solved and I fully expect that refrigerators will become an important factor in the acceptance of the technology.

X. Will SQUIDs always be confined to magnetic shields in laboratories?

Environmental noise is a real problem for both SQUID NDT and biomagnetism. Figure 51 is a plot of magnetic field noise versus frequency, ranging from the low field in the Berlin magnetically shielded room to the seven-orders-of-magnitude larger magnetic noise in a Helsinki hospital. The challenge is to be able to measure magnetic fields of the brain at the level of a few femtotesla in the presence of all this noise. In support to my answer of "No!" to the question of whether SQUIDs are doomed to remain inside shields in research laboratories, we need to look at some of the tricks that are being used to get SQUIDs out of shielded rooms.

Gradiometer pickup coils can be fabricated in various configurations to reject the background noise, as shown in Fig. 52. Most of the biomagnetic measurements to date have been done with axial gradiometers that are hand-wound with wires on a cylindrical substrate (Fig. 52b) so that they measure $\partial B_z/\partial z$. With care, this type of gradiometer can be balanced to a part in 10^6, *i.e.* to provide a common mode rejection ratio for uniform fields of 120 db. This approach can be quite successful: in 1973, Doug Brenner, Lloyd Kaufman and Sam Williamson used this approach to measure evoked responses in an unshielded room on the ninth floor of Meyer Hall of Physics at New York University, 12 floors above the BMT subway, although they subsequently found that wide-bandwidth measurements were easier in a shielded room. The Finnish Neuromag system uses a pair of orthogonal planar gradiometers that measure $\partial B_z/\partial x$ and $\partial B_z/\partial y$; when used together they provide a vector representation of the approximate strength and direction of the current source beneath the gradiometer. The advantage of the planar gradiometers is that they can be mass-produced with thin-film technology using either low or high temperature superconductors, and can either be fabricated on the same substrate as the SQUID, or coupled to the SQUID as a "flip-chip." Their disadvantage is that they are less sensitive to deep sources than are long-baseline axial gradiometers, but it is difficult to mass produce axial gradiometers, except by wrapping a flexible, planar coil around a cylindrical substrate, a technology that has yet to be extended to high temperature superconductors. NDT measurements have been made with axial and planar gradiometers, including the radially symmetric configurations in Fig. 52e and f, which measure $\partial B_z/\partial r$ and $\partial^2 B_z/\partial r^2$. The relative merits of various gradiometer configuration are still being discussed, and undoubtedly more work remains in this area.

A reference magnetometer can be used with a set of coils to cancel external fields. David Cohen at MIT had such a system for his shielded room. Between 1983-1988, Andrey Matlashov and his colleagues at the Institute of Radio Engineering and Electronics of the Russian Academy of

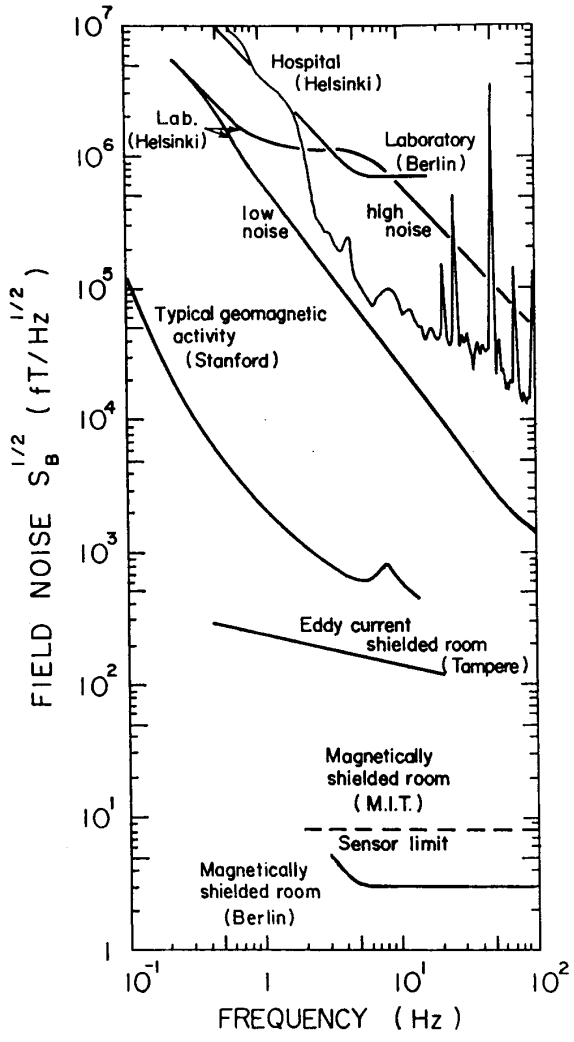

Fig. 51. The frequency dependence of environmental magnetic noise. The sensitivity of SQUIDs has improved substantially since this drawing was made in 1982! (From [135], with permission)

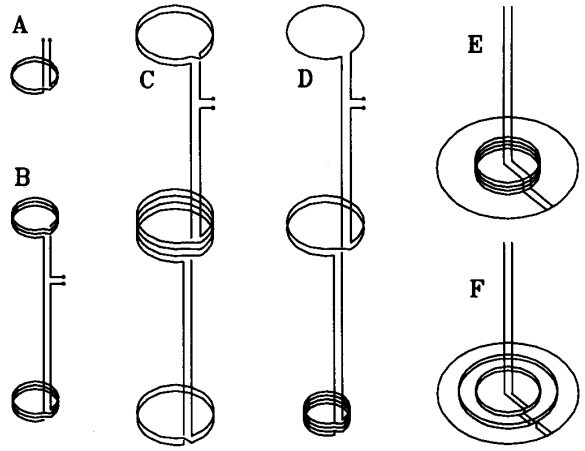

Fig. 52. Various SQUID pickup coil configurations. a) Magnetometer. b) First-order axial gradiometer. c) Symmetric second-order axial gradiometer. d) Second-order asymmetric gradiometer designed for increased face-coil sensitivity. e) Planar first-order gradiometer. f) Planar second-order gradiometer. (Adapted from[136] and[80])

Sciences in Moscow used three fluxgates and a set of coils for active cancellation of the external ac noise field that allowed them to make biomagnetic measurements with a 1 channel SQUID gradiometer that was balanced to only one part in a hundred. Since then, it has been recognized that the canceling field need not be applied externally, but could be applied directly to the pickup coils of the SQUIDs as long as there was little direct pickup by the SQUIDs themselves. This has led to the concept of a SQUID system that contains not only the standard pickup coils, but also one or more reference magnetometers. Direct feedback, simple off-line subtraction, or adaptive signal processing can then be used to remove the background contamination from the desired signal; depending upon the spatial variation of the noise field and the characteristics of the primary magnetometers or gradiometers, it may be necessary to utilize first order reference gradiometers as well.

This concept can be taken even further to form a large array of synthetic gradiometers. The group at CTF has invested a great deal of work in developing 64 and 140 channel systems that synthesize second and third-order gradiometers from data acquired from first order gradiometers[27], [28]. A proprietary calibration process and algorithm are used to determine fixed weighting coefficients that are then used to combine the outputs of 140 signal channels and 28 reference channels. The data in Figs. 53 and 54 show that this approach is successful and can be used to measure auditory evoked responses in an unshielded environment. It is important to note that even outside a shield, their system is close to the brain noise limit!

There are two possible limitations to the synthetic gradiometer approach as presently implemented: the coef-

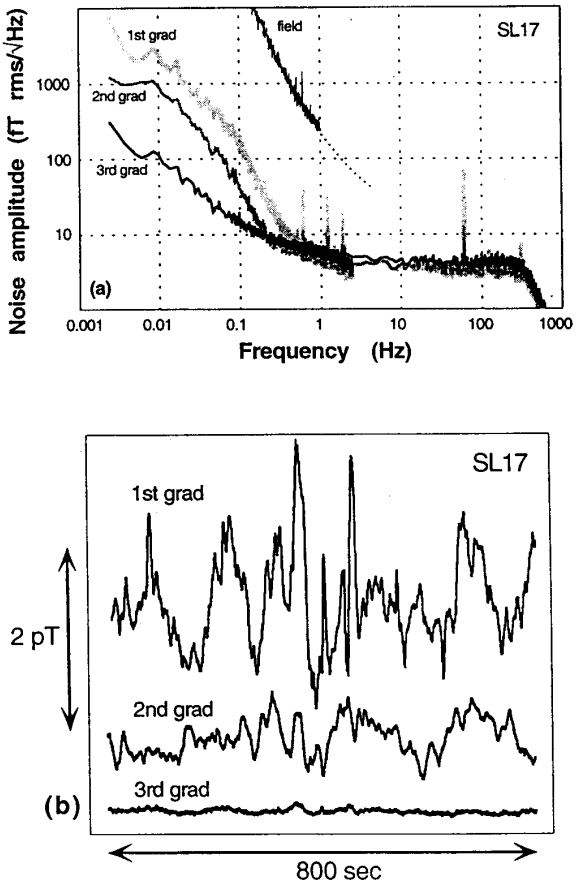

Fig. 53. Noise of the 64-channel CTF MEG system in a shielded room[27]. (Courtesy of Jiri Vrba of CTF).

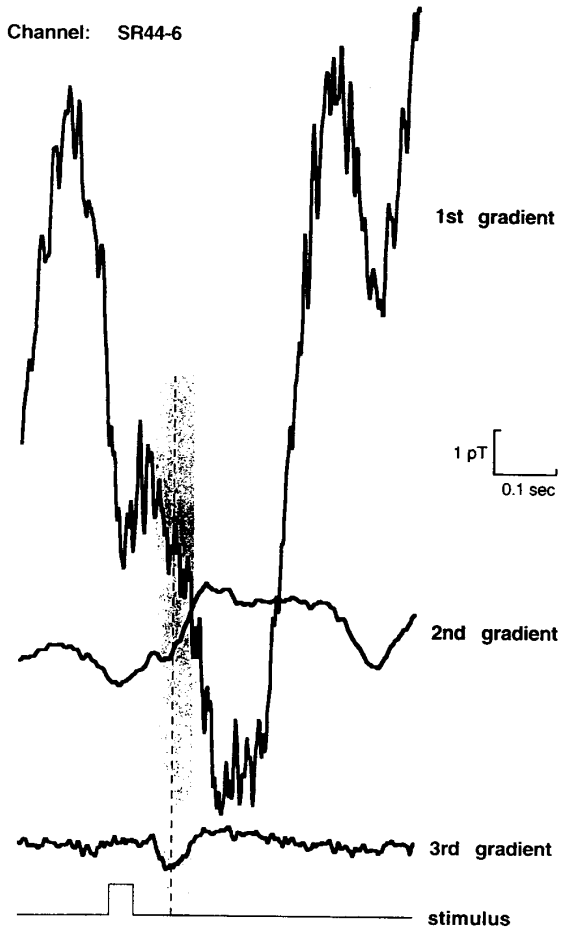

Fig. 54. An auditory evoked field experiment in an open environment using the CTF 64-channel MEG system. The second and third gradient signals are synthesized from signals from multiple first-order gradiometers. (Courtesy of Jiri Vrba of CTF)

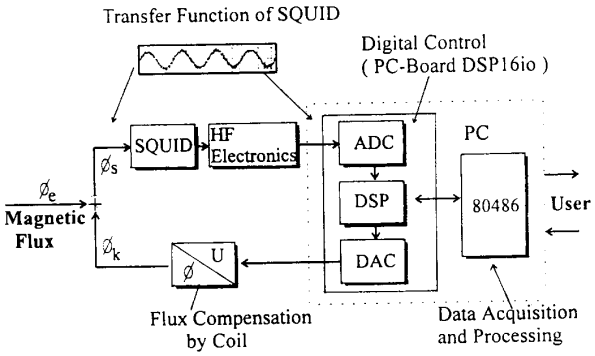

Fig. 55. The KFA rf SQUID system with digital feedback electronics[139]. (Courtesy of Helmut Soltner of KFA)

ficients are fixed to form third-order gradiometers that rely solely on the rapid field fall-off from distant sources, and substantial capital is tied up in the reference channels, which contribute SQUID noise to the synthetic gradiometer output but do not contribute any signal. (While the SQUID noise for the primary and reference sensors should be uncorrelated and hence would add in quadrature, it still represents a net loss in sensitivity. Note that this also occurs in a similar manner with standard gradiometers, in that the signal energy that is coupled into the reference coil is not coupled to the SQUID; the use of asymmetric pickup coils as in Fig. 52d can minimize this effect but not eliminate it[137]). The solution to the first problem might be to use adaptive weighting coefficients, but it is not clear how stable such a system would be for time-dependent noise sources with differing spatial characteristics. A possible solution to the second problem was proposed by Steve Robinson of the University of New Mexico: Place all of your SQUID sensors adjacent to the field source, for example the scalp in a MEG helmet system, and use numerical cross-correlation and inverse techniques to solve for the location of all effective signal sources. The sources outside of the helmet are assumed to be noise and are simply ignored, and those inside of the helmet are assumed to be signal. While conceptually elegant, this approach is not yet proven.

XI. Is there a role for digital SQUIDs?

We need to consider the future role of digital SQUIDs. There are two different flavors: room temperature and superconducting. Drung at Karlsruhe[138], Vrba at CTF[27], Alex Braginski's group at KFA in Jülich[139], and others replace the analog feedback loop with an analog-to-digital converter, a digital signal processor, and then a digital-to-analog converter, as shown for the KFA rf SQUID in Fig. 55. This process linearizes the flux-voltage characteristics, replaces many of the room temperature subsystems such as the electronic lock-in amplifier with signal processor code, and avoids interchannel phase delays arising from differences in component values in the analog circuitry. I expect this will prove to be a powerful approach that will reduce the cost of SQUID electronics. Other approaches may also lead to low cost electronics; in no design has the volume of SQUID electronics sales reached a level where the cost savings from mass production can be fully realized.

The more challenging approach is the integrated digital SQUID, where the pickup coil and the SQUID are on the same substrate as the Josephson digital logic required for feedback. In 1988, Fujimaki at Fujitsu used a SQUID comparator and an up-down counter to add or subtract flux quanta from an integrating loop, and the signals from the counter also provided the digital signals that were brought to room temperature[140]. The Fujitsu SQUID had limited dynamic range and sensitivity, but demonstrated the feasibility of the concept.

Integrated digital SQUIDs are quite appealing. The room temperature electronics would be inexpensive, since in principle only a modest preamplifier and a counter are required. A digital SQUID would have a high slew rate, set by the internal clock frequency, and a dynamic range that is limited only by the critical current of the feedback circuit. If the digital counter is placed on the chip, phenomenally high slew rates (10^9 ϕ_o/s) could in theory be achieved. The combination of high slew rates and dynamic range would allow the SQUIDs to treat as signal what is normally a major limiting factor in SQUID performance: rf interference. With such SQUIDs, it may eventually be possible to use SQUID magnetometers rather than gradiometers, which in turn would simplify the mathematical rejection of noise in large arrays; similarly, digital SQUIDs would simplify or eliminate the requirements for magnetically shielded rooms. Most importantly, it is easy to multiplex the digital signals from multiple SQUIDs, and it hence would be unnecessary to have signal and feedback wires between each SQUID and room temperature. The net result is that you can have a thousand channel SQUID array with ten wires coming to room temperature instead of six thousand. The potential applications of this approach will include multichannel systems and magnetic cameras. Since it will be possible to mass produce a complete SQUID magnetometer on an integrated circuit production line, and then mount the finished, packaged chips in a small dewar, the cost of the systems should plummet. This in turn could promote the large-volume production of inexpensive, compact, portable magnetometer systems.

Digital SQUIDs are getting quite close to commercialization. Figures 56 and 57 show the layout of one of several digital SQUIDs under development at Hypres. The circuit shown has a measured dynamic range of 80 db, a sensitivity of 10^{-4} $\phi_o/\mathrm{Hz}^{1/2}$, and a slew rate of 10^3 ϕ_o/s with a 100 kHz clock. Ongoing improvements, described elsewhere in these proceedings[141], [142], include the ad-

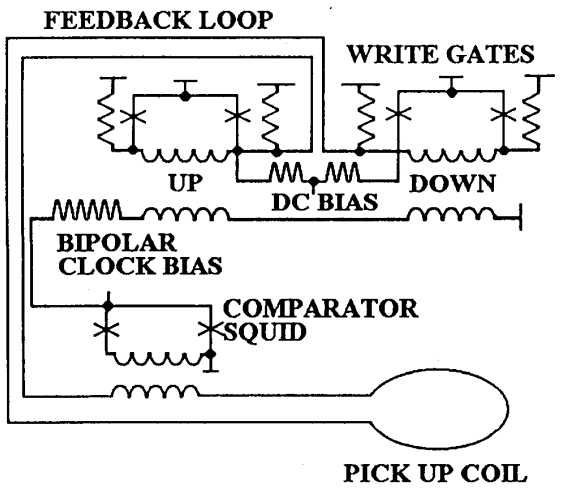

Fig. 56. A circuit design for one of the Hypres digital SQUIDs[141]. (Courtesy of Masoud Radparvar of Hypres)

dition of a SQUID preamplifier in front of the comparator, with an expected dynamic range of greater than 160 db, a sensitivity of better than $10^{-4}\ \phi_o/\mathrm{Hz}^{1/2}$, and a slew rate of $10^5\ \phi_o/\mathrm{s}$ with a 10 MHz clock. Figure 58a shows, for a square wave input signal, how one side of the bipolar output has no 50 kHz counter pulses when the field changes in one direction. If you integrate the up-down signals corresponding to a triangular input signal (Fig. 58c), you get the triangular output signal in Fig. 58d. Thus digital SQUIDs are a reality; I think they will be doing quite well before too long.

XII. Will SQUIDs using high-temperature superconductors be of any practical use?

A lot of people ask "Do high temperature SQUIDs have any value?" Innumerable groups are developing high-T_c SQUIDs, as indicated by the numerous papers in these proceedings. The simple and inexpensive Mr. SQUID^{tm} sold by Conductus has already been used for an NDE demonstration[143],[144]. Figure 59 shows the very low $1/f$ knee that has been achieved with the KFA rf high-T_c SQUID[145]. Figure 60 shows the results of a collaborative project between John Clarke's group at Berkeley and PTB in Berlin[146],[25], and demonstrates that high temperature SQUIDs can provide the very respectable white-noise floor of 18 $\mathrm{fT/Hz}^{1/2}$ and a $1/f$ knee at 1 Hz. This is quite respectable and 10 years ago would have been a state-of-the-art low-temperature SQUID, as can be seen by comparing this graph to the "sensor limit" in Fig. 51. The performance of high-T_c SQUIDs continues to improve, as shown by Fig. 61.

It's important to realize that high temperature SQUIDs are already adequate for clinical magnetocardiography. There is an ongoing study by a collaboration between the

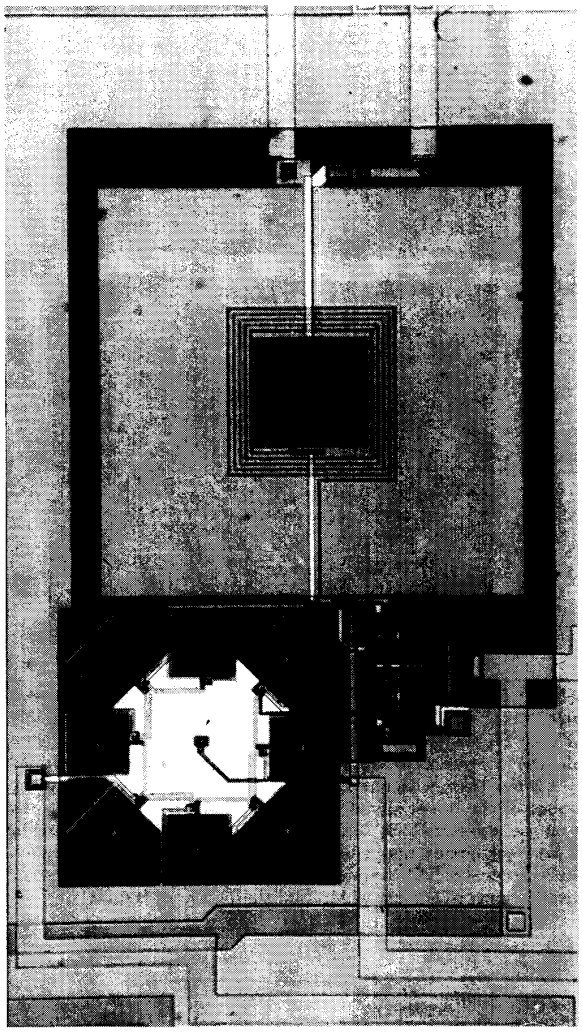

Fig. 57. The circuit layout for one of the Hypres digital SQUIDs[141]. The large square structure at the top is the input/feedback coil; the octagon at the lower left is the comparator, and the structures to the right are the write gates. (Courtesy of Masoud Radparvar of Hypres)

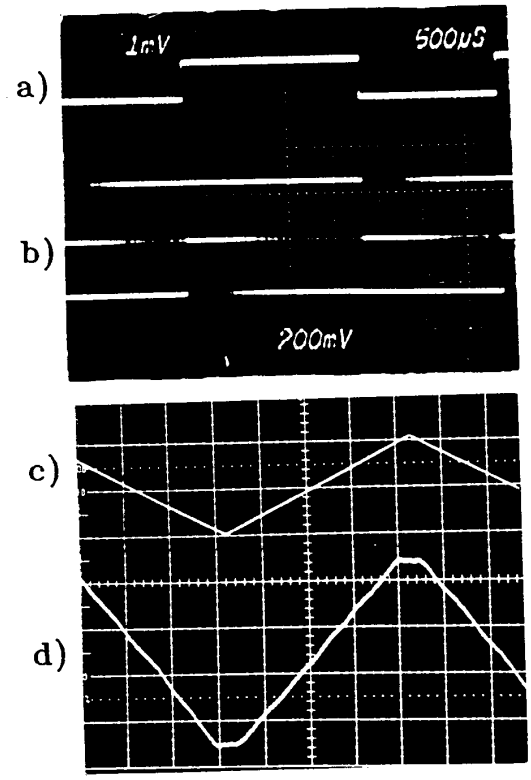

Fig. 58. Demonstration of one of the Hypres integrated digital SQUIDs[141], [142]. a) Square wave input signal of approximately 50μA. b) Bipolar digital output with a 50 kHz clock. At this time scale, the individual clock pulses are not resolvable, but the dropout of the lower trace with the rising edge of the input signal and the dropout of the upper signal with the falling edge are evident. In actual use, a faster clock would be used so that the settling time in the feedback circuit would be shorter. c) A triangular test signal. d) The reconstructed output obtained by integrating the bipolar digital output. (Courtesy of Masoud Radparvar of Hypres)

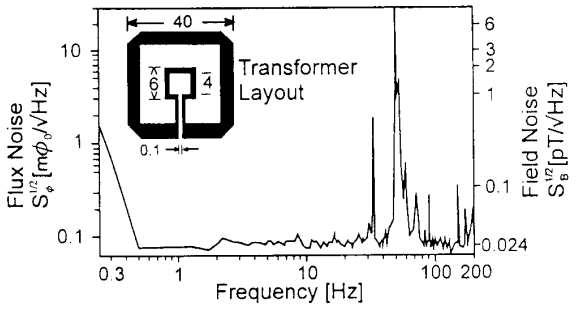

Fig. 59. Noise spectrum of the KFA single-layer $YBa_2Cu_3O_7$ rf SQUID magnetometer with a direct-coupled pickup coil and a flip-chip flux transformer[145]. The field noise at 1 Hz is $\leq$ 40 fT/Hz$^{1/2}$ at 77 K and in a magnetic shield. (Courtesy of Helmut Soltner of KFA)

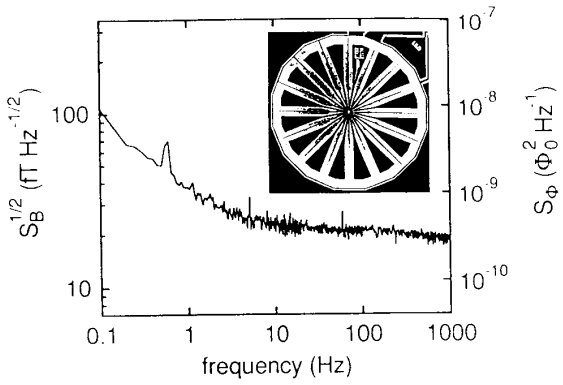

Fig. 60. RMS magnetic field noise versus frequency at 77 K for a 16-turn multiloop magnetometer involving $YBA_2Cu_3O_{7-x}$–$SrTiO_3$–$YBA_2Cu_3O_{7-x}$ multilayers[146] and[25]. The noise is 18 fT/Hz$^{1/2}$ at 1 kHz and 37 fT/Hz$^{1/2}$ at 1 Hz. The device (inset) is only 7 mm in diameter. (Adapted from[146] and[25], courtesy of John Clarke of the University of California at Berkeley)

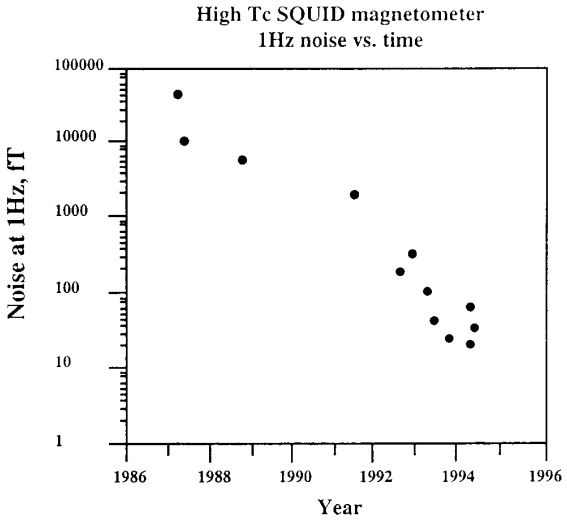

Fig. 61. The 1 Hz noise of high-T_c SQUID magnetometers as a function of time. (Courtesy of John Rowell of Conductus and John Clarke of the University of California at Berkeley)

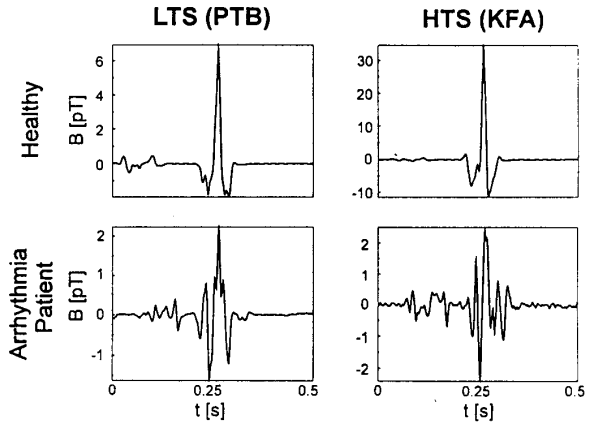

Fig. 62. Identification of patients prone to malignant cardiac arrhythmia using a bandpass-filtered, signal-averaged MCG[108], [109]. The LTS (low temperature superconductivity) MCGs were recorded with the PTB magnetically shielded room and liquid-helium temperature SQUID system of 1990, and the HTS (high temperature superconductivity) MCGs were recorded with the KFA rf digital high-T_c SQUID in liquid nitrogen. The high amplitude of the HTS MCG is due to the reduced distance from the skin. Filtering by nonrecursive binomial filters allows the analysis of the entire QRS interval for high frequency components. When comparing healthy and VT-patients, the fragmentation of the filtered QRS-complex of the MCG appears to be significantly more pronounced for patients with sustained ventricular tachycardia. Similar, however less significant results were found for the ECG. One should keep in mind that VT-patients are under medication. (Courtesy of Helmut Soltner of KFA and Lutz Trahms of PTB)

PTB in Berlin and KFA in Jülich in which the PTB group has been studying the high-frequency magnetocardiogram of healthy individuals and individuals with arrhythmias, where they are trying to identify which of these arrhythmias are potentially life threatening[108], [109]. As indicated in Fig. 62, the group at KFA has shown that their new magnetometer, which has a 24 $fT/Hz^{1/2}$ noise at 1 Hz, provides comparable data. The HTS signals are bigger because the magnetometer is closer! As I have indicated before, the rapid ($1/r^3$ or faster) fall-off of the high spatial-frequency information with distance from the source makes close magnetometer spacing worthwhile in most applications, and HTS SQUIDs should make this easier.

One of the difficulties with high temperature superconducting materials is that it is not yet possible to fabricate low-noise, persistent current axial gradiometers since there is no suitable wire. Planar gradiometers as in Fig. 63a have been demonstrated, but there are problems: if you want lots of sensitivity, you need a very large chip; it is hard to shield the SQUIDs from rf interference[147]; and these multilayer devices at present seem to be prone to flux noise and low process yield. An alternative approach is to use two or more simple magnetometers and to subtract their outputs electronically[148], [149], as in Fig. 63b, but this approach requires that the feedback loop of each SQUID maintain lock independently. The

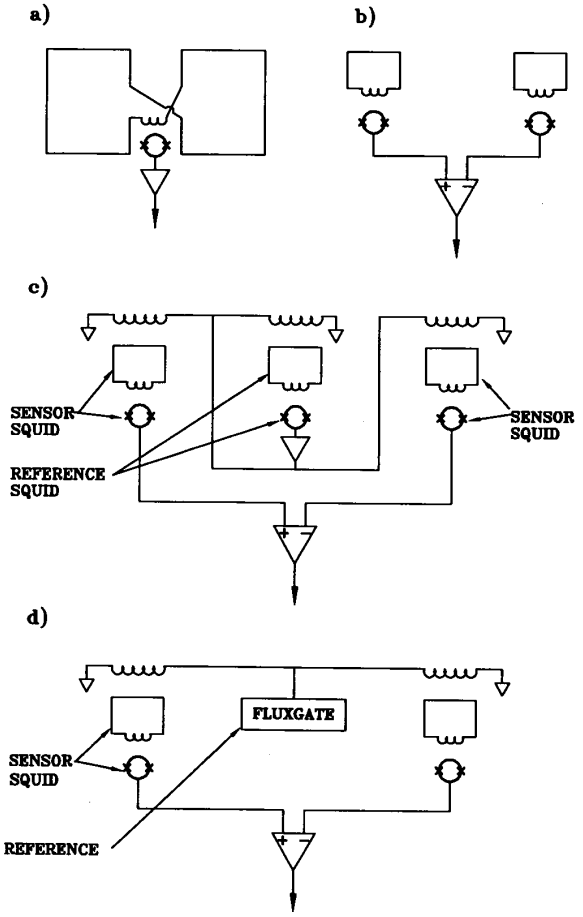

Fig. 63. Four approaches to high-T_c gradiometers. a) Planar gradiometer with thin-film gradiometer pickup coil, either on the same substrate as the SQUID or as a flip chip. b) Two SQUIDs whose outputs are subtracted electronically. c-d) Three-SQUID gradiometers[150], [151] with c) a SQUID and d) with a fluxgate as a reference magnetometer. (Adapted from a drawing by Roger Koch of the IBM Thomas J. Watson Research Center.)

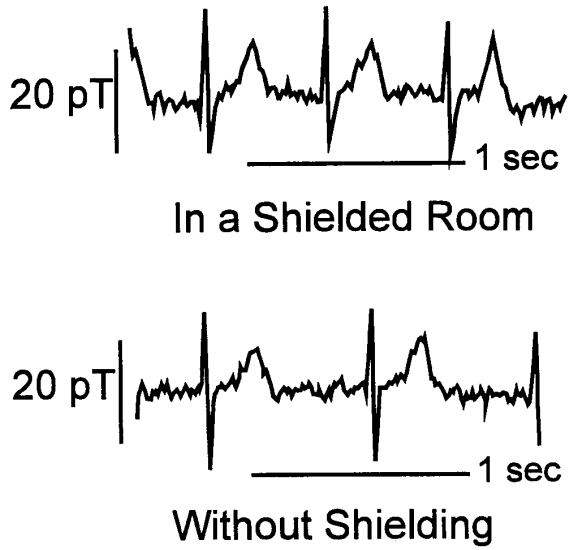

Fig. 64. Magnetocardiograms recorded inside and outside a shield with a KFA-type electronic gradiometer of first and second order using two or three washer-type rf SQUIDs with 25 mm flux concentrators and digital electronics[148], [149]. (Courtesy of Helmut Soltner of KFA)

data in Fig. 64 from KFA demonstrates that this is possible, and that high quality MCGs can be recorded in an unshielded environment. The solution devised by Roger Koch at IBM is elegant[150], [151]. As shown in Fig. 63c, the three-SQUID gradiometer uses a reference SQUID and two sensor SQUIDs. The reference SQUID feeds back to the other two input circuits and cancels at each sensor SQUID the field sensed by the reference SQUID. Even if the reference SQUID is noisy, its noise is coupled equally to the two sensor SQUIDs, which can be very sensitive, and the differential amplifier removes any common-mode noise introduced by the reference SQUID. The neatest aspects of this approach are that the reference magnetometer can be a fluxgate magnetometer, only the SQUIDs need to be superconducting, and the SQUIDs can be in separate dewars. When fields from distant sources are detected, for example from submarines or mines, it is possible to achieve long baseline gradiometers without large dewars. Thus two high-T_c SQUIDs and a fluxgate with a clever feedback system can give you a very high sensitivity, high temperature SQUID gradiometer with a high degree of balance and no need for superconducting wires.

There are, of course, a number of problems yet to be solved with high temperature SQUIDs, most notably the relatively high frequency at which the $1/f$ knee occurs with some junction technologies, and the problems of excess noise that arises from flux creep in the pickup coils when the SQUID is moved in the earth's magnetic field.

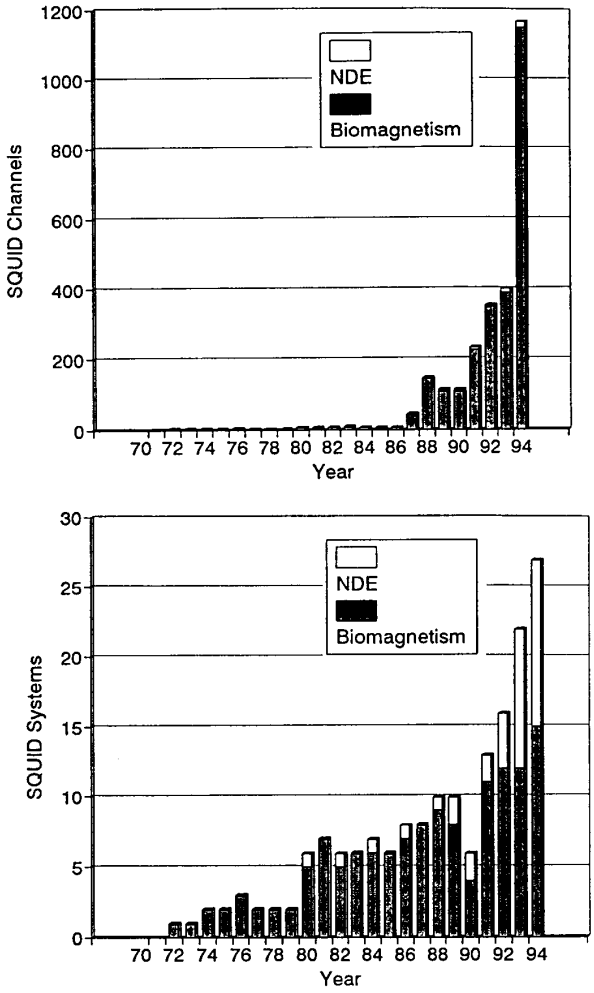

Fig. 65. Estimated annual SQUID production for biomagnetism and NDT as of October, 1994. Top: Number of SQUID channels. Bottom: Number of SQUID systems.

XIII. Will anyone ever make money with $QUID$?

Another big question is whether anyone will ever make money making or using SQUIDs? I think they will, but it's not guaranteed. Figure 65 shows my estimate, obtained by polling companies and research groups that are major SQUID builders,of the annual production of SQUIDs for biomagnetism and NDT for the past 24 years, both in units and in the number of systems sold. Some of these SQUIDs systems were sold, and some were produced for internal use in labs or companies and never delivered to a customer. These numbers probably err on the low side, since some companies chose not to report the internal development systems. Also, these numbers do not include SQUID sensors and electronics sold separately. The 1994 data includes systems that have been sold and scheduled

for delivery in 1994 but had not been completed by October 1994. Over the past few years, the number of channels sold is reasonably accurate because it is driven by a few large array systems produced by four groups: BTi, CTF, Instrumentarium, and SSL.

The number of systems sold is being increasingly dominated by NDT systems, but these systems typically have very few channels and contribute negligibly to the SQUID channel statistics. Because of the difficulty in accounting for a number of single channel systems built by research groups, by CTF and BTi in their early days, and by companies that are no longer manufacturing SQUIDs, such as Develco and Siemens, the error in the annual number of systems may be as large as ±50%. By my estimates, this year is the first time that SQUID production has crossed the thousand channel mark, and it appears to be rising very quickly. I estimate that a total of about 3000 functioning SQUIDS have been produced worldwide in the past 24 years, and that they have been used in around 200 systems. In comparison with biomagnetism, the NDT market is still young and small - I estimate between 15 and 20 NDT systems worldwide were built in the past year or two, containing less than 40 SQUIDs.

XIV. What do we need in the future?

We can conclude this paper by asking what we need to do in the future; obviously any list I provide will be incomplete, and cannot reflect future discoveries, but will provide some idea of the direction of current research in SQUIDs for NDT and biomagnetism. SQUID NDT is gaining in popularity in part because of the increased public emphasis on our aging technological infrastructure; however, our biological infrastructure is also aging, and I expect that SQUIDs for biomagnetic NDT will find increasing utilization for the study of dementias, stroke, and cardiac and intestinal disease. For both structural and human NDT, we need improved synthetic gradiometers and active noise cancellation: we can and will be more clever in using the capability of SQUIDs to eliminate more noise. We need more advanced imaging algorithms that provide better and more realistically constrained solutions to the inverse problem. I believe that we need to devise measures of distributed brain activity to compete with the slow, metabolic images provided by positron emission tomography. There is no magnetic equivalent yet. Particularly in the NDT applications, it is necessary to develop simple, user-friendly control systems – the NDT industry is used to simple screen displays on an eddy-current instrument, or visual images that don't require hours on a supercomputer to produce. Obviously, virtually every application I have mentioned will benefit from adding more channels, eventually to the extent of producing a SQUID magnetic camera. Helmet MEG systems need to have their pickup coils closer to the scalp, and the systems need to be made more compact and easier to manufacture. The price of MEG systems must be brought down. Integrated digital SQUIDs may provide the path to follow.

It is also important to recognize what types of applications might benefit from SQUIDs. So far, we have shown that SQUIDs should be used when the application requires high sensitivity between dc and 10 kHz, wide dynamic range and linearity to track noise, and gradiometers to reject distant noise sources. The ability to operate at dc or frequencies below 100 Hz will prove useful when it is necessary to detect deep flaws. Superconductivity makes it easy to apply steady or strong magnetic fields. The small size of SQUIDs is useful when you need high spatial resolution or multiple channels for simultaneous field mapping, high scanning speed, or noise correlation studies. SQUIDs are ideal for measuring diamagnetic or paramagnetic susceptibilities. SQUIDs are ideal for measurements at a distance.

As a closing word of caution, one of the lasting impressions that I gained during the early years of biomagnetism is that many physicists and engineers were intrigued with and challenged by the construction of SQUIDs, and while few knew any medicine or physiology, many became convinced that SQUIDs would undoubtedly help solve someone's medical problem. Biomagnetism earned a reputation of being a solution in search of a problem. After 20 years of research by a number of dedicated individuals and companies such as BTi, and the investment of substantial amounts of governmental and commercial support, biomedical applications are now being identified that may be ideally suited for SQUIDs. When these applications are proven and accepted, biomagnetism will judged on its merits and not its history. Today, with the advent of high temperature SQUIDs, we have a new generation of SQUID builders in search of applications for their devices and funding to support further development. The shift of our nation's attention from new technology for medicine to our aging infrastructure places nondestructive testing in a position similar to that held by biomagnetism 10 to 20 years ago: a promising technique that seems destined to solve someone's NDT problem. Lest we repeat the long time between device development and commercial application, it is important at the outset to identify problems that are suitable for SQUIDs, to establish collaborations with people who need to have these problems solved today, and at every step to keep track of what competing techniques have to offer. Ideally, the applications for SQUIDs will be ones where SQUIDs are the best, and hopefully the only solution. It is most important, in the words of Harold Weinstock, to use SQUIDs only when nothing else will suffice.

XV. Acknowledgment

I thank Terry Orlando and the other members of the Program Committee of the Applied Superconductivity Conference for the opportunity to present this plenary lecture and to write this paper. I am indebted to the very large number of people who have contributed over 600 slides and numerous papers for the lecture and this paper: Steve Baughman of Lockheed Aeronautical Systems Company; Randy Black and Frederick C. Wellstood of the University of Maryland; William C. Black, Eugene C. Hirschkoff, Dave Kynor and James V. Schumacher of Biomagnetic Technologies, Inc.; Alex Braginski and Helmut Soltner of Forschungszentrym Jülich GmbH, (KFA); L. Alan Bradshaw, James Cadzow, Cheryl D. Cosby, Anthony P. Ewing, J. Michael Fitzpatrick, William G. Jenks, Delin Li, Xingkang Li, Yu Pei Ma, Calvin R. Maurer, Nestor G. Sepulveda, Daniel J. Staton and Ian M. Thomas of Vanderbilt University; John Clarke of the University of California, Berkeley; Gordon Donaldson, Sandy Cochran, Luke Morgan and Colin M. Pegrum of the University of Strathclyde; David Cohen of MIT; Joe Anderberg, Laura M. Crowley, Duane Crum, Richard J. Kirby and John Rowell of Conductus, Inc.; Anne Deery of Siemens Medical Systems; Olaf Dössel of Philips GmbH, Hamburg; Edgar Edelsack; Robert L. Fagaly of General Atomics, Inc.; Gerald L. Fitzpatrick of Physical Research, Inc.; Christopher C. Gallen of Scripps Research Institute, La Jolla; John George and Christopher Wood of Los Alamos National Laboratory; Alan S. Gevins of EEG Systems Laboratory and SAM Technology, Inc.; Irina Gorodnitsky of the University of California, San Diego; Matti Hämäläinen and Olli V. Lounasmaa of Helsinki University of Technology; Teresa Healey and Steven R. Martell of Sonoscan, Inc.; Andy Hibbs of Quantum Magnetics, Inc.; Greg Jablunovsky of Wright Patterson Air Force Base; Hisashi Kado and Haruhisa Toyoda of the Superconducting Sensor Laboratory; Mark B. Ketchen and John R. Kirtley of the IBM Thomas J. Watson Research Center; Richard Kinzie of Robbins Air Force Base; Stan Lapidus and Greg Zimmerman of Optra, Inc.; Jeffrey D. Lewine of the University of New Mexico; Jaakko Malmivuo of the Ragnar Granit Institute of the Tampere University of Technology; Andrey N. Matlashov of the Institute of Radio Engineering and Electronics, Russian Academy of Sciences; Michael Murias, Michael I. Posner and Don M. Tucker of the University of Oregon; Mashiro Otaka of Hitachi, Ltd.; Alberto Pasquarelli of Consiglio Nazionale delle Ricerche, Rome; Walter Podney of SQM Technology, Inc.; Masoud Radparvar and Elie Track of Hypres, Inc.; Sidney Smith of General Electric, Inc.; Lutz Trahms and Zvonko Trontelj of Physickalisch-Technicshe Bundesanstalt, Berlin (PTB); Jiri Vrba of CTF Systems, Inc.; Ron Wakai of the University of Wisconsin; Harold Weinstock of the Air Force Office of Scientific Research; Samuel J. Williamson of New York University. I appreciate comments on this manuscript by Bill Black, Alan Bradshaw, Bill Jenks, and Leonora Wikswo. I especially want to thank Licheng Li for her care in preparing and cataloging the almost-innumerable slides and the illustrations for both the lecture and this paper.

References

[1] *Biomagnetism, An Interdisciplinary Approach,* S.J. Williamson, G.-L. Romani, L. Kaufman and I. Modena, Eds., New York: Plenum Press, 1983,

[2] H. Weinstock and M. Nisenoff, "Non-destructive evaluation of metallic structures using a SQUID gradiometer," in *SQUID '85, Proc. 3rd International Conference on Superconducting Quantum Devices*, H.D. Hahlbohm and H. Lubbig, Eds., Berlin: de Gruyter, 1985, pp. 843-847.

[3] G.B Donaldson, "SQUIDs for everything else," in *Superconducting Electronics*, H. Weinstock and M. Nisenoff, Eds., New York: Springer Verlag, 1989, pp. 175-207.

[4] *Advances in Biomagnetism*, S.J. Williamson, M. Hoke, G. Stroink, and M. Kotani, Eds., New York: Plenum Press, 1990, pp. 1-18.

[5] H. Weinstock, "A review of SQUID magnetometry applied to nondestructive evaluation," *IEEE Trans. Mag.*, vol. 27, no. 2, pp. 3231-3236, 1991.

[6] W.G. Jenks, S.S.H. Sadeghi, and J.P. Wikswo, Jr., "A review of SQUID magnetometers for non-destructive testing," *Journal of Physics D*, in press.

[7] J. Clarke, "Principles and applications of SQUIDs," *Proc. IEEE*, vol. 77, pp. 1208-1223, 1989.

[8] R.L. Fagaly, "Neuromagnetic instrumentation," in *Advances in Neurology*, vol. 54: Magnetoencephalography, S. Sato, Ed., New York: Raven Press, 1990, pp. 11-32.

[9] Edgar A. Edelsack, Washington, DC, personal communication.

[10] G. Baule and R. McFee, "Detection of the magnetic field of the heart," *Am. Heart J.*, vol. 55, p. 95, 1963.

[11] D. Cohen, E.A. Edelsack, and J.E. Zimmerman, "Magnetocardiograms taken inside a shielded room with a superconducting point-contact magnetometer," *Appl. Phys. Lett.*, vol. 16, no. 7, pp. 278-280, April 1970.

[12] D. Cohen, "Magnetoencephalography: Detection of the brain's electrical activity with a superconducting magnetometer," *Science*, vol. 175, pp. 664-666, February 1972.

[13] D. Cohen, "Magnetoencephalography: Evidence of magnetic fields produced by alpha-rhythm currents," *Science*, vol. 161, pp. 784-786, June 1968.

[14] J.P. Wikswo, Jr. and J.M. van Egeraat, "Cellular magnetic fields: Fundamental and applied measurements on nerve axons, peripheral nerve bundles, and skeletal muscle," *J. of Clin. Neurophys.*, vol. 8, no. 2, pp. 170-188, 1991.

[15] M.N. Deeter, A.H. Rose, and G.W. Day, "Iron-garnet magnetic field sensors with 100 $pT/Hz^{1/2}$ noise-equivalent field," *Proc. 7th Int. Conf. Optical Fiber Sensors*, Sydney, 1990.

[16] M.N. Deeter, A.H. Rose, and G.W. Day, "Sensitivity limits to ferrimagnetic Faraday effect magnetic field sensors," *J. Appl. Phys.*, vol. 70, no. 10, pp. 6407-6409, November 1991.

[17] M.N. Deeter, G.W. Day, T.J. Beahn, and M. Manheimer, "Magneto-optic field sensor with 1.4 $pT/Hz^{1/2}$ minimum detectable field at 1 kHz," *Electron. Lett.* vol. 29, pp. 993-994, May 1993.

[18] Greg Zimmerman, Optra, Inc., Topsfield, MA, personal communication.

[19] Y.C. Okada, "Neurogenesis of evoked magnetic fields," in *Biomagnetism, An Interdisciplinary Approach*, S.J. Williamson, G.-L. Romani, L. Kaufman and I. Modena, Eds., New York: Plenum Press, 1983, pp. 399-408.

[20] J.P. Wikswo, Jr., "Biomagnetic sources and their models," in *Advances in Biomagnetism*, S.J. Williamson, M. Hoke, G.

Stroink, and M. Kotani, Eds., New York: Plenum Press, 1990, pp. 1-18.

[21] H.J.M. ter Brake, J. Flokstra, W. Jaszczuk, R. Stammis, G.K. van Ancum, A. Martinez, et. al., "The UT 19-channel dc SQUID based neuromagnetometer," *Clin. Phys. Physiol. Meas.*, vol. 12, Suppl. B, pp. 45-50, 1991.

[22] A.N. Matlashov, V.Y. Slobodchikov, A.A. Bakharev, Y.E. Zhuravlev, and N. Bondarenko, "Biomagnetic multichannel system built with 19 cryogenic probes," in *Proc. 9th Inter. Conf. on Biomagnetism, Vienna*, L. Deecke, C. Baumgartner, G. Stroink, and S.J. Williamson, Eds., in press.

[23] A. Matlashov, Y. Zhuravlev, V. Slobodchikov, N. Bondarenko, A. Bakharev, and D. Rassi, "Miniature dc SQUID magnetometers for clinical use," in *Proc. 9th Inter. Conf. on Biomagnetism, Vienna*, L. Deecke, C. Baumgartner, G. Stroink, and S.J. Williamson, Eds., in press.

[24] O. Dössel, B. David, M. Fuchs, J. Krüger, K.-M. Lüdeke, and H.-A. Wischmann, "A 31-channel SQUID system for biomagnetic imaging," *Appl. Supercond.*, vol. 1, nos. 10-12, pp. 1813-1825, 1993.

[25] D. Drung, "The PTB 83-SQUID system for biomagnetic applications in a clinic," *IEEE Trans. Appl. Supercond.*, these proceedings.

[26] S. Yamasaki, T. Morooka, N. Matsuda, J. Kawai, N. Mizutani, K. Tsukada, et al., "Design and fabrication of multichannel dc SQUIDs for biomagnetic applications," *IEEE Trans. Appl. Supercond.*, vol. 3, pp. 1887-1889, March 1993.

[27] J. Vrba, K. Betts, M. Burbank, T. Cheung, D. Cheyne, A.A. Fife, et al., "Whole cortex 64 channel system for shielded and unshielded environments," *Proc. of the 9th International Conference on Biomagnetism*, Amsterdam: Elsevier, 1993, in press.

[28] J. Vrba, B. Taylor, T. Cheung, A.A. Fife, G. Haid, P.R. Kubik, et al., "Noise cancellation by a whole-cortex SQUID MEG system," *IEEE Trans. Appl. Supercond.*, these proceedings.

[29] M. Ueda, A. Kandori, H. Ogata, Y. Takada, T. Komuro, K. Kazami, et al., "Development of a biomagnetic measurement system for brain research," *IEEE Trans. Appl. Supercond.*, these proceedings.

[30] A. Matlashov, A. Bakharev, Y. Zhuravlev, and V. Slobdobchikov, "Biomagnetic multi-channel system consisting of several self-contained autonomous small-size units," in *Superconducting Devices and Their Applications*, vol. 64, H. Koch and H. Lübbig, Eds., Berlin: Springer-Verlag, 1992, pp. 511-516.

[31] A.N. Matlashov, "New approaches to biomagnetic measurements and signal processing," *International Journal of Applied Electromagnetics in Materials*, vol. 4, Amsterdam: Elsevier, 1993, pp. 185-188.

[32] A.D. Hibbs, R.E. Sager, D.W. Cox, T.H. Aukerman, T.A. Sage, and R.S. Landis, "A high-resolution magnetic imaging system based on a SQUID magnetometer," *Rev. Sci. Instrum.*, vol. 63, no. 7, pp. 3652-3658, July 1992.

[33] A. Hibbs, R. Chung, and J.S. Pence, "Corrosion measurements with a high resolution scanning magnetometer," *Review of Progress in QNDE*, vol. 13, D.O. Thompson and D.E. Chimenti, Eds., New York: Plenum Press, 1994, pp. 1955-1962.

[34] W.N. Podney, "Performance measurements of a superconductive microprobe for eddy current evaluation of subsurface flaws," *IEEE Trans. Appl. Supercond.*, vol. 3, no. 1, pp. 1914-1917, March 1993.

[35] W. Podney, "A superconductive electromagnetic microscope for eddy current evaluation of materials," *Review of Progress in QNDE*, vol. 13, D.O. Thompson and D.E. Chimenti, Eds., New York: Plenum Press, 1994, pp. 1947-1954.

[36] G.L. Romani, S.J. Williamson, and L. Kaufman, "Tonotopic organization of the human auditory cortex," *Science*, vol. 216, p. 1339-1340, 1982.

[37] E. Maclin, Y.C. Okada, L. Kaufman, and S.J. Williamson, "Retinotopic map on visual cortex for eccentrically placed patterns: First noninvasive measurement," *Il Nuovo Cimento*, vol. 2D, pp. 410-419, 1983.

[38] H.A. Schlitt, L. Heller, R. Aaron, E. Best, and D.M. Ranken, "Evaluation of boundary element methods for the EEG forward problem: Effect of linear interpolation," *IEEE Trans. Biomed. Eng.*, in press.

[39] H.A. Schlitt, L. Heller, E. Best, D.M. Ranken, and R. Aaron, "Effect of conductor geometry on source localization: Implications for epilepsy studies," in *NABMAG2 - Proceedings of the Second North American Biomagnetism Action Group Meeting*, N. Tepley, Ed., Henry Ford Hospital, Detroit, Michigan.

[40] C.R. Maurer, Jr., G.B. Aboutanos, B.M. Dawant, S. Gadamsetty, R.A. Margolin, R.J. Maciunas, and J.M. Fitzpatrick, "Effect of geometrical distortion correction in MR on image registration accuracy," in *Medical Imaging VIII: Image Processing*, Proc. SPIE, vol. 2167, pp. 200-213, 1994.

[41] J.S. Ebersole, "EEG dipole modeling in complex partial epilepsy," *Brain Topography*, vol. 4, no. 2, pp. 113-123, 1991.

[42] R. Cooper, A.L. Winter, H.J. Crow, and W.G. Walter, "Comparison of subcortical, cortical, and scalp activity using chronically indwelling electrodes in man," *Electroenceph. Clin. Neurophysiol.*, vol. 18, pp. 217-228, 1969.

[43] M. Fuchs, M. Wagner, H.-A. Wischmann, K. Ottenberg, and O. Dössel, "Possibilities of functional brain imaging using a combination of MEG and MRI," in *NATO Advanced Studies Symposium Oscillatory Event Related Brain Dynamics*, Tecklenburg, 1993.

[44] J.C. Mosher, P.S. Lewis, and R.M. Leahy, "Multiple dipole modeling and localization from spatio-temporal MEG data," *IEEE Trans. Biomed. Eng.*, vol. 39, no. 6, pp. 541-557, June 1992.

[45] I.F. Gorodnitsky, J.S. George, and B.D. Rao, "Neuromagnetic source imaging with FOCUSS: A recursive weighted minimum norm algorithm," unpublished.

[46] Z.-L. Lü, S.J. Williamson, and L. Kaufman, "Human auditory primary and association cortex having differing lifetimes for activation traces," *Brain Res.*, vol. 527, pp. 236-241, 1992.

[47] L. Kaufman, S. Curtis, J.-Z. Wang, and S.J. Williamson, *Electroenceph. Clin. Neurophysiol.*, vol. 82, pp. 266-284, 1992.

[48] R. Hari, R. Salmelin, S.O. Tissari, M. Kajola, and V. Virsu, "Visual stability during picture naming," *Nature*, vol. 367, pp. 121-122, January 1994.

[49] R. Salmelin, R. Hari, O.V. Lounasmaa, and M. Sams, "Dynamics of brain activation during picture naming," *Nature*, vol. 368, pp. 463-465, March 1994.

[50] T.T. Yang, C.C. Gallen, B.J. Schwartz, and F.E. Bloom, "Noninvasive somatosensory homunculus mapping in humans by using a large-array biomagnetometer," *Proc. Natl. Acad. Sci. USA*, vol. 90, pp. 3098-3102, April 1993.

[51] T.T. Yang, C. Gallen, B. Schwartz, F.E. Bloom, V.S. Ramachandran, and S. Cobb, "Sensory maps in the human brain," *Nature*, vol. 368, pp. 592-593, April 1994.

[52] R.T. Wakai, M. Wang, and C.B. Martin, "Spatiotemporal properties of the fetal magnetocardiogram," *Am. J. Obstet. Gynecol.*, vol. 170, no. 3, pp. 770-776, March 1994.

[53] Y.E. Zhuravlev, D. Rassi, and S.J. Emery, "Clinical assessment of fetal magnetocardiography," *IEEE Trans. Appl. Supercond.*, in press.

[54] M. Burghoff, G. Curio, W. Haberkorn, B.-M. Mackert, and L. Trahms, *Quellenbildgebung aus biomagnetischen Feldern peripherer Nerven. Proceedings of the Congress, Biomedizinische Technik*, 1994.

[55] I. Modena, G.B. Ricci, S. Barbanera, R. Leoni, G.L. Romani, and P. Carelli, "Biomagnetic measurements of spontaneous brain activity in the brain following repetitive sensory stimulation," *Electroenceph. Clin. Neurophysiol.*, vol. 54, pp. 622-628, 1982.

[56] D.S. Barth, W. Sutherling, J. Engel, Jr., and J. Beatty, "Neuromagnetic localization of epileptiform spike activity in the human brain," *Science*, vol. 218, pp. 891-894, November 1982.

[57] R. Hari, A. Ahonen, N. Forss, M.-L. Granström, M. Hämäläinen, M. Kajola, et al., "Parietal epileptic mirror focus detected with a whole-head neuromagnetometer," *NeuroReport*, vol. 5, no. 1, pp. 45-48, October 1993.

[58] W.W. Orrison and J.D. Lewine, "Magnetic source imaging in neurosurgical practice," *Prospectives in Neurosurgical Surgery*, vol. 4, no. 2, pp. 141-147, 1993.

[59] E.C. Benzel, J.D. Lewine, R.D. Bucholz, W.W. Orrison, "Magnetic source imaging: A review of the *Magnes* system of Biomagnetics Technology Incorporated," *Neurosurg.*, vol. 33, pp. 252-259, August 1993.

[60] J.D. Lewine and W.W. Orrison, "Magnetoencephalography amd Magnetic Source Imaging," in *Functional Brain Imaging*, W.W. Orrison, J.D. Lewine, J.A. Sanders, and M. Hartshorne, Eds., St. Louis: Mosby Yearbooks, pp. 369-416, 1995.

[61] W.H. Barry, D.C. Harrison, W.M. Fairbank, K. Lehrman, J.A.V. Malmivuo, and J.P. Wikswo, Jr., "Measurement of the human magnetic heart vector," *Science*, vol. 198, pp. 1159-1162, 1977.

[62] D.J. Staton, R.N. Friedman, and J.P. Wikswo, Jr., "High resolution SQUID imaging of octupolar currents in anisotropic cardiac tissue," *IEEE Trans. Appl. Supercond.*, vol. 3, no. 1, pp. 1934-1936, 1993.

[63] W. Richards, A. Bradshaw, L. Garrard, D. Staton, J. Golzarian, F. Liu, et al., "Magnetoenterography (MENG): Noninvasive measurement of bioelectric activity in human small intestine," unpublished.

[64] W.O. Richards, D.J. Staton, J. Golzarian, R.N. Friedman, and J.P. Wikswo, Jr., "Non-invasive SQUID magnetometer measurement of human gastric and small bowel electrical activity," in *Proc. 9th Inter. Conf. on Biomagnetism, Vienna*, L. Deecke, C. Baumgartner, G. Stroink, and S.J. Williamson, Eds., in press.

[65] J.P. Wikswo, Jr., Y.P. Ma, N.G. Sepulveda, S. Tan, I.M. Thomas, and A. Lauder, "Magnetic susceptibility imaging for nondestructive evaluation," *IEEE Trans. Appl. Supercond.*, vol. 3. no. 1, pp. 1995-2002, 1993.

[66] B.J. Roth, N.G. Sepulveda, and J.P. Wikswo, Jr., "Using a magnetometer to image a two-dimensional current distribution," *J. Appl. Phys.*, vol. 65, pp. 361-372, 1989.

[67] R.L. Fagaly, "SQUID detection of electronic circuits," *IEEE Trans. Mag.*, vol. 25, pp 1204-1218, 1989.

[68] Y.E. Zhuravlev, A.A. Bakharev, A.N. Matlashov, V.Y. Slobodchikov, I.D. Velt, S.L. Nikulin, et al., "Application of dc-SQUID magnetometers for nondestructive testing of multilayer electronic cards," in *Superconducting Devices and Their Applications*, vol. 64, H. Koch and H. Lübbig, Eds., Berlin: Springer-Verlag, 1992, pp. 511-516.

[69] S. Tan, Y.P. Ma, I.M. Thomas, and J.P. Wikswo, Jr., "High resolution SQUID imaging of current and magnetization distributions," *IEEE Trans. on Applied Superconductivity*, vol. 3, no. 1, pp. 1945-1948, 1993.

[70] Y.P. Ma and J.P. Wikswo, Jr., "Detection of a deep flaw inside a conductor using a SQUID magnetometer," *Review of Progress in QNDE*, vol. 11, pp. 1153-1159, 1992.

[71] Y.P. Ma and J.P. Wikswo, Jr., "Imaging subsurface defects using SQUID magnetometers," *Review of Progress in QNDE*, vol. 12, pp. 1137-1143, 1993.

[72] J.P. Wikswo, Jr., Y.P. Ma, N.G. Sepulveda, D.J. Staton, S. Tan, and I.M. Thomas, "Superconducting magnetometry: A possible technique for aircraft NDE," in *Nondestructive Inspection of Aging Aircraft*, M.T. Valley, N.K. Grande, and A.S. Kobayashi, Eds., SPIE Proceedings, vol. 2001, pp. 164-190, 1993.

[73] Y.P. Ma and J.P. Wikswo, Jr., "Detection of subsurface flaws using SQUID eddy current technique," *Nondestructive Inspection of Aging Aircraft*, M.T. Valley, N.K. Grande, and A.S. Kobayashi, Eds., Proc. SPIE, vol. 2001, pp. 191-199, 1993.

[74] D.C. Hurley, Y.P. Ma, S. Tan, and J.P. Wikswo, Jr., "Imaging of small defects in nonmagnetic tubing using a SQUID magnetometer," *Res. Nondestr. Eval.*, vol. 5, pp. 1-29, 1993.

[75] D.C. Hurley, Y.P. Ma, S. Tan, and J.P. Wikswo, Jr., "A comparison of SQUID imaging techniques for small defects in nonmagnetic tubes," *Review of Progress in QNDE*, vol. 12, pp. 633-640, 1993.

[76] Y.P. Ma and J.P. Wikswo, Jr., "SQUID eddy current techniques for detection of second layer flaws," *Review of Progress in QNDE*, vol. 13, D.O. Thompson and D.E. Chimenti, Eds., New York: Plenum Press, 1994, pp. 303-309.

[77] J.A. Cadzow and X. Li, "Blind deconvolution," unpublished.

[78] J. Banchet, J. Jouglar, P.-L. Vuillermoz, P. Waltz, and H. Weinstock, "Evaluation of stress in steel via SQUID magnetometry," *Review of Progress in QNDE*, vol. 14, D.O. Thompson and D.E. Chimenti, Eds., New York: Plenum Press, in press.

[79] A. Cochran and G.B. Donaldson, "Improved techniques for structural NDT using SQUIDs," in *Superconducting Devices and Their Applications*, vol. 64, H. Koch and Lübbig, Eds., Berlin: Springer-Verlag, 1992, pp. 576-581.

[80] A. Cochran, G.B. Donaldson, S. Evanson, and R.J.P. Bain, "First-generation SQUID-based nondestructive testing system," *IEE Proceedings-A*, vol. 140, no. 2, pp. 113-120, March 1993.

[81] Sandy Cochran, University of Strathclyde, Glasgow, Scotland, personal communication.

[82] A. Cochran, G.B. Donaldson, L.N.C. Morgan, R.M. Bowman, and K.J. Kirk, "SQUIDs for NDT: the technology and its capabilities," *British J. NDT*, vol. 35, pp. 173-182, April 1993.

[83] M. Otaka, K. Enomoto, M. Hayashi, S. Sakata, and S. Shimizu, "Detection of fatigue damage in stainless steel using a SQUID sensor," in *The American Society Mechanical Engineers*, PVP-vol. 276, book no. G00844: Determining Material Characterization, J.C. Spanner, Jr., Ed., pp. 113-117, 1994.

[84] I.M. Thomas, Y.P. Ma, S. Tan, and J.P. Wikswo, Jr., "Spatial resolution and sensitivity of magnetic susceptibility imaging," *IEEE Trans. Appl. Supercond.*, vol. 3, no. 1, pp. 1937-1940, 1993.

[85] I.M. Thomas, Y.P. Ma, and J.P. Wikswo, Jr., "SQUID NDE: Detection of surface flaws by magnetic decoration," *IEEE Trans. Appl. Supercond.*, vol. 3, no. 1, pp. 1949-1952, 1993.

[86] D. Li, Y. Ma, W.F. Flanagan, B.D. Lichter, and J.P. Wikswo, Jr., "The use of superconducting magnetometry to detect corrosion in aircraft alloys," in *Proc. of the 1994 Tri-Service Conference on Corrosion*, in press.

[87] T.E. Dixon, M.G. Silk, and D.J. MacKeith, "Review of market opportunities for advanced sensors in non-destructive testing. Part 1. Technical background and overview of developing techniques and new areas," *Insight*, vol. 36, no. 4, pp. 256-263, 1994.

[88] M.G. Silk, T.E. Dixon, and D.J. MacKeith, "Review of market opportunities for advanced sensors in non-destructive testing. Part 2. Future market opportunities and market size predictions," *Insight*, vol. 36, no. 5, pp. 342-347, 1994.

[89] D.S. Barth, W. Sutherling, and J. Beatty, "Fast and slow magnetic phenomena in focal epileptic seizures," *Science*, vol. 226, pp. 855-857, November 1984.

[90] J.P. Wikswo, Jr., "High-Resolution Measurements of Biomagnetic Fields," *Advances in Cryogenic Engineering*, R.W. Fast, Ed., vol. 33, pp. 107-116, 1988.

[91] J.P. Wikswo, Jr., J.M. van Egeraat, Y.P. Ma, N.G. Sepulveda, D.J. Staton, S. Tan, and R.S. Wijesinghe, "Instrumentation and techniques for high-resolution magnetic imaging," in *Digital Image Synthesis and Inverse Optics*, A.F. Gmitro, P.S. Idell, and I.J. LaHaie, Eds., Proc. SPIE, vol. 1351, pp. 438-470, 1990.

[92] J.P. Wikswo, Jr., R.N. Friedman, A.W. Kilroy, J.M. van Egeraat, and D.S. Buchanan, "Preliminary measurements with MicroSQUID," in *Advances in Biomagnetism*, S.J. Williamson, M. Hoke, G. Stroink, and M. Kotani, Eds., New York: Plenum Press, pp. 681-684, 1990.

[93] I.M. Thomas, S.M. Freake, S.J. Swithenby, and J.P. Wikswo, Jr., "A distributed quasi-static ionic current source in the 3-4 day old chicken embryo," *Phys. Med. Biol.*, vol. 38, pp. 1311-1328, 1993.

[94] W.O. Richards, D.J. Staton, J. Golzarian, R.N. Friedman, and J.P. Wikswo, Jr., "Non-invasive SQUID magnetometer measurement of human gastric and small bowel electrical activity," in *Proc. 9th Inter. Conf. on Biomagnetism, Vienna*, L. Deecke, C. Baumgartner, G. Stroink, and S.J. Williamson, Eds., in press.

[95] I.M. Thomas, T.C. Moyer, and J.P. Wikswo, Jr., "High resolution magnetic susceptibility imaging of geological thin sections: Pilot study of a pyroclastic sample from the Bishop tuff," *Geophys. Res. Lett.*, vol. 19, no. 21, pp. 2139-2142, 1992.

[96] I.M. Thomas and R.N. Friedman, "Study of macrophage activity in rat liver using intravenous superparamagnetic tracers," in *Proc. 9th Inter. Conf. on Biomagnetism, Vienna*, L. Deecke, C. Baumgartner, G. Stroink, and S.J. Williamson, Eds., in press.

[97] R.C. Black. A. Mathai, F.C. Wellstood, E. Dantsker, A.H. Miklich, D.T. Nemeth, et al., "Magnetic microscopy using a liquid nitrogen cooled $YBa_2Cu_3O_7$ superconducting quantum interference device," *Appl. Phys. Lett.*, vol. 62, no. 17, pp. 2128-2130, April 1993.

[98] L.N. Vu and D.J. Van Harlingen, "Design and implementation of a scanning SQUID microscope," *IEEE Trans. Appl. Supercond.*, vol. 3, no. 1, pp. 1918-1921, March 1993.

[99] J.R. Kirtley, M.B. Ketchen, K.G. Stawiasz, J.Z. Sun, W.J. Gallagher, S.H. Blanton, et al., "High- resolution scanning SQUID microscope," unpublished

[100] C.C. Tsuei, J.R. Kirtley, C.C. Chi, L.S. Yu-Jahnes, A. Gupta, T. Shaw, et al., "Pairing symmetry and flux quantization in a tricrystal superconducting ring of $YBa_2Cu_3O_{7-\delta}$," *Phys. Rev. Lett.*, vol. 73, no. 4, pp. 593-596, July 1994.

[101] N.G. Sepulveda and J.P. Wikswo, Jr., "Differential operators and their applications to magnetic measurements using SQUID magnetometers," unpublished.

[102] J.P. Wikswo, Jr., D.B. Crum, W.P. Henry, Y.P. Ma, N.G. Sepulveda, and D.J. Staton, "An improved method for magnetic identification and localization of cracks in conductors," *Journal of Nondestructive Evaluation*, vol. 12, no. 2, pp. 109-119, 1993.

[103] J.P. Wikswo, Jr., A. Gevins, and S.J. Williamson, "The future of the EEG and MEG," *EEG Clin. Neurophysiol.*, vol. 87, pp. 1-9, 1993.

[104] J.P. Wikswo, Jr. and J.P. Barach, "Possible sources of new information in the magnetocardiogram," *J. Theoretical Biol.*, vol. 95, pp. 721-729, 1982.

[105] J.P. Wikswo, Jr., "Theoretical aspects of the ECG-MCG relationship," in *Biomagnetism, An Interdisciplinary Approach*, S.J. Williamson, G.-L. Romani, L. Kaufman and I. Modena, Eds., New York: Plenum Press, 1983, pp. 311-326.

[106] J. Lant, G. Stroink, B. Ten Voorde, M. Horachek, and T.J. Montague, "Complementary nature of electrocardiographic and magnetocardiographic data in patients with ischemic heart disease," *J. Electrocardiology*, vol. 23, pp. 315-322, 1990.

[107] G. Stroink, J. Lant, P. Elliot, and M. Gardner, "Magnetic field and body surface potential mapping of patients with ventricular tachycardia," in *Biomagnetism: Clinical Aspects*," M. Hoke, S.N. Erne, Y.C. Okada, and G.L. Romani, Eds., Amsterdam: Elsevier, 1992, pp 471-475.

[108] Y. Zhang, H. Bousack, M. Burghoff, L. Trahms, and J. Borgmann, "Erste Vergleichende Untersuchungen von Tieftemperatur- und Hochtemperatur-SQUIDs bei der Aufnahme des Magnetokardiogramms," *Institut fur Schicht und Ionentechnik Forschungszentrum Jülich (KFA), Internal Report, 1994*, in press.

[109] L. Trahms, H.-D. Hahlbohm, D. Kreiseler, K. Brockmeier, M. Oeff, D. Schmidt, et al., "Fragmentation of the magnetocardiogram of patients prone to malignant arrhythmia," unpublished.

[110] D. Cohen and L. A. Kaufman, "Magnetic determination of the relationship between the S-T segment shift and the injury current produced by coronary artery occlusion, *Circulation Res.*, vol. 36, pp. 414-424, 1975.

[111] B.J. Roth and J.P. Wikswo, Jr., "Electrically-silent magnetic fields," *Biophysical J.*, vol. 50, pp. 739-745, 1986.

[112] J.P. Wikswo, Jr., "Tissue anisotropy, the cardiac bidomain and the virtual cathode effect," in *Cardiac Electrophysiology: From Cell to Bedside, Second Edition*, D.P. Zipes and J. Jalife, Eds., Orlando: W.B. Saunders, 1994, pp. 348-361.

[113] G.L. Barkley, N. Tepley, S. Nagel-Leiby, J.E. Moran, R.T. Simkins, and K.M.A. Welch, "Magnetoencephalographic studies of migraine," *Headache J.*, vol. 30, no. 7, June 1990.

[114] D.M. Tucker, "Spatial sampling of head electrical fields: The geodesic sensor net," *Electroenceph. Clin. Neurophysiol.*, vol. 87, pp. 154-163, 1993.

[115] A.S. Gevins, D. DuRosseau, and J. Libove, "Electrode system for brain wave detection," *U.S. Patent 5,038,782*, August 1991.

[116] A.S. Gevins, J. Le, P. Brickett, B. Reutter, and J. Desmond, "Seeing through the skull: Advanced EEGs use MRIs to accurately measure cortical activity from the scalp," *Brain Topography*, vol. 4, no. 2, New York: Human Sciences Press, Inc., 1991, pp. 125-131.

[117] S. Tan, B.J. Roth, and J.P. Wikswo, Jr., "The magnetic field of cortical current sources: The application of a spatial filtering model to the forward and inverse problems," *Electroenceph. Clin. Neurophys.*, vol. 76, pp. 73-85, 1990.

[118] J. Malmivuo and R. Plonsey, "*Bioelectromagnetism - Principles and Applications of Bioelectric and Biomagnetic Fields*," New York: Oxford University Press, 1994.

[119] G. Anogianakis, G.F.A. Harding, M. Peters, M. Apostolakis, G. Foroglou, J. Vieth, et al., "Biomagnetic methodologies for the noninvasive investigations of the human brain (Magnobrain)," *Computer Methods and Programs in Biomedicine*, in press.

[120] *Surgical Treatment of the Epilepsies*, J. Engel, Jr., Ed., New York: Raven Press, 1993, p. 26.

[121] Gene Hirschkoff, Biomagnetic technologies, Inc., San Diego, personal communication.

[122] G.L. Fitzpatrick, D.K. Thome, R.L. Skaugset, and E.Y.C. Shih, "The present status of magneto-optic eddy current imaging technology," *Review of Progress in QNDE*, vol. 12, D.O. Thompson and D.E. Chimenti, Eds., New York: Plenum Press, 1993, pp. 617-624.

[123] Richard Kinzie, Warner Robbins Air Logistics Center, Robbins Air Force Base, GA personal communication.

[124] V. Argawala, Naval Air Warfare Center, Warminister, PA, personal communication.

[125] U.G. Goranson and M. Miller, "Aging jet transport structural evaluation programs," in *Structural Integrity of Aging Airplanes*, Atluri, Sampath and Tong, Eds., Berlin: Springer-Verlag, 1991, pp. 131-140.

[126] A. Hoggard, "Fuselage longitudinal splice design," in *Structural Integrity of Aging Airplanes*, Atluri, Sampath and Tong, Eds., Berlin: Springer-Verlag, 1991, pp. 167-181.

[127] S.N. Bobo, "The aging aircraft fleet: A challenge for nondestructive inspection," *Rev. Prog. NDE*, vol. 9, pp. 2097-2109, 1990.

[128] G.F. Fulop, "NDT: Slow market growth in traditional areas," *Quality*, vol. 32, no. 9, pp. 28-29, September 1993.

[129] C.D. Wells, "The commercial role of NDT in the context of a changing world," *Insight*, vol. 36, no. 5, pp. 334-341, 1994.

[130] Market Intelligence Research Corporation, "Non-destructive test equipment markets," 1992.

[131] G.A. Klemic, D.S. Buchanan, Y.M. Cycoqicz, and S.J. Williamson, "Sequential spatially distributed activity of the human brain detected magnetically by CryoSQUIDs," in *Advances in Biomagnetism*, S.J. Williamson, M. Hoke, G.

Stroink, and M. Kotani, Eds., New York: Plenum Press, pp. 685-688, 1990.

[132] D.S. Buchanan, D. Paulson, and S.J. Williamson, "Instrumentation for clinical applications of neuromagnetism," in *Advances in Cryogenic Engineering*, vol. 33, R.W. Fast, Ed., New York: Plenum Press, 1988, pp. 97-106.

[133] W.A. Little, "Microminiature refrigeration," *Rev. Sci. Instrum.*, vol. 55, pp. 661-680, 1984.

[134] W.A. Little, "Advances in Joule-Thomson cooling," *Adv. Cryogenic Engr.*, vol. 35, pp. 1305-1314, 1990.

[135] G.L. Romani, S.J. Williamson, and L. Kaufman, "Biomagnetic instrumentation," *Rev. Sci. Instrum.*, vol. 53, pp. 1815-1845, 1982.

[136] J.P. Wikswo, Jr., "Optimization of SQUID differential magnetometers," *AIP Conf. Proc.*, vol. 44, pp. 145-149, 1978.

[137] J.E. Zimmerman, "SQUID instruments and shielding for low-level magnetic measurements," *J. Appl. Phys.*, vol. 48, no. 2, pp. 702-710, February 1977.

[138] D. Drung, E. Crocoll, R. Herwig, M. Neuhas, and W. Jutzi, "Measured performance parameters of gradiometers with digital output," *IEEE Trans. Mag.*, vol. 25, pp. 1034-1037, 1989.

[139] G. Brandenburg, U. Clements, H. Halling, F. Zimmermann, *Internal Report, Zentrallabor für Elektronik, Forschungszentrum Jülich (KFA)*, 1994, in press.

[140] N. Fujimaki, H. Tamura, H. Suzuki, T. Imamura, S. Hasuo, and A. Shibatomi, "A single-chip SQUID magnetometer," *IEEE Trans. Elect. Dev.*, vol. 35, p. 2412-2417, 1988.

[141] M. Radparvar and S. Rylov, "An integrated digital SQUID magnetometer with high sensitivity input," *IEEE Trans. Appl. Supercond.*, these proceedings.

[142] P.-F. Yuh and S. Rylov, "An experimental digital SQUID with large dynamic range and low noise," *IEEE Trans. Appl. Supercond.*, these proceedings.

[143] A. Cochran, J.C. Macfarlane, L.N.C. Morgan, J. Kuznik, R. Weston, L. Hao, et al., "Using a 77 K SQUID to measure magnetic fields for NDE," *IEEE Trans. Appl. Supercond.*, vol. 4, no. 3, pp. 128-135, September 1994.

[144] L.N.C. Morgan, C. Carr, A. Cochran, D.McA. McKirdy, and G.B. Donaldson, "Electromagnetic nondestructive evaluation with simple HTS SQUIDs: Measurements and modelling," *IEEE Trans. Appl. Supercond.*, these proceedings.

[145] Y. Zhang, U. Krüger, R. Kutzner, R. Wördenweber, J. Schubert, W. Zander, et al., "Single-layer $YBa_2Cu_3O_7$ rf SQUID magnetometers with direct-coupled pickup coils and flip-chip flux transformers," *Appl. Phys. Lett.*, in press.

[146] F. Lidwig, E. Dantsker, R. Kleiner, D. Koelle, J. Clarke, S. Knappe, D. Drung, et al., "Integrated high-T_C multiloop magnetometer," unpublished.

[147] R.H. Koch, V. Foglietti, J.R. Rozen, K.G. Stawiasz, M.B. Ketchen, D.K., Lathrop, et al., "Effects of radio frequency radiation on the dc SQUID," *Appl. Phys. Lett.*, vol. 65, no. 1, pp. 100-102, July 1994.

[148] Y. Tavrin, Y. Zhang, M. Mock, A.I. Braginski, and C. Heiden, "$YBa_2Cu_3O_7$ thin film SQUID gradiometer for biomagnetic measurements," *Appl. Phys. Lett.*, vol. 62, no. 15, pp. 1824-1826, April 1993.

[149] Y. Tavrin, Y. Zhang, W. Wolf, and A.I. Braginski, "A second-order SQUID gradiometer operating at 77 K," *Supercond. Sci. Technol.*, vol. 7, pp. 265-268, 1994.

[150] R.H. Koch, "Gradiometer having a magnetometer which cancels background magnetic field from other magnetometers," *U.S. Patent 5,122,744*, June 1992.

[151] R.H. Koch, J.R. Rozen, J.Z. Sun, and W.J. Gallagher, "Three SQUID gradiometer," *Appl. Phys. Lett.*, vol. 63, no. 3, pp. 403-405, July 1993.